Assessing the Demand Response Potential of Heat Pumps in All-Electric Buildings Equipped with PV, EV (V2G) and BES to Minimize Energy Costs.

D.A Gaona Reinoso

Master of Science Thesis

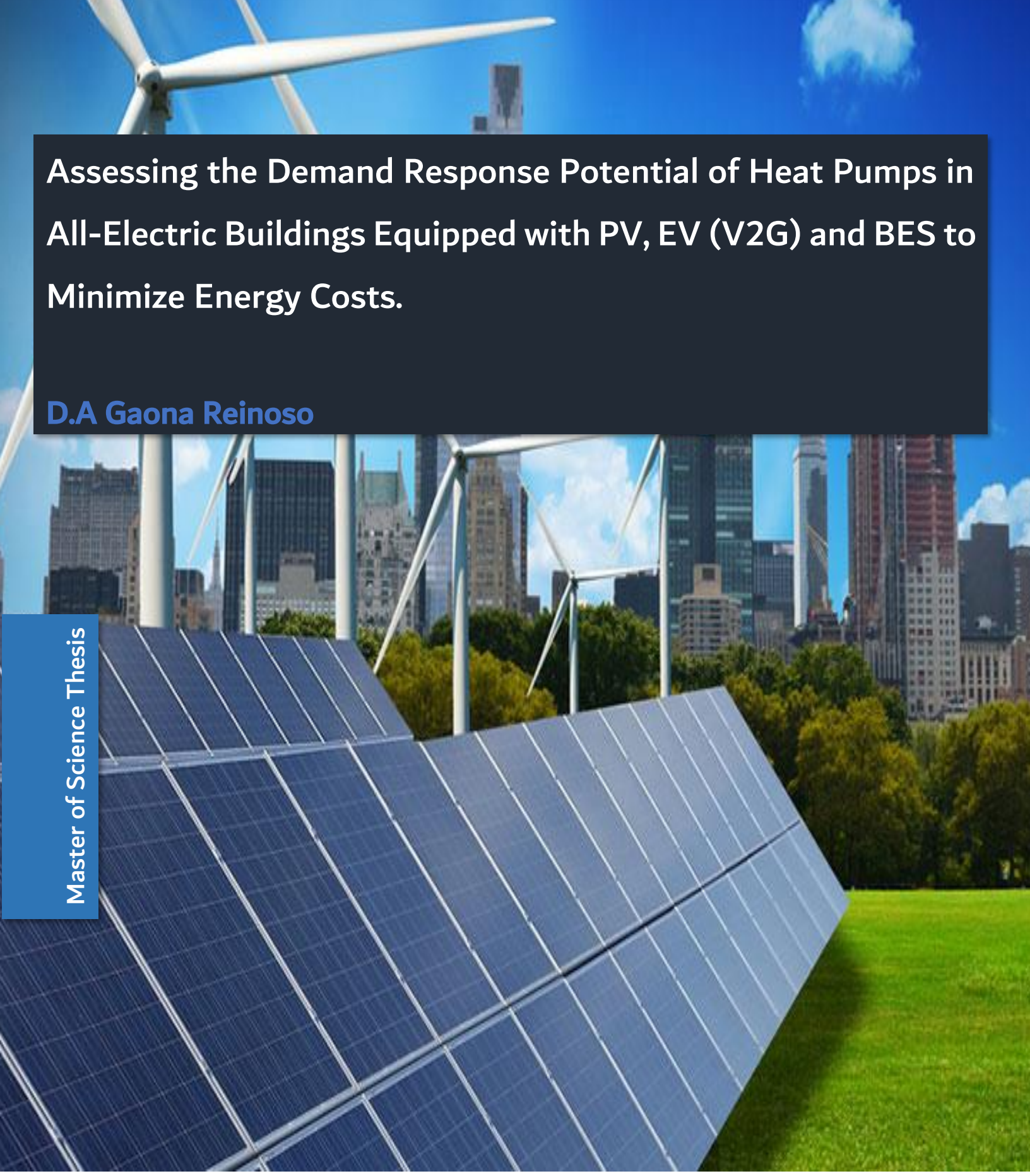

TU Delft Delft University of Technology

Assessing the Demand Response Potential of Heat Pumps in All-electric Buildings Equipped with PV, EV (V2G) and BES to Minimize Energy Costs

By

D.A. Gaona Reinoso

in partial fulfilment of the requirements for the degree of

Master of Science
in Sustainable Energy Technologies

at the Delft University of Technology,
to be defended publicly on Wednesday October 21, 2020 at 09:00.

Supervisor:	dr.ir. G.R. Chandra Mouli	TU Delft
Thesis committee:	Prof.dr.ir. P. Bauer,	TU Delft
	dr. ir. G.R. Chandra Mouli,	TU Delft
	Prof. dr. Ir. C. Ferreira T	TU Delft

TU Delft

Preface

Energy has been the drive force for the development of mankind since our ancestors understood and mastered its mysteries to use it practically to perform any task. Historically, fossil fuels have been the main energy resources that have allowed all the economic sectors to grow significantly in a relatively short period since their discovery. However, their extensive use has engendered risks for the environment as result of the exponential increase of CO_2 emissions in the atmosphere. This has triggered a series of global effects that are threatening living being's survival if no actions are immediately taken to reduce these emissions without compromising the future and economic stability of society. Looking for alternative resources that can satisfy the current and future energy demand and reduce the greenhouse effects is an arduous task, but not impossible.

Fortunately, we dispose of interminable clean energy resources that can become part of the solution to the worldwide energy crisis. When they are merged with sustainable technologies and enthusiastic well-educated people, different strategies and procedures can be proposed and developed to lead the world towards diversifying its energy matrix where renewable energies must be predominant over fossil fuels.

As a Chemical Engineer, I have always been interested in studying and proposing new, clean, and efficient processes and technologies aligned with the principles of sustainability that can be evidenced as reliable alternatives. Consequently, I considered the development of this project a milestone within the study of renewable energy systems as I tried to incorporate different energy elements that can demonstrate the economic and energetic benefits of using them in a smart and integrated way. Principally, I was motivated to work on this thesis project as it offered me the opportunity to study how to optimize the power consumption of two of the most energy intensive sectors such as the residential and transport by incorporating different technologies such as batteries, electric vehicles and heat pumps into one single problem.

Through this thesis, I wanted to demonstrate the feasibility of using heat pumps as an alternative to gas to satisfy the heating demand in the residential sector and how their operational flexibility helps to minimize the operational energy costs in an integrated energy system. I consider this research of paramount importance as it offers a more realistic approach towards understanding how renewable energies and demand response programs can be incorporated to reach self-sustainability in terms of energy and costs.

By the end of this research, I hope the reader would be motivated and convinced to take actions on starting a transition towards the use of renewable energies to become part of the millions of people who want a greener and sustainable world not only for us, but for our future generations.

"The most sustainable way is to not make things. The second most sustainable way is to make something especially useful, to solve a problem that hasn't been solved". T. Sigsgaard

D.A. Gaona Reinoso
Delft, October 2020

Contents

Abstract

Mitigating and reducing greenhouse gas emissions have become global agreements to combat climate change, and to lead the world towards a sustainable low carbon future without compromising society's development. Currently, many countries have started a transition onto the increase of renewable energies participation to reduce their dependency on fossil fuels in their most energy intensive sectors. On December 7th, 2016, the Dutch government submitted its *Energieagenda* outlining its plan to decarbonize the Dutch economy and to electrify the transport and residential sectors to achieve 80-90% reduction of CO_2 emissions by 2050 [1]. In the residential sector, natural gas has been the main consumed energy resource for surface heating (SH) and domestic hot water (DHW) during cold seasons for decades, and substituting this energy carrier with electricity generated from renewable resources imposes challenges not only in economic but also technical terms.

The electricity production from these sources is constrained to their inherent intermittent nature because their availability is highly dependent on the seasonal stage and the weather conditions of the location, thus the electricity supply will not be constant and it will not match the electricity demand, decreasing the reliability of the electricity generation sector. Therefore, this fluctuation in the electricity supply must be mitigated to prevent them from causing shortcomings and instability in the transmission and distribution grids where electric devices could receive too much or too little power resulting in a malfunctioning of the entire system. In this context, the integration of flexible energy devices such as heat pumps (HP), electric vehicles (EV), and batteries (BES) within demand response programs present as a promising option to reduce the effects of intermittent electricity production from renewable resources for the residential and transportation sectors.

In this thesis, an integrated energy system formed by PV panels, EV, BES, and a HP coupled with thermal storage tanks (TES) has been studied. The research aimed to minimize the total energy costs by scheduling the optimal power consumption of each device as response to two external signals as part of a demand response program. One of the signals corresponded to a selling electricity price tariff or feed-in tariff (FIT) to account for the ability of the system to sell energy towards the grid. On the other hand, the second signal corresponded to the buying electricity price tariff to account for the system's energy consumption from the grid. This control scheme allowed to determine the optimal energy consumption of the HP and its flexibility potential to shift its load towards times of low electricity prices.

To do this, an HP-TES optimization model was developed to meet SH and DHW demands during winter and summer. By conducting time-dependent energy balances, the temperature of the water in the tanks, the temperature of the building, and the optimum power consumption of the HP were obtained. In addition, the HP's coefficient of performance was modelled to account for its variability in time as a function of the temperature difference between the storage tanks and the outside air. Similarly, a correlation between the SH demand and the ambient temperature has been developed to perform a temporal interpolation and to obtain the SH demand data at the desired time resolution. Additionally, the impact of the SH storage tank size on the HP's performance was investigated.

The developed HP-TES model was implemented into a second model detailing the functioning of the PV, EV, and BES components. In this way, a non-linear programming (NLP) optimization model was obtained to minimize the total energy costs of the entire system. The General Algebraic Modelling System (GAMS) software was used to optimize the system for a five-day horizon with a time resolution of 15 min. Additionally, the influence of the FIT on the cost minimization was treated. Two scenarios involving a high and a reduced FIT were addressed to assess the system operation strategy to minimize the costs. Finally, the optimization results were compared with those obtained in a non-optimized case where no demand response was carried out.

In the high FIT scenario, the results showed that the system's strategy to minimize the energy costs consisted of purchasing and injecting energy at low and high prices, respectively. It was calculated that a 49% in cost savings could be achieved relative to the non-optimized system. On the other hand, in the reduced FIT case, the system's energy intake was reduced, and no energy was injected to the grid, resulting in 44% in cost reduction. During summer, a similar behaviour was encountered for both high and reduced FIT cases. In the first case, the energy costs were 128% lower

than the non-optimized case, generating revenues for the customer. This was due to minimum PV-self consumption, which resulted in large amounts of energy being sold to the grid. In the second case, the minimized costs were 68% lower than the non-optimized system, showing a considerable PV-self consumption.

Looking at the HP behaviour, no operational flexibility was obtained when using a small tank because the HP operated almost continuously, demanding 2 kW in average. Contrarywise, operational flexibility by means of load shifting was achieved when using a big tank. In this case, peaks of 6 kW took place at times of low prices mainly to charge the storage tanks such that sufficient energy was available for the periods when the HP remained OFF. It was calculated that the number of hours the HP did not operate was 9.45 h per day, so the SH and DHW demands were entirely met by the storage tanks. Consequently, it was determined that 56.09 kWh of electricity was shifted towards times of low prices. Besides, it was calculated that 53 m^3 of gas would be avoided by using the heat pump, which resulted in a 17% cost reduction for the customer's heating bill.

Consequently, this study has showed the technical and economic value of the inclusion of heat pumps to efficiently provide heat from electricity in an all-electric concept as a promising option to reduce not only the effects of intermittent electricity production, but also the customer's energy bill.

Acknowledgments

This thesis is the final requirement for obtaining the degree of Master of Science in Sustainable Energy Technologies at the Delft University of Technology. The work done during this project could not have been the same without the support and guidance I received throughout the entire process. I would like to take this opportunity to express my gratitude to all the people who helped me achieve this new goal in my professional career.

First, I would like to express my sincere gratitude to my daily supervisor Wiljan Vermeer. Your continuous support and guidance motivated me to keep working and improving this research each day specially those times where the problem seemed to be infeasible. I learned a lot from you, and I enjoyed working and sharing ideas about this topic with you.

I would also like to recognize the support offered by my thesis supervisor dr. Gautham Chandra, whose knowledge and critical remarks to my mistakes encouraged me to keep working hard until I finally solved all the problems. Besides, I would like to thank Gautham for his support during the pandemic times, I really appreciated your help regarding my economic circumstances.

Furthermore, I would like to acknowledge the valuable support of MSc. Diego Jijón from the Instituto de Investigación Geológico y Energético (IIGE) in Ecuador. Your knowledge in weather data treatment, programming, and your patience to explain to me things that were out of my expertise field were extremely valuable for the development of this thesis.

I would like to express my gratitude to my parents, siblings, and friends for their constant support during those times when I felt lost and unmotivated to continue working. Your love and patience gave me the strength to never give up.

I would like to thank the Ex-President Rafael Correa Delgado for being the first and unique President in the Ecuadorian history that recognized education as a key factor in Ecuador's development and offered an opportunity to professionals like me to keep studying and perfecting his knowledge in benefit of the country throughout the scholarship program he initiated.

Finally, I would like to thank the Ecuadorian Government and the Secretaría Nacional de Educación Superior, Ciencia Tecnología e Innovación (SENESCYT) for granting me a full scholarship to cover my studies at the Delft University of Technology.

D.A. Gaona Reinoso
Delft, October 2020

1. Introduction

1.1. Research context

Following the international climate change agreement, the Netherlands is facing the challenge to reduce drastically its greenhouse gases emissions to reach the climate neutrality goal by the second half of the 21st century. To accomplish this, a restructuring of the energy systems into more sustainable forms will be required by distinguishing how the energy is used in four main functions: energy for space heating, energy for industrial process heat, energy for power and light, and energy for transport [2]. Traditionally, to satisfy its energy consumption, the Dutch energy system has relied mainly on natural gas and fossil fuels while a small proportion of renewable energies has been included, as it was demonstrated by [1] where it showed that only 7% of the total energy produced comes from wind and solar technologies as the principal renewable sources.

Considering this, the energy transition will require not only major technological changes towards renewable systems but also societal-behaviour adjustments that help to match the supply with the demand. Nevertheless, the Netherlands is well situated in terms of technology development, research and government investment in new and efficient energy systems, and this represent a great opportunity to study and develop clean and efficient energy systems [3]. Figure 1 illustrates the evolution of renewable electricity production since 2007 in the Netherlands where the use of wind and solar has increased notably

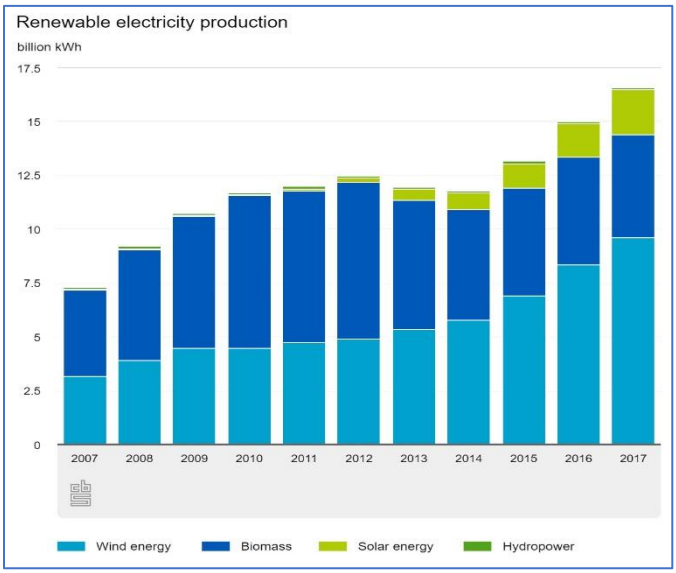

Figure 1-1: Renewable electricity production in the Netherlands, [4]

As the substitution of fossil-driven power generation by renewable energies continues as part of the energy transition, a new problem arises from the use of these resources which comprises mainly the constancy of power production. Fossil-fuelled power systems are characterized for producing stable electricity, meaning that the power output can be controlled over time to satisfy the demand constantly, but this does not occur with renewable energy technologies. Due to their intermittent nature, the electricity production will fluctuate causing major problems to balance the supply with the demand at every time spot within the energy market [5].. As this tendency will keep growing, it is important to integrate systems and programs intended to solve the problem of intermittent energy production effectively.

In this context, different approaches, technologies, and strategies have been investigated to manage the variable renewable electricity from wind and solar. All these tactics have as main characteristic the study of the "flexibility potential" that new energy systems can offer to attenuate the effects of intermittency and to help the grid to keep their stability. On the demand side, the main approach is to address the problem towards demand response programs (DR), where the final consumers are willing to modify their current consumption tendency by using smart technologies that

respond to some signals. Here, the final users perform their daily activities under an optimized scheduling framework that assures the satisfaction of their needs while consuming the least amount of energy at the lowest cost.

The importance of this approach lies on reducing the requirement of the most energy demanding sectors such as the residential or transport without jeopardizing consumer's comfort and satisfaction. Most of the research has been focused on the residential side as this segment is considered the second most energy intensive sector within the energy mix of a country due to the nature of the energy required. Space heating/cooling and domestic hot water are the most demanded forms of energy in households. Currently, maintaining the thermal comfort during summer or winter, and providing hot water for domestic daily activities involve consuming a vast amount of fossil fuels and electricity, which results in a considerable increase of the CO_2 emissions per year. The integration of renewable sources such as PV or wind, the use of alternative devices to produce heat like heat pumps and their integration in demand side management (DSM) applications present as feasible options to reduce the dependence on fossil fuels for heating services, and to boost the energy transition towards clean and renewable energy.

Considering all mentioned above, this research project seeks principally to promote and support the use of heat pumps as a solution to reduce the variability of renewable energy sources, and to provide flexibility potential to energy systems through its application in demand side management programs (DSM).

1.2. Problem statement

Increasing the share of renewable energies in the electricity production will bring about a reduction in the reliability of the electricity generation to meet the electricity demand as result of the intermittent nature of renewable energy sources. According to [6], a grid with high penetration of renewable sources will cause power fluctuations where the supply does not match demand, and the devices connected to the grid will receive too little or too much power causing them a malfunctioning. Additionally, future buildings will be all-electric systems where heating will be done electrically possibly in the form of heat pumps. Together with the electrification of transport, this results in a drastic increase in electricity demand, which the current grid is unable to supply. To face these issues, coupling energy storage systems (ESS), flexible electric devices, and energy demand response programs (DR) have been of great interest for researchers during recent years as an alternative to mitigate these effects and to increase their self-consumption.

Flexible devices are defined as systems who can change their energy consumption based on external signals to reduce costs and to optimize the use of the energy required by balancing the supply and demand at each time spot [7]. The most common flexible devices studied by researchers are electric vehicles (EV's), battery systems (BES), power to gas (P2G), and heat pumps (HP) coupled with thermal storage systems (TES) as their operation can be scheduled depending on the amount of energy supplied or generated.

In this way, the proposed thesis intends to investigate the flexibility potential achieved with heat pumps in an integrated power system composed of photovoltaic panels (PV), battery storage system (BS), electric vehicle charging point V2G (EV) to achieve economic savings, and higher PV self-consumption. Therefore, the main research questions to be answered under this research are:

- *What is the demand response potential of heat pumps (HP) and thermal storage system (TES) in all-electric buildings equipped with PV and electric energy storage devices (EES)?*

- *What is the minimized energy cost for this integrated system?*

1.3. Relevance of the research

This research will intend to provide a model to perform an energy cost minimization and to encourage the use of renewable energy systems to satisfy residential energy demands. By simulating a demand response program, this thesis aims to achieve a reduction in the energy consumption for residential heating by determining the optimal operation a heat pump. In this way, determining how flexible the system becomes when heat pumps and thermal storage systems are included is vital to know the limits of the proposed solution.

This thesis is relevant as it will offer an approach to determine the extent of the flexibility achieved in integrated power systems in households, and it can contribute to encourage the inclusion of heat pumps as a flexibility service for future energy systems. From the results of this project, different parties within the energy sector can get insights about the possibilities and benefits of using all-electric systems as a reliable option to minimize the consumer's energy bill.

The main academic aspect of this proposal is to develop an optimization model to assess the demand response potential of heat pumps as effective devices to satisfy heating demands while minimizing the energy costs. Consequently, this proposal is an opportunity to study different energy systems that can be flexible and controllable. In addition, this research is related to the Sustainable Energy Technology field because it combines the use of renewable energies with demand response programs as a sustainable option to meet the total demand of a household. Furthermore, this thesis emphasizes the main feature of the SET program on developing, optimizing, and integrating different energy subsystems into one system than can manage the fluctuating energy supply and demand.

The proposed research gives the opportunity to develop a system level thinking instead of focusing on one specific component, and it delivers a model which includes the technological aspects of an integrated power system for a typical house where heat pumps (HP), electric vehicles (EV) and battery systems (BES) play a critical role in the system's flexibility. On the other hand, an economic analysis is included to elucidate the feasibility of developing and including these technologies as part of the future energy systems.

1.4. Research approach

To address the presented problem, an extensive literature review will be done focusing on the following areas: heat pump technologies, building's heating with heat pumps and thermal storages, distributed generation problems, and energy flexibility in integrated energy systems. Each one of these areas will support the development of the desired model to find a solution to the main problem of this research. The literature review will be based on scientific papers from recognized and influential journals in the energy field, and some thesis developed in TU Delft whose information lies on the field of this research.

After the literature review, a description of the integrated energy system to be studied is presented. This description will let the reader to understand how the system works and the role of each one of the components. As the principal focus of this project is to investigate the impact of heat pumps (HP) and thermal storage (TES) on the energy consumption in households, a thermal modelling must be established to understand the behavior of the heat loads involved in a typical dwelling. Through a flow diagram, the coupling of a heat pump, a water storage tank, and a household will be represented to determine the main variables and energy streams involved. This flow diagram is a key component to establish the required input data, degrees of freedom (variables), constraints, and considerations that describe the dynamics of the thermal system mainly. Furthermore, some fair assumptions justified by the literature review will be considered to simplify the model while keeping its effectiveness and reliability.

For modeling the thermal part, time-dependent energy balances and heat transfer principles will be applied in each component of the system HP-TES-Building to determine how the main variables change in time. First, this system will be modelled as a sub-optimization problem aimed to minimize the power consumption of a heat pump while maintaining the thermal comfort inside the building. Based on an electricity price signal from a transmission system operator (TSO), the heat pump must work to charge the storage tank when the energy price is low, and when the electricity price becomes higher, the storage tank is discharged to satisfy the heat demand of the building. The problem will be optimized using the General Algebraic Modeling System (GAMS) software, which is a high level-modeling system for mathematical optimization designed for solving linear, nonlinear, and mixed integer optimization problems.

Once the thermal model of the HP-TES-Building gives reasonable results, it will be adapted to a pre-existing model developed by MSc. Wiljan Vermeer and Dr. Gautham Mouli of TU Delft which describes the operation of the PV panels, battery (BES), and an electric vehicle V2G to minimize the energy costs of the entire system. This entire model will represent the integration of different devices in one household, for the optimization results presented here must be considered only as a local optimum and not as a global optimum.

After optimizing the entire system, the flexibility potential of the system will be analyzed using a base case scenario where heating is done by an electric heater, and in the optimal scenario the heat pump is used. Furthermore, an analysis of the amount of energy consumed from the solar panels will be presented together with a sensitivity analysis of the energy storage devices (BES, TES, and EV) to determine which device offers more flexibility. Finally, an economic evaluation is performed to establish the feasibility of the system in terms of Levelized Cost of Electricity (LCOE) and Pay Back Period (PBP).

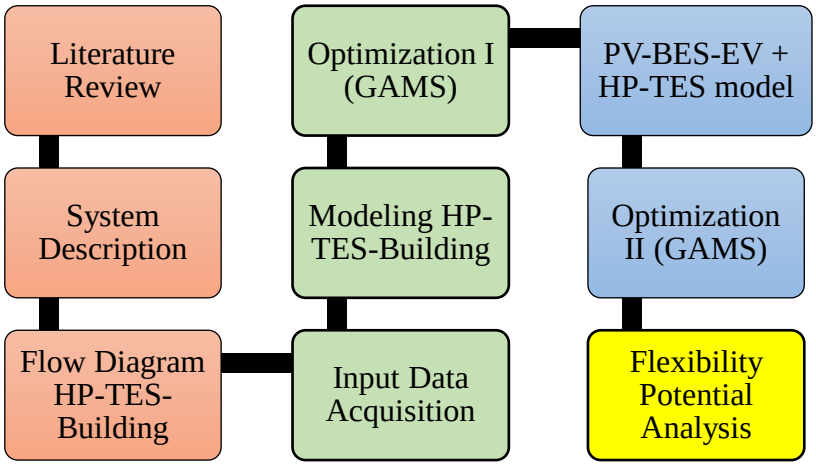

Figure 1-2: Research approach

1.5. Report outline

The contents of this thesis have been organized into the following parts. This section gives a detailed description of the contents of each chapter.

- Chapter 2 summarizes the literature review and state of the art on the use of heat pumps in residential buildings and its coupling with thermal energy storage devices. First, it describes what energy flexibility and demand side management are, and how demand response potential can be achieved in households. Second, a brief description of what a heat pump is, how it works, and the types of heat pumps available in the market is presented. Finally, the integration of heat pumps (HP) and thermal energy storage (TES) for demand response applications is described.

- Chapter 3 includes a description of the system to be studied and minimized. First a brief explanation of the main components is presented through a flow diagram of the heat pump (HP), thermal storage (TES) and the building. Next, the mathematical formulation of the optimization problem for the HP-TES system is developed together with a detailed explanation of the model and the reasoning behind it. Furthermore, the model development for the PV-EV-BES-HP system is exhibited emphasizing on the PV-BES-EV system considerations, assumptions, and constraints. Finally, the formulation of the objective function aimed to be minimized is presented and detailly explained to demonstrate how the optimization works.

- Chapter 4 presents the results obtained from the optimization problem of the integrated system. First, the results for winter season are displayed. Here, the behavior of the individual system's components is explained in terms of power profiles and operational costs. Besides, the influence of the size of the thermal storage components on the integrated system's behavior is analyzed. Next, an explanation of the effect of the feed-in tariff (FIT) on the operational strategy to minimize the energy costs is offered. This exhaustive analysis was performed for summer to demonstrate how PV self-consumption can be enhanced. Additionally, the results of the optimized problem were compared with an uncontrolled system where no optimization is performed to establish the benefits of the proposed integrated system. Finally, the estimation of different flexibility potential indicators is performed.

- Chapter 5 involves the discussion of the main results and recommendations for future work. Finally, Chapter 6 comprises the main conclusions of the project.

2. Literature Review

2.1. Energy system flexibility and demand side management (DSM)

2.1.1. Energy flexibility

In electric systems, the supply and the demand need to match at operational timescales to be in balance to operate properly to avoid any problems in the distribution grids. This means that electric systems must be built in such a way that it is capable of managing uncertainty and variability in both supply and demand [7]. In traditional electric systems, flexibility refers to grid frequency, voltage control, and power ramping rate which is provided through power plants with different response times to adapt to the load side at every time spot. Technically, the flexibility of an electric service has been defined as the power adjustment sustained at a given moment for a given duration from a specific location within the network [8]. Additionally, the operational flexibility of an electric service can refer to the capability of supporting the power system in terms of speed, range, and duration of the power output as well as its ability to respond to the frequency or voltages changes that might occur due to the penetration of distributed energy resources (DER) [9].

When discussing flexibility, it is remarkable to recognize how systems on the supply side can offer a great flexibility potential. This potential might be analyzed first based on their large range of absolute output power between its minimum and maximum capability limits. The larger the range, the bigger the flexibility potential as it has greater ability to adjust to the changes in the power system conditions. Furthermore, easiness of being turned on or off provides great flexibility to a system as its operating output power can be taken between zero and its maximum limit. In the same way, high ramping rates and startup times make energy systems more flexible because the system can adapt and respond faster to the changes in the system energy conditions. [9]. Therefore, the flexibility of a service can be characterized by three namely attributes: direction, electrical composition in capacity or power, and availability defined by its starting time and duration.

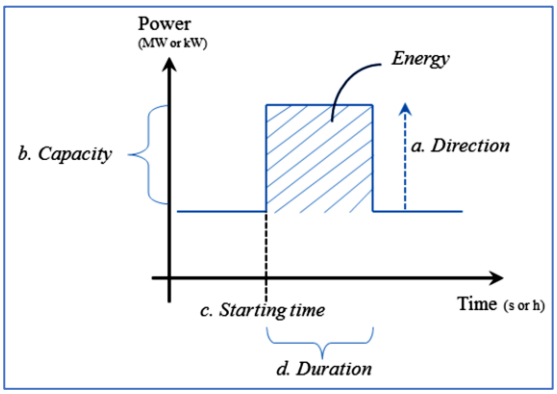

Figure 2-1: Characterization of flexibility products, [10]

On the other hand, electricity flexibility can be offered in the demand side by different type of resources such as electric vehicles (EV), electric heaters (EH), battery systems, thermal storage devices, and combined heat and power (CHP) units. The flexibility of these resources can be characterized using the attributes given in figure 2. For instance, household loads such as water heaters can be only unidirectional, but battery systems can be bidirectional as they can produce and consume electricity. Besides, the availability of the system plays an important role as in the case of EV's which are only available normally during night times [10]. Taking advantage of the different types of flexibility that systems can offer on the demand side belongs to the concept of demand response programs or demand side management (DSM).

2.1.2. Demand side management (DSM)

The objective of DSM programs is to reduce the impact of DER on the low voltage transmission grid, which due to the presence of these resources will be used as energy carrier of bidirectional electricity flows. In this context, DSM has been defined as a set of measures addressed to modify the pattern and magnitude of end-electricity consumption by reducing, increasing, or rescheduling energy load in order to lessen the effects of intermittency on the grid [7]. By implementing a DSM program, the load profile can be controlled and modified indirectly to achieve two main utility objectives: to have a load factor close to 1, and to have a peak load within the proper margin. By accomplishing these objectives, the maximum amount of energy from the installed units would be obtained, and at the same time the total profit can be maximized by minimizing the average cost per kWh produced [11]. There are five types of programs within DSM theory focused on modifying the load profile: valley filling, load shifting, peak clipping, energy conservation, and load growth.

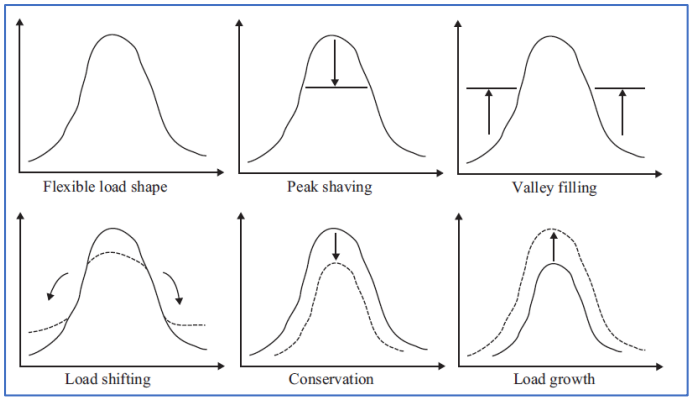

Figure 2-2: Categories of demand side management, [12]

In valley filling, the load is increased during off-peaks while maintaining the same peak load. This can be the case of charging EV's at night times to smooth out the load profile so that the utility does not have to produce much power during the day. Load shifting program tries to move the times of peak energy use to times where excess of produced electricity exists, for the peak demand is distributed among the off-peak periods [11]. This type of DSM requires energy storage systems such as batteries or heat storage to flatten the load profile. Peak clipping is used to decrease the peak load, but this load cannot be spread over the off-peak periods, for one way to achieve this program is to force the end-users indirectly to reduce their load. In the conservation program, the load can be reduced all over the consumption period while keeping the demand satisfied by using high efficiency components [12]. Flexibility options can be offered on the supply and the demand sides. On the demand side, flexibility can be reached by demand response (DR) or energy storage (ES) or a combination of both. In demand response, the consumer reduces his load as a response to an operator's signal (i.e. price signal), while in energy storage the operator has the capability of withdrawing or supplying power to the grid [13].

2.1.3. Demand response potential in households

The growing trend to satisfy energy demand is renewable electricity generation from photovoltaic (PV) and wind plants. On the level of individual households, this implies the appearance of prosumers, systems that consume and produce electricity at different times on a day to seek independence from the grid in the form of standalone systems [14]. To achieve this independence while using DER, these systems needs a demand response (DR) control for all the possible domestic shiftable loads such as heating/cooling systems, washing machines, plug-in EV's etc. Most of the energy consumed in a house comes from the need for space heating (SH) and domestic hot water (DHW), for the DR program is aimed to match the generated electricity and demand by controlling heating, ventilation, and air conditioning (HVAC) without altering the thermal comfort and the building energy efficiency.[13].

In this research, a heat pump (HP) and a thermal storage tank (TST) will be used as the main flexible loads to satisfy the SH and DHW demands in an all-electric household running mainly on PV energy, for their demand response potential will be determined. The focus of this research is based on heat pumps and thermal storage due to these

devices are the link between the electric and heat sector, and provide flexibility to the system as the load of HP can be shifted while the produced heat can be stored for later use to meet demand [14]. In this research, it is assumed that heat demand of the individual household cannot be reduced, for the demand response effect aimed to produce by using HP-TSTS is load shifting and not load reduction.

2.2. Heat pumps brief description

In this section a brief description of the relevant features of residential heat pumps and its applications is provided. This description encompasses the most common types of HP used for residential heating, a comparison between them, and its applications in renewable energy systems.

2.2.1. Heat pumps features

Heat pumps provide heat using thermal energy from a heat source (reservoir) of low temperature and transmit it to a sink of high temperature by using additional energy to perform work in order the heat to flow. For residential purposes, the heat source can be the outside air surrounding the building envelope or ground water with low enthalpic content, and the sink, where heat is disposed, corresponds to the interior of the building. Forcing heat to flow from low temperature to high temperature requires additional energy that must be supplied to the system, typically in the form of electricity. The operation principles of a heat pump are based on 4 thermodynamic processes the working fluid, a refrigerant, must perform: evaporation, compression, condensation, and expansion [14].

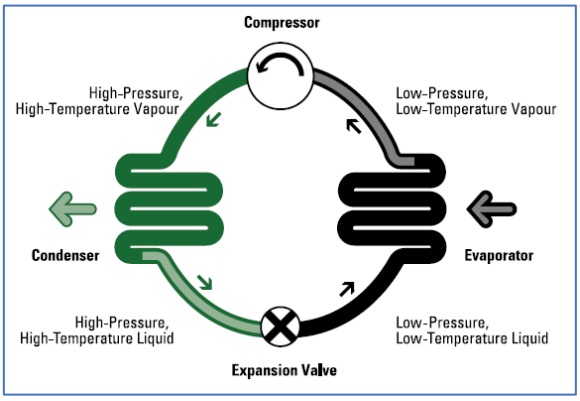

Figure 2-3: Basic heat pump cycle, [15]

As heat pumps work in an inverted Carnot cycle, the "efficiency" of the system is determined by the coefficient of performance (COP), which is the ratio of the energy output of the heat pump and the amount of electricity needed to run the device at a specific temperature. The higher the COP, the more efficient is the heat pump, but the COP is also an inverse function of the temperature difference between the sink and source temperatures. The smaller the difference, the higher the COP, for in winter, the COP can be lower than in summer as more electricity will be needed because extracting heat from colder air becomes more difficult [15].

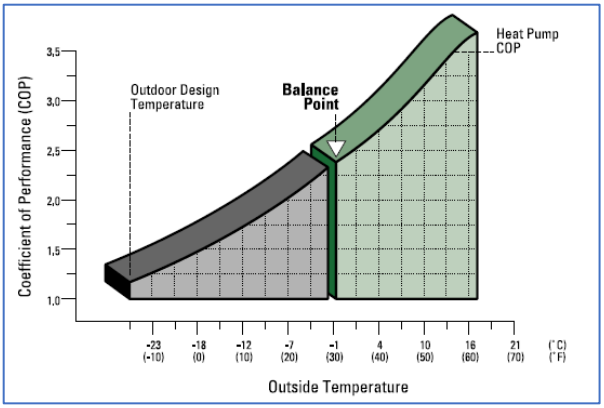

Figure 2-4: COP vs ambient temperature, [15]

2.2.2. Types of heat pumps in the market

The most common types commercially available in the market are air-source (ASHP) and ground-source heat pumps (GSHP). ASHP uses the outside air as the thermal source from which heat will be extracted and transferred to a secondary source typically water or air that will be used for the space conditioning and hot water provision. Air to water heat pumps (AWHP) are considered a promising solution to satisfy heat demand in households, and they have had an increasing share representing the fastest growth in heat pumps in the European heating market [16]. This type of heat pump is coupled with hydronic heat distribution systems and thermal storage tanks offering in this way extra flexibility potential.

The advantage of these type of devices is the unlimited availability of the main energy source, and as air has low density, heat exchangers are sized to be compact and with low thermal resistance, for the capital costs are considerably low and the system becomes relatively economic. Besides, the space needed for installing the device is suitable compared to the traditional heating systems (gas or electric boilers) that require large spacing rooms [17]. Nevertheless, these devices present two considerable disadvantages in terms of the features of the energy source. First, air's temperature is volatile as it fluctuates depending on the geographical location and seasonal weather conditions, and as mentioned before, the lower the temperature of the source the less efficient is the heat pump. Additionally, frosting of the evaporator can occur especially during high demands and air temperatures near or below the freezing point, so he moisture from the air will freeze and a defrosting operation will be required involving extra energy consumption and lowering the overall efficiency of the device. The sizing of these devices must be calculated to cover the 80-90% of the annual heating load in cold zones as trying to cover the total demand will require oversized systems [15].

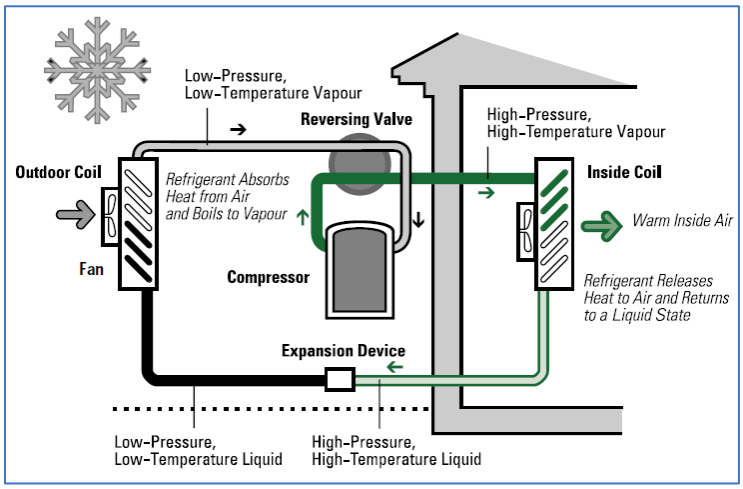

Figure 2-5: Heating cycle of ASHP, [15]

On the other hand, GSHP uses the ground soil or ground water as the thermal source, and as in the first case, a secondary source will be used for satisfying the heat demand of the household. These devices require an earth connection to transfer heat into or out of the ground or the water source, and it takes the form of an outdoor heat exchanger as a coil or a pipe which carries a heat transfer fluid depending on the sink type [18]. Compared to ASHP, it presents some limitations respect to the availability of the heat source, especially when water is the thermal source as aquifers, lakes or rivers are not always accessible. Furthermore, site specific parameters influence the performance of these devices such as soil properties, available space for the ground heat exchanger, and presence of other ground neighbor systems.

Knowing the soil properties in advance is critical for determining the suitability of the place as heat source, for carrying out prior studies are mandatory to ensure a high-performance operation [19]. These studies together with drilling operations and other processes to conditioning the ground make GSHP expensive in terms of capital costs, but the operational costs are low as they are durable and require little maintenance [20]. Nevertheless, water sources, soil and geological formations have the advantage of having a higher thermal capacity as its temperature

varies less than air's. Consequently, its temperature will be closer to room temperature, and the thermal difference between the source and the building's interior will be smaller, for its efficiency will be enhanced by displaying a higher COP compared to ASHP. This makes GSHP attractive for the market as one of the most efficient, comfortable and quiet heating technologies available today [17].

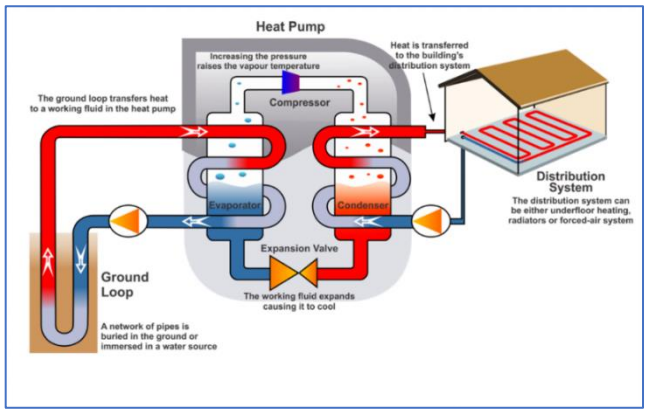

Figure 2-6: Heating cycle of a GSHP, [21]

Considering the features, advantages and disadvantages that both heat pump systems show, ASHP has been selected as the study object of this research because its availability in the market has proliferated widely, it does not require prior suitability studies or space conditioning for its installation and operation, and its investment cost will be lower compared to GSHP.

2.3. Integration of HP and TES for demand response

In this section, the integration of heat pumps as part of demand response programs in smart grids will be introduced and explained. First, a short explanation of what a smart grid means, then, how heat pumps in a smart grid provide demand response potential, and finally, applications of heat pumps in demand response programs.

2.3.1. Smart grid (SG)

In the energy power system field, the concept of smart grids has emerged as a solution to the problem of matching variable electricity generation with demand without altering the comfort of end consumers and keeping benefits for producers. There is no exact definition of a smart grid, but it is described as an electric grid capable of delivering electricity in a controlled and smart way from producers to consumers who can modify their consumption behavior based on signals, incentives and information [14]. It is relevant to notice that this definition includes the idea of flexibility on the demand side only in terms of electricity consumption, and it does not mention any other type of energy such as heat. Therefore, it is necessary to couple the approach of the electric smart grid concept and demand flexibility with the residential heating sector, and heat pumps are the ideal devices to link both terms. In this context, heat pumps are the part of the demand side that can be managed in a smart grid to satisfy the heat load of the residential sector.

2.3.2. Heat pump's flexibility potential limitations

Many factors determine the flexibility potential of heat pumps to balance fluctuations in the power grid. There are 5 considerations which widely influences the flexibility potential of heat pumps systems: thermal demand, heat pump capacity and properties, storage type and size, system's dynamic properties, and flexibility requirements from the power system [14]. The thermal demand and the heat profile of the building determines the amount of energy that can be shifted over time, but the amount of energy that can be shifted cannot be higher than the demand during the day. Additionally, the total heat demand must include surface heating (SH) and domestic hot water (DHW), and this will vary depending on the number of people, building type (i.e. materials, configuration) and location. The heat pump capacity imposes limitations to the flexibility in operation by constraining the increase or decrease of the electricity consumption by switching it on or off, and by its ramping rate [22]. The difference between the real

heat demand and the heat produced by the heat pump at a specific time will determine the energy content and dynamic behavior of both the heat pump and the storage system simultaneously. The heat pump capacity, expressed in BTU/h, is defined as the amount of heat that a heat pump can extract from cold air at a determined outdoor temperature and effectively inject it into a system. Thus, the heat pump capacity is seen as the amount of thermal energy that the heat pump can supply per unit of time. Under this consideration, if the heat pump capacity is greater than the heat demand, two flexibility options are present: the heat pump can ramp up its power consumption to increase its heat output and charge the storage system, or it can be ramped down and discharge the storage system. The choice between these flexibility options will be limited by the energy content of the storage system. Contrary, if the heat pump capacity is smaller than the actual demand, the only flexibility option is to ramp the HP down and discharge the storage system if there is energy available in there.[14].

$$if: HP_{capacity} > Demand_{building}^{heat} \therefore P_{HP}\ ramped\ up \rightarrow charge\ storage\ tank \quad 2\text{-}1$$

$$if: HP_{capacity} > Demand_{building}^{heat} \therefore P_{HP}\ ramped\ down \rightarrow discharge\ storage\ tank \quad 2\text{-}2$$

$$if: HP_{capacity} < Demand_{building}^{heat} \therefore P_{HP}\ ramped\ down \rightarrow discharge\ storage\ tank \quad 2\text{-}3$$

Water storage tanks (WST) are the main used thermal storage technology when heating distribution system uses water as it can be easily stored and used for later purposes, for the heat supply to the building can be shifted for a certain period [23]. The storage system's energy capacity will restrict the flexibility potential depending on the amount of energy that needs to be shifted, and the maximum allowed temperature that the heat pump can produce as this will limit the temperature that the storage tank will reach. Furthermore, the decrease of the ambient temperature causes the storage heat capacity to reduce significantly as the heat produced by the heat pump is also a function of the ambient temperature, for the minimum required temperature in the storage tank will increase in order to keep the thermal comfort [24].

The maximum temperature that a HP can produce is determined according to the standard EN 14511:2018: "*Air conditioners, liquid chilling packages and heat pumps for space heating and cooling and process chillers, with electrically driven compressors"*. Here, it is stablished that the minimum and maximum water's temperature a HP can produce must be measured considering the dry bulb (DB) and wet bulb (WB) temperatures of the outside air.

The amount of energy that can be shifted with storage tanks depends on the thermal demand profile, and the load profile that the heat pump must balance, and the charging and discharging frequencies. High frequency charge/discharge cycles allow a great amount of energy to be shifted and a relatively small storage size will be needed. Infrequent charging and discharging of storage involve a higher tank capacity as the energy stored for a longer time will be higher than in the case of high frequency [22]. The dynamic properties of the heat pump reduce its flexibility potential due to mechanical constraints that must be considered to keep the operating life cycle of the device. Minimum run and pause-time requirements, avoiding frequent switching on/off, ramping speed response of the compressor, and power consumption over time are some of the restrictive parameters that limit the flexibility potential [14].

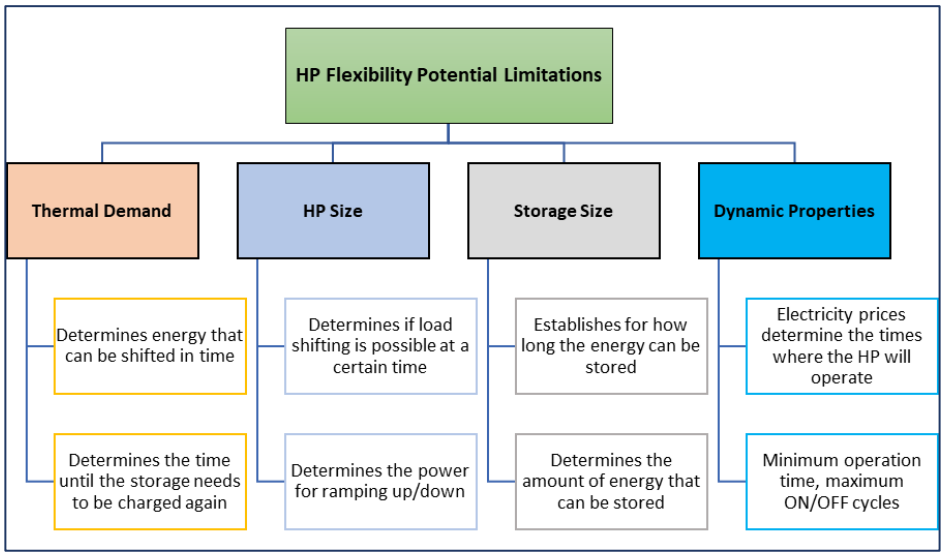

Figure 2-7: Factors influencing the flexibility potential of heat pumps

2.3.3. Demand response potential modelling overview of HP and TES

Extensive research has been performed to approach the problem of demand response programs with heat pumps and try to find an optimal alignment that buffers the variability nature of renewable energy systems while maintaining the grid within the operational technical requirements. Heat pumps alone might not achieve significant energy savings in households; hence, they need to be paired with distributed energy resources (DERs) such as PV or wind, and electric storage components such as batteries or vehicles-to-grid (V2G) technologies to enlarge the flexibility potential of the entire system [25]. The objective with this energy-mixed system is to create cost-effective electricity billing and positive-energy buildings, for the successful implementation of these systems relies on performing an optimal configuration and control.

Many mathematical models have been developed to represent future all-electric systems, structures whose components run mainly on electricity, and its optimization has been attempted using a wide range of techniques and algorithms. A common target on the optimization of energy systems is the minimization of operational costs and the maximization of renewable electricity self-consumption to motivate end-consumers to participate in demand response programs and save money by being self-sufficient. In the following paragraphs a brief description of this is presented.

- In Sichilalu, Mathaba & Xia (2017) an optimal control of a hybrid wind-PV system with heat pump and water storage systems is presented. Here, the authors developed a mathematical model to minimize the grid energy cost considering the time-of-use electricity tariff (TOU) to satisfy the thermal demand using an air-water heat pump (AWHP) and a water storage tank (WST). The novelty of this model is the prediction of the optimal water temperature that the heat pump must reach based on the known hot water demand and without requiring to reach the temperature set-point. The system has been modeled as a mixed integer linear programing problem (MILP) with a time horizon of 24 h. By using a switching strategy, the power supply to the heat pump is controlled while the excess renewable power is injected to the grid, and the dynamics of the hot water temperature inside the water tank is modelled as a linear function and discretized in time. As results, the authors state that 51.23% of energy saving can be achieved, the payback period is 3 years, and energy trade-off can be performed optimally.

- Steen, Stadler [26] proposes a MILP model for the design of thermal storage systems (TES) to determine the feasibility of investing in TES in combination with DER. The model describes a linearization of the TES with calculation of thermal losses based on the energy contained in the storage tank and allows the use of heat pumps only for low temperature storage charging. Besides, the storage system has been considered as a stratified tank with two well differentiate zones assuming mixing does not occur. The objective function

is to minimize the total energy cost which includes the different energy sources (PV, gas, etc.) costs, the amortized capital cost of DER equipment, cost of storage system, and revenues from energy sales to the grid. The model was tested using residential data for San Francisco and San Diego cities, and the authors have stated that the implementation of heat pumps is possible, and the TES investments are favorable.

- Wind integration using heat pumps and different storage options has been analyzed by Hedegaard, Mathiesen [27]. In this research, heat accumulation tanks and passive heat storage are investigated as storage options in terms of their ability to increase wind power use while providing cost-effective fuel savings. The model has been applied to the Danish construction sector with 50% wind power share. The authors present a model to determine the flexibility potential of both storage options and heat pumps applying an hourly time resolution and covering a whole year. GSHP and ASHP have been considered in combination with a WST and a small buffer tank connected to the main central heating system of the building. The buffer tank is aimed to minimize the heat pumps start-up cycles, but it does not enable shifting operation from one hour to the other.

- Terlouw, AlSkaif [28] have proposed an optimal demand response model for all-electric residential systems with heat and electricity storage through a battery and an electric vehicle. This model includes surface heating (SH) and domestic hot water (DHW) provision through an ASHP capable of providing both SH and DHW simultaneously. One novelty of this research compared to the others is the COP has been modeled as a function of the thermal difference between the outside temperature and the supply temperature. Hence, the COP will vary depending on the operating mode of the HP when it is used for SH or DHW. ASHP sizing is done to supply the annual peak of heat demand of the household respect to the minimum CoP, that is calculated based on the minimum temperature requirements of the system, and the HP can operate using the electricity provided by PV, a battery or the grid. The WST is a stratified tank, and its sizing has been modeled in terms of volume and the number of inhabitants while its storage capacity depends on the minimum and maximum temperatures limits for SH and DHW.

- In Wolf [29] a model-based assessment of heat pump flexibility was performed by simulating a pool of heat pumps and creating different thermal load profiles for space heating and domestic hot water. The author states that two different heat pumps, a back-up electric heater, and a DWH storage tank have been used to model the entire system. The heat pumps are an ASHP and GSHP which have been modeled based on regressions of manufacturer data, and the DHW tank was modelled using energy balances. For flexibility assessment, building/heat-pump pool relation is defined, and five external signals were selected to cause a load demand response of the heat-pump pool. The heat pump system was modelled considering first only one heat pump, and then a combination of heat pump with a back-up heater, while the storage system is composed by two separated tanks for SH and DHW to avoid the use of stratified tanks. As results, the author concludes that a high active operation of the heat pump pool provokes high electric load shifting by switching on at mid-day time due to a super-heat signal. In an off signal, 15% of the load cannot be shifted due to the restriction of minimum running time. An economic assessment of the system is not presented to evaluate the feasibility of the model.

- Hedegaard and Balyk [30] established a model to determine the effects on investment of energy systems incorporating heat pumps with thermal storage in buildings and buffer tanks in a Danish case. This model analyzes individual heat pumps and storage systems to optimize investments and operation, and it incorporates the thermal building dynamics and covers the use of passive heat storage by using the thermal inertia of the building, active heat storage by heating floor systems, and storage tanks for space heating and domestic hot water. The objective function is to minimize the total system costs that includes the investment cost of the storage tank, cost of passive storage in the building, but it does not include the investment cost of the heat pump. As results, the authors have concluded that without investment on heat storage capacity, heat pumps cannot operate flexibly, and they are restricted to cover the net heat demand in each hour.

3. System Description and Modelling

This chapter describes the structure of the integrated energy system to be studied, and the modeling for the thermal components. Section 3.1 includes a brief description of the elements conforming the physical system and which of them are relevant for the purpose of this thesis. The general model will be described considering the main features and statements for each part of the system in section 3.2. Finally, the definition of variables, energy streams and required input data for the thermal components will be determined in section 3.3 through a flow diagram and the derivation of the thermal model.

3.1. Components of the general system

The integrated energy system shown in Figure 3-1 is composed by solar panels (PV), a battery energy storage system (BES), and electric vehicle (EV-V2G) connected to the DC side of a multi-port power converter (MPPC). On the AC side, a heat pump (HP) is connected for building heating/cooling, and at the same time, the heat pump is coupled to a thermal energy storage tank (TES) to provide extra flexibility to the system, satisfy the thermal demand of the building, and reduce the electricity consumption of the heat pump. Additionally, a smart grid operator (SGO) is considered to provide the purchasing and selling electricity price signals under which the system will act as part of the demand respond program. The PV, BES, and EV components have been already modeled by Msc. Wiljan Vermeer and Dr. Gautham Mouli, and they will be integrated into the developed HP-TES model to perform the optimization of the entire system.

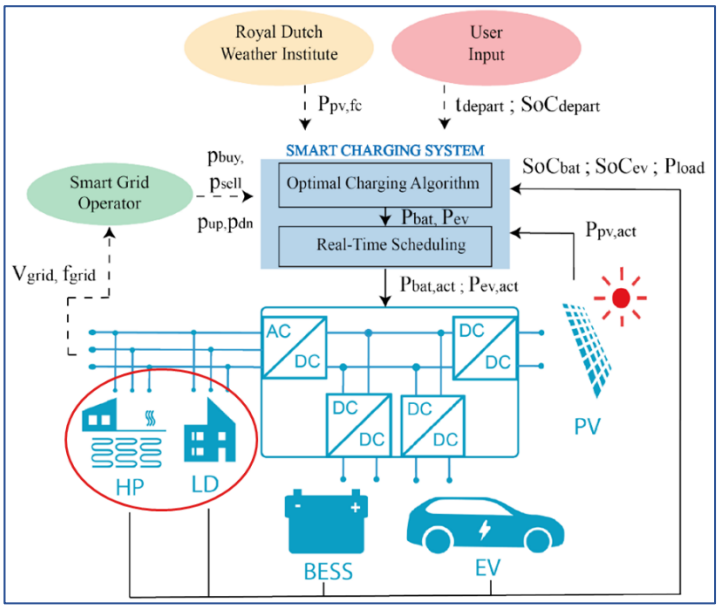

Figure 3-1: Schematic diagram of the general system (Wiljan Vermeer, TU Delft)

In chapter 2, it was shown that ground source and air source heat pumps are the most common types within the market for heating/cooling building applications. Air source heat pumps (ASHP) are the most studied and used due to their relative low costs and good performance, for this thesis will consider only this type to perform the heating of the building, although the model can also be adapted to use ground source heat pumps (GSHP).

The function of the HP is to supply heat to the TES tank where the temperature must be maintained between maximum and minimum limits to allow the thermal tank to satisfy the heat demand of the building. The amount of heat supplied to the tank depends on the desired temperature and the temperature of the source, which in this case is the outside air. Based on the literature review, current heat pumps can adjust their capacity by controlling the frequency of the compressor such that they can operate in different modes depending on the type of application (surface heating or domestic hot water) [31]. In this thesis, it has been assumed that the ASHP can work under these

considerations, but no controller or model has been developed to express the relation between pump's capacity and compressor's frequency. The thermal storage tanks (TES) are responsible for decoupling the electricity consumption of the heat pump from the heating demand of the building as they act as a buffer and provide thermal inertia for demand response applications, for the water tanks will be heated up to satisfy both surface heating (SH) and domestic hot water (DHW) demands.

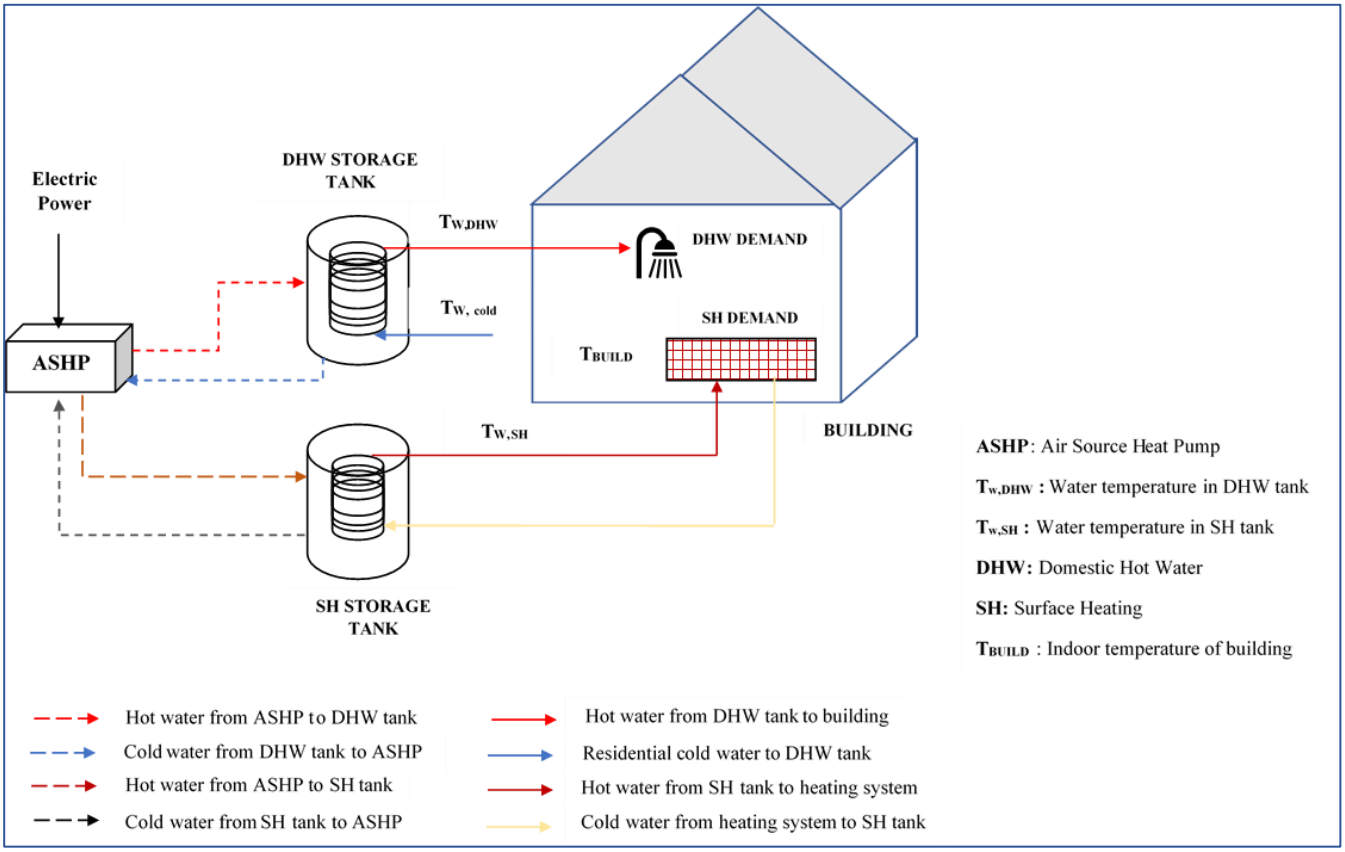

Figure 3-2: Basic schematic diagram of the thermal components

In addition, the model incorporates degradation costs of EV and BES due to their charging/discharging cycles to provide a more realistic approach. The BES and EV have a bidirectional operation, meaning that they can absorb and inject energy to the grid if it is needed, providing in this way ancillary services to maintain the stability of the grid. Furthermore, based on the solar irradiation received, it is expected that the PV panels will generate as much power as possible to feed the entire system and reduce the power intake from the grid, and if any excess is present, it will be injected to the grid.

For this project, the HP-TES model was developed and tested to find if the formulation of the problem would lead to logical results and if it could be effectively used. To solve the model, a sub-optimization problem was formulated in GAMS having as objective function the minimization of the power intake from the grid while meeting the heating demand of building. After analyzing the results, it was incorporated to the PV-BES-EV model to optimize the entire system. This approach is depicted in Figure 3-3.The model considers energy balances in all the components (thermal and electric balances) that describe the production and consumption of power during the operation of the system.

To determine the temperature of the water in the tanks, the temperature of the building, and the power consumption of the heat pump, time-dependent energy balances have been performed. In this way, the HP's power consumption is related to the amount of heat supplied to the thermal tank and the thermal demand of the building . The model also must maintain the water temperature within the desired limits to ensure its effectiveness on keeping the thermal comfort inside the household.

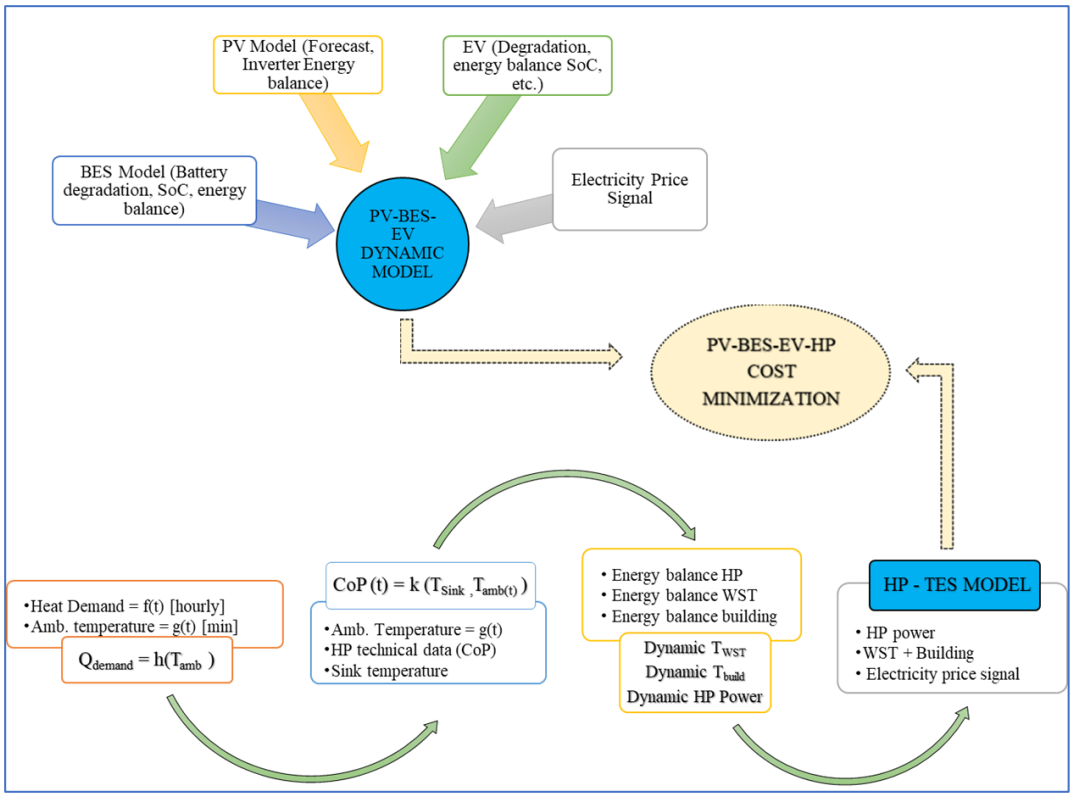

Figure 3-3: General optimization model scheme for PV-BES-EV-HP-TES system

3.2. HP-TES model formulation

This section describes the formulation of the HP-TES system as a sub-optimization problem of the general model. Some key features and relevant assumptions have been made to simplify the problem. The modeling of the heat balances and heat transfer are based on physical laws, and the results were obtained by applying a numerical method.

3.2.1. Model considerations and assumptions

As showed in Figure 3-2, the heating system is constituted by an air source heat pump (ASHP), two storage tanks (TES) for SH and DHW, and a household. The HP will supply heat for SH and DHW individually to the water tanks to meet the total heating demand of the household. The main state variables will be the water temperature of the SH and DHW tanks (T_{SH}, T_{DHW}), and the temperature of the air inside the building (T_{BUILD}) that must be maintained within desired limits. The power consumption of the HP will depend if it is providing heat for the SH tank or the DHW tank. Additionally, the following assumptions have been considered while modeling the system:

- The heat pump is a variable speed pump capable of changing its power consumption by changing the speed of the compressor. This means the heat pump can modulate its power output based on the requirement of the system and its nominal capacity.
- Surface heating (SH) and domestic hot water (DHW) demands will be satisfied by using the storage water inside the tanks for each purpose. The energy content of each tank is subject to boundary constraints in terms of a maximum and minimum acceptable temperature.
- The discharging process of the tanks is done indirectly through coils located within the tanks. The temperature variation along the tanks has been considered homogeneous by assuming perfectly mixed tanks.
- The charging process occurs directly, so the heat pump will extract the water from each tank, it will heat it up, and it will return it to the tank, so the net mass change in the system is zero.

- Subsystems like water pumps, valves, and smart controllers have not been considered here as this is out of scope of the research.
- The building has been considered as a single zone whose state is represented by a single temperature corresponding to the air's temperature inside the household.
- The storage tanks are located inside the building, so their heat losses correspond to the temperature difference between the room's temperature and the water temperature in the tanks.
- Heat losses of the building include convection , conduction, and natural ventilation. These losses depend on the design of the building.
- Heat gains due to the presence of people, electric appliances, and solar irradiation have not been considered.
- The model of the HP-TES is focused mainly on providing heat for cold seasons (winter), and cooling has not been included for summer. Cooling demand data for the Netherlands is not available as the residential sector barely consumes energy for this purpose. However, the model could incorporate cooling of the building if data were available. For this, a $COP_{cooling}$ model is additionally presented in section 3.3.4. For summer, the heat pump will be mainly used to meet the DHW demand, and if possible, to store any excess of PV energy.

Based on these considerations, the modeling of the HP-TES system is presented in the following subsections.

3.2.2. Data acquisition and treatment

Residential demand profiles and ambient temperature profile are required to determine how the system must operate to satisfy these energy requirements, and how much heat loss the building will face. For this specific problem, a typical Dutch house in the city of Delft has been selected. The demands for surface heating (SH) and domestic hot water (DHW) have been obtained from the Applied Natural Science Research (TNO) organization and [32] respectively as seen in Figure 3-4. The data set provided by TNO corresponds to a study case for year 1987 where the most extreme winter was registered.

In this study, TNO intended to assess the effect of different heating devices such as air source heat pumps (ASHP), and water source heat pumps (GSHP) on the electric grid. Based on this study, different electricity demands from the heating devices were available, so it was necessary to express this electricity demand into heating demand to be used in the optimization problem. Unfortunately, there was not available technical data of the heat pumps used by TNO, consequently, the COP was estimated using technical data provided by LG as shown in section 3.3.4. To do this, it was assumed that the HP provided heat directly to the building without using a buffer storage tank. Furthermore, it was considered that the HP provided a minimum water temperature of 35 ˚C by using the outside air as heat source, and the building temperature was set to 20˚C as recommended by [33].

In this way, the COP could be estimated for each hour of the year to obtain an hourly heat demand profile of the building. The type of building in this study was a terraced house with a medium insulation level, and it was identified as a B-level energy performance building according to [34]. Figure 3-4 shows the generated heating demand profile and the temperature profile during this worst-case weather scenario from TNO.

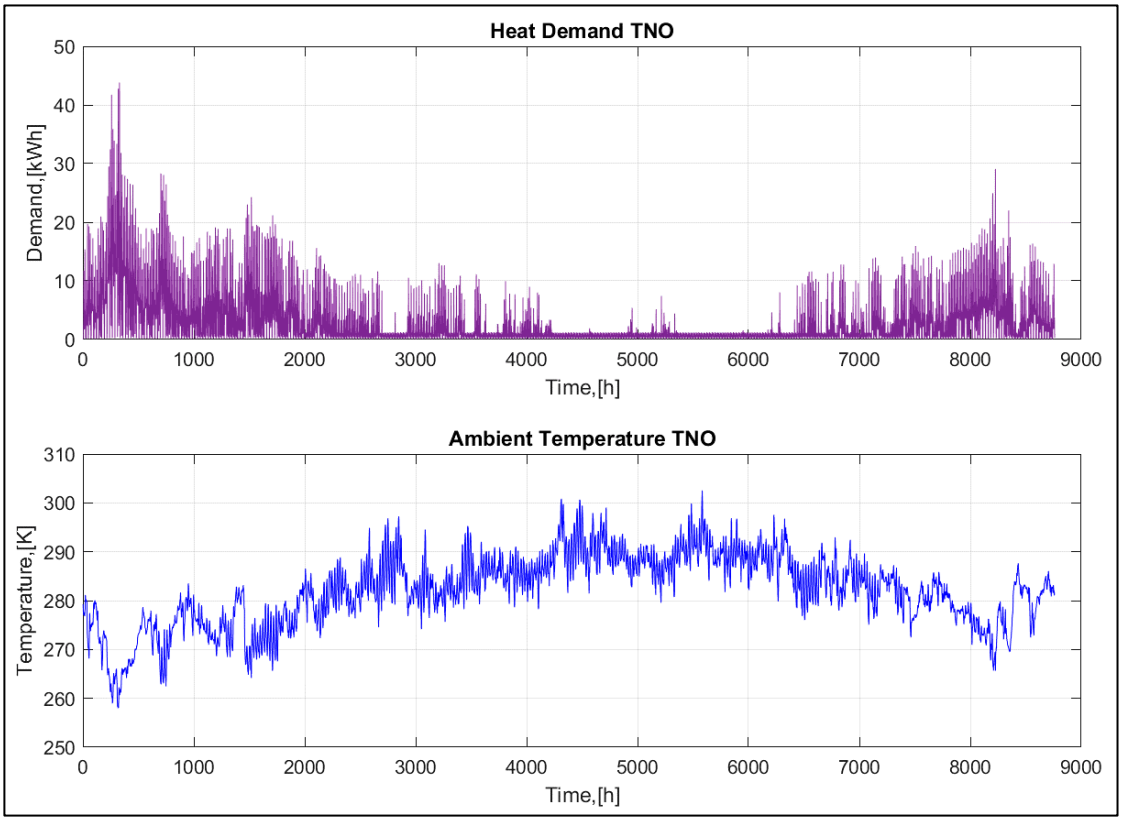

Figure 3-4: Hourly heat demand ASHP and ambient temperature TNO study case for year 1987

Having both temporal series is extremely useful as the heating demand can be mathematically correlated with the ambient temperature, for the heat demand can be interpolated for any ambient temperature. It is important to recognize that the heat demand is not only a function of the ambient temperature as there might be other weather variables that can influence this demand such as the wind speed or the incident solar irradiation on the building, however, in terms of heat transfer principles, the temperature difference between the inside of the building and the ambient temperature rules the heat demand for comfort space. Considering this, both temporal series were used to establish a mathematical correlation between these two variables. This must be done because both data series have an hourly resolution, but the optimization problem required heat demand data to be in a 15 minute-resolution, so a temporal interpolation of the data must be performed to obtain the data at the desired resolution.

First, the heat demand was plotted against the ambient temperature to infer what type of correlation might exist, and this is presented in Figure 3-5. As expected, the heat demand decreases with the increase of the ambient temperature, showing an exponential relationship among them. From this plot, it can be seen how the heat demand relates to the ambient temperature, and how the data distributes based on probability of occurrence. Throughout this analysis, atypical data can be identified and omitted to have a more precise regression model.

In figure 3-5a, it is perceptible that a high percentage of the data is strongly grouped in a specific range of temperature values. This means that the probability of occurrence of these demands is higher than the rest, while the others can be considered as atypical. For instance, heat demands between 30 and 45 kW are rare to happen, while heat demands between 0 and 10 kW have high occurrence frequency, so most of the heating demand data will be grouped within this range. To determine which group of data can be selected with a high confidence interval, a data distribution analysis is performed using percentiles to realize how the data will allocate and if they can be used to assert the mathematical regression model.

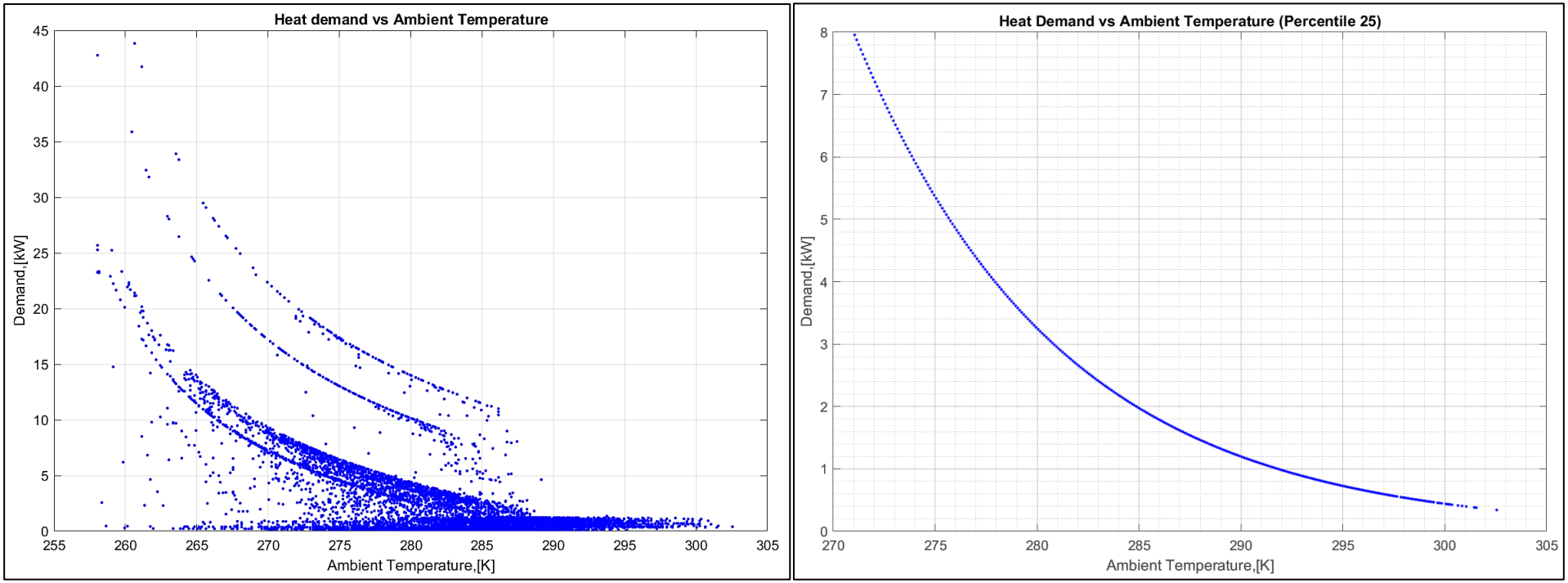

a) *b)*

Figure 3-5: Relation Heat demand and ambient temperature for study case: a) Data Distribution; b) Fitting correlation for Percentile 25

From this analysis, it was found that the percentiles 25 (P25) and 35 (P35) have the best fitting correlations. For this project, the percentile 25 correlation has been used to interpolate the heat demand data considering Delft's average ambient temperature data. Figure 3-5b displays the fitting between the heat demand and the ambient temperature for percentile 25. The percentile 25 indicates that only 25% of the heating data are higher than the weighted mean, while 75% of the data are below or equal to the weighted mean. Based on this, the mathematical correlation between the heating demand and the ambient temperature is:

$$\dot{Q}_{demand,SH} = 4.588 * 10^{12}\, e^{-0.09991 * T_{amb}} \qquad 3\text{-}1$$

This equation can be used to determine the heat demand rate in kW for any ambient temperature in the range of 258 to 303 K. For a specific time resolution, the independent term must be divided by a factor that characterizes that time resolution, for in this case the time resolution needed is 15 minutes, the dividing factor must be 4 (there are 4 groups of 15 minutes in one hour), and the ambient temperature data needs to be in 15 minute-time resolution. It is important to notice that this equation represents a mathematical model for the demand of an specific type of house, therefore it cannot be considered as a general model (first-principles model) but an empirical model as it comes from measured data. However, the principle can be applied for any other available data for different types of households.

On the other hand, domestic hot water (DHW) demand data have been obtained from [32] where various demand profiles have been developed to study DHW solar systems in Quebec, Canada by measuring the water consumption in 73 houses with a time resolution of 5 min. The consumption patterns were created considering 3 different types of consumers: sparing consumers, who consume DHW in the mornings, average consumers who tend to use DHW in the evenings, and dispersed consumers whose demand is dispersed during the day. For this thesis, the average consumer's profile has been selected as shown in Figure 3-6 where the hourly DHW for one year is depicted. This profile has been selected considering that this demand depends on the behavior of the house's inhabitants, and that the water heating process will be done electrically by means of a heat pump, and to minimize costs, it is preferred that the heat pump operates at times where the electricity price is low, which generally occurs at night time. However, a different type of profile can be used too as the model will adapt to these demands and will look for the optimal operation strategy for the heat pump.

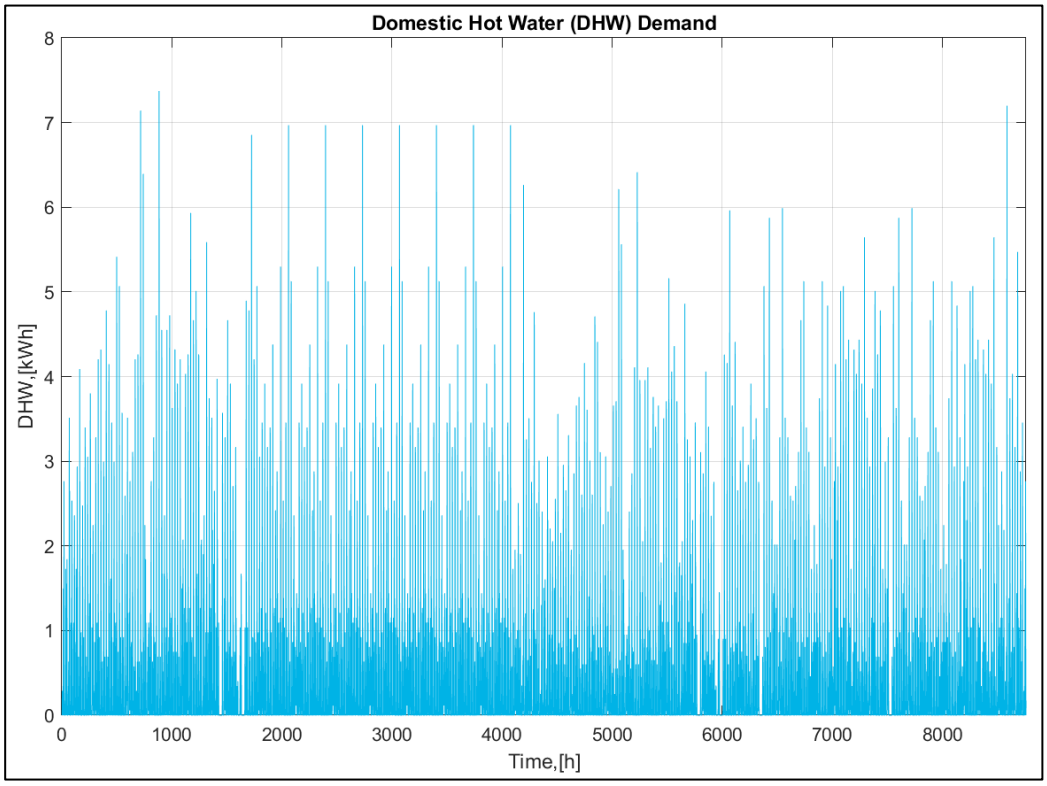

Figure 3-6: Hourly DHW demand profile for an average consumer

3.2.3. Heat pump performance

To achieve a minimal energy consumption, the heat pump must exhibit an adequate performance in transforming the electric power into useful heat. This performance or "efficiency" is called coefficient of performance (COP), and it is defined as the ratio of the heat produced by the heat pump to the total work done. The total work developed by the heat pump is equal to the electric power consumption of the compressor, so the COP can be expressed mathematically as:

$$COP = \frac{\dot{Q}_{HP}}{P_{el}}$$

Where $\dot{Q}_{HP}$ represents the heat produced by the HP during a heating process, and P_{el} represent the electricity power consumption of the HP. Thermodynamically, the coefficient of performance is determined by the thermal difference between two defined reservoirs, and independently on the process the heat pump is performing heating or cooling, these reservoirs are known as the sink and source. The sink corresponds to the place where heat is transferred to,

while the source is the place where heat is extracted from as it can be seen in Figure 3-8. Both reservoirs are characterized by a defined temperature, for it can be inferred that the COP is a function of the temperature of the reservoirs. Therefore, the COP also can be expressed in terms of these temperatures applying the second law of thermodynamics. Recognizing that the heat transferred to the hot reservoir is equal to the performed work plus the heat extracted from the cold reservoir, the COP can be expressed as stated in equation 3-8.

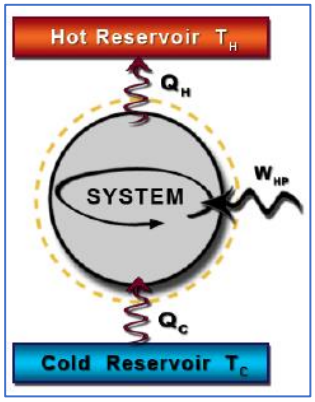

Figure 3-7: Heat pump simplified thermodynamic cycle [31]

$$\boldsymbol{COP} = \frac{\dot{Q}_{hot,r}}{\dot{Q}_{hot,r} - \dot{Q}_{cold,r}} = \frac{T_H}{T_H - T_{cold}} \qquad 3\text{-}2$$

Where $\dot{Q}_{hot,r}$ is the heat flux injected in the hot reservoir, $\dot{Q}_{cold,r}$ is the heat flux extracted from the cold reservoir. Thus, T_H and T_{cold} are the temperatures of the hot and cold reservoirs, respectively. This simple relation has been considered for this thesis. By using technical data provided by the company LG for one of their HP models, a fitting analysis to express the COP as a function of the temperature difference between both reservoirs has been performed. Since an ASHP has been selected, the heat source corresponds to the outside air characterized by the variable $T_{amb,}$ which is the outdoor ambient temperature, while the sinks are the storage tanks for SH and DHW. Figure 3-8 displays the COP of the HP versus the outdoor temperature for various produced water temperatures T_w for heating mode, while Figure 3-9 shows the COP of the HP versus the outdoor temperature for cooling mode. The variable T_w corresponds to the temperature the water in the storage tanks can reach based on the HP operation.

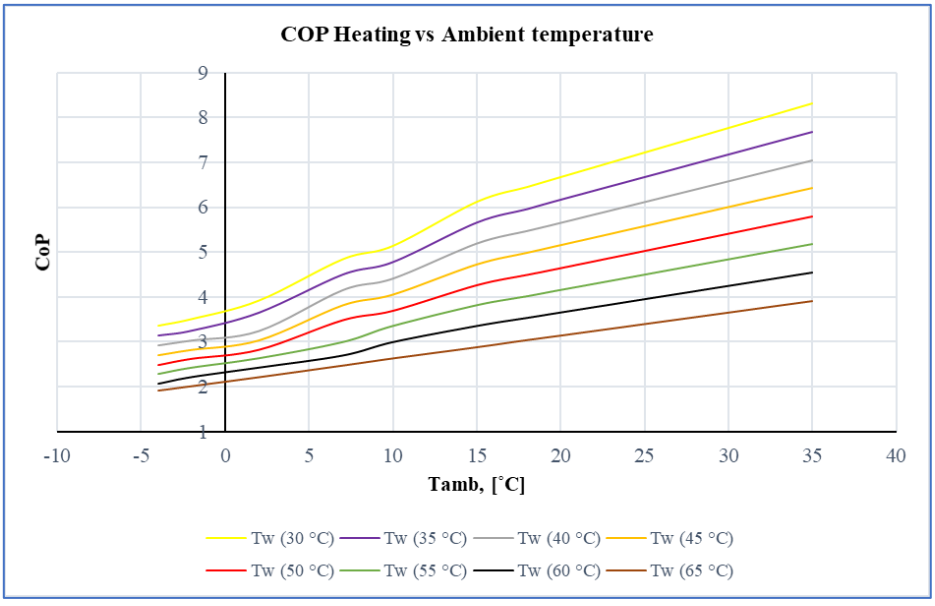

Figure 3-8: COP heating vs ambient temperature for various supply temperatures

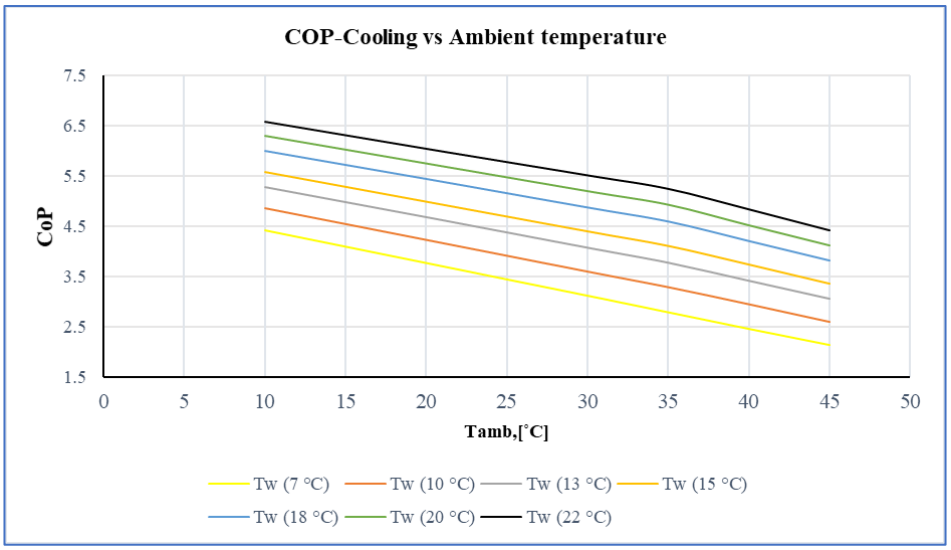

Figure 3-9: COP cooling vs ambient temperature for various supply temperatures

In this way, the mathematical correlation of the COP and reservoirs' temperatures has been performed. It is important to mention the COP for cooling has also been calculated in case future works include cooling demands during summer. As it can be seen in both figures, the higher the difference between the water temperature T_w and ambient temperatures, the lower the COP, which means the heat pump needs to perform more work to extract heat from colder air in heating mode, or to inject heat to the outside air in cooling mode. Therefore, the efficiency of the heat pump is limited by the weather conditions and the desired production temperature, so the ideal performance is to work with a low thermal difference between both reservoirs in order to maximize the heat production and reduce the energy consumption. Because the heat pump's COP decreases when the temperature difference between the reservoirs increases, it is vital to express this relationship in mathematical terms such that the COP can be determined. Through a least square approach from the technical data for the HP model of LG company plotted in Figures 3-8 and 3-9, the relationship between the COP and the temperature difference between the water temperature T_w and the outside ambient temperature T_{amb} has been determined for both heating and cooling modes as it can be seen in Figures 3-10 and 3-11 respectively.

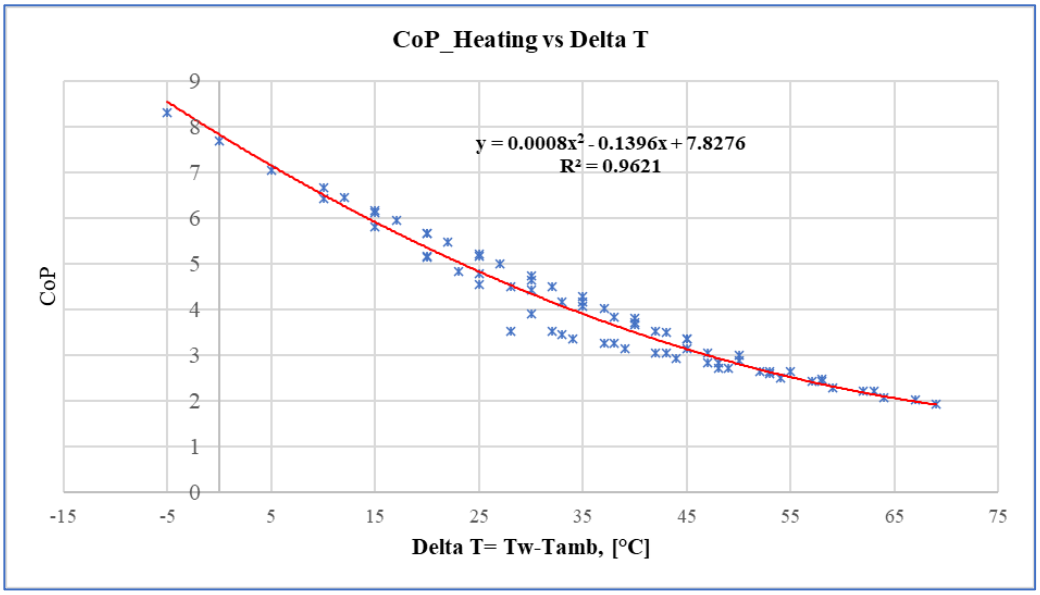

Figure 3-10: COP heating vs temperature difference (T_{sup} -T_{amb})

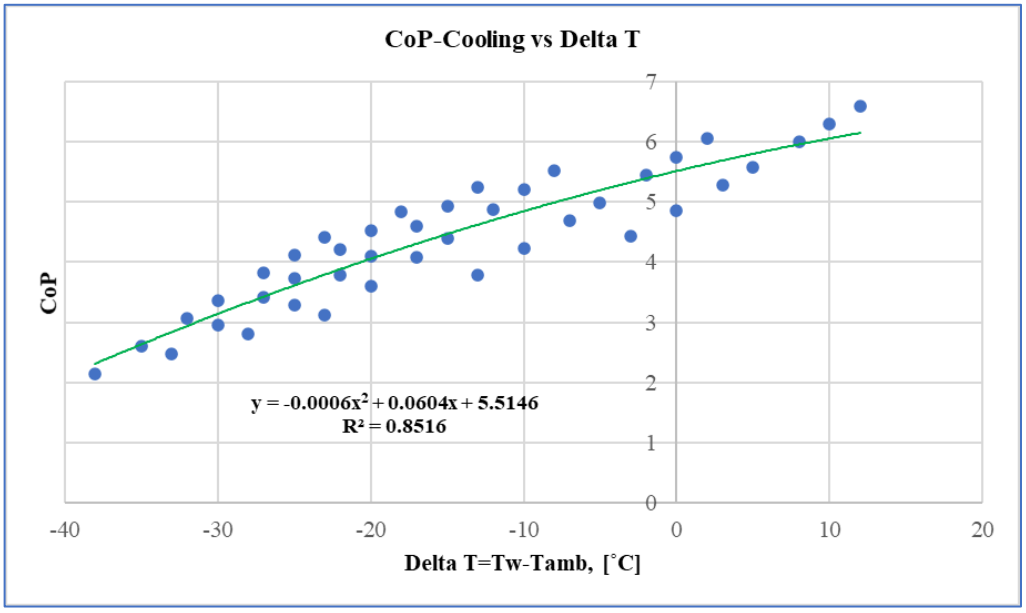

Figure 3-11: COP cooling vs temperature difference (T_{sup} -T_{amb})

The COP exhibited a quadratic behavior versus the temperature difference between the reservoirs according to the following equations:

$$\boldsymbol{COP_{heating}} = a_0 - a_1\,(T_w - T_{amb}) + a_3(T_w - T_{amb})^2 \qquad 3\text{-}3$$

$$\boldsymbol{COP_{cooling}} = a_{0c} + a_{1c}\,(T_w - T_{amb}) - a_{3c}\,(T_w - T_{amb})^2 \qquad 3\text{-}4$$

where $COP_{heating}$ and $COP_{cooling}$ are the coefficient of performance for heating and cooling respectively, T_w is the temperature at which the water has been heated, and T_{amb} corresponds to the outside ambient temperature. The coefficients of both equations are presented in table 3-3. It can be seen that the COP for heating is higher than for cooling as it is more difficult to cool down an environment that heat it up, for in cooling mode the heat pump will consume more power depending on the cooling demand of the building. Both equations have been used in the optimization model where T_{sup} is replaced by the time dependent temperatures of the storage tanks depending on the operation mode as mentioned before.

Table 3-1: COP model regression coefficients

Coefficient	Value	Unit
a_0	7.8276	-----
a_1	0.1396	K^{-1}
a_2	0.0008	K^{-2}
a_{0c}	5.5146	----
a_{1c}	0.0604	K^{-1}
a_{2c}	-0.0006	K^{-2}

3.2.4. Thermal energy balance modeling

The assumptions made in section 3.2.1 allow us to perform energy balances for each one of the components of the thermal system. It is necessary to identify inputs, outputs, state conditions, variables, and energy flows by means of a flow diagram to express the relationships in the system as it can be seen in Figure 3-12.

Applying the general energy balance equation to the tanks, and building, continuous-time equations can be obtained. The fundamental laws of physics states that energy cannot be created nor destroyed, but only transformed, thus energy is always conserved. This means that if the energy content of a system changes, this change must be result of an external process by which the system has received or has given energy. In this way, the change of energy of the system can be tracked by looking at the amount of energy that is entering the system, leaving the system, or generated and consumed inside the system due to chemical reactions. This tracking process is known as an energy balance, and it can be expressed in the following form:

$$\frac{\boldsymbol{Change\ in\ energy}}{\boldsymbol{unit\ of\ time}} = Energy\ flux\ in - Energy\ flux\ out + Generation - Consumption$$

In a differential form, the above expression can be written as:

$$\frac{\boldsymbol{dQ}}{\boldsymbol{dt}} = \dot{Q}_{in} - \dot{Q}_{out} + \dot{Q}_{Generation} - \dot{Q}_{consumption} \qquad 3\text{-}5$$

Where $\frac{dQ}{dt}$ represents the change of energy in the system per unit time, $\dot{Q}_{in}$ and $\dot{Q}_{out}$ are the energy fluxes incoming and leaving the system, respectively, $\dot{Q}_{Generation}$ and $\dot{Q}_{consumption}$ are the energy fluxes generated or consumed by the system due to chemical reactions. Therefore, equation 3-5 expresses the general energy balance for any thermal system. The units for the energy fluxes and the change in energy respect to time are expressed in Watts (W). For the present system, the terms generation and consumption will not be considered because no chemical reactions are involved.

As mentioned in section 3-1, the energy balance will be performed in differential form because the process is continuous, for all the terms in the balance equation correspond to rate terms so that the balance describes the behavior of the system in an instant of time, having in this way ordinary differential equations. The approximation of the differential equations was accomplished by applying the forward finite difference method (FFD) to obtain the numerical solution as this is a problem with boundary values.

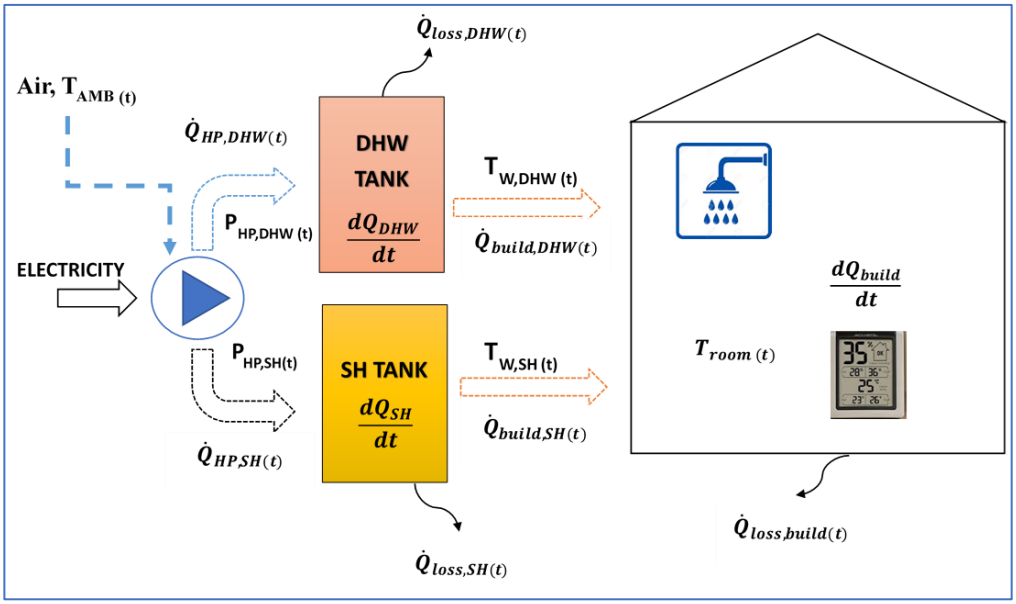

Figure 3-12: Flow diagram of thermal system

The variables showed in Figure 3-12 represent the state variables of the system. Their time evolution will give an indirect measure of the rate of change in the energy content of each component. The meaning of these variables is

explained in table 3-2. On the other hand, the electric energy consumed by the HP for SH or DHW is totally converted into heat by neglecting mechanical losses. Figure 3-12 can be interpreted as follows: the HP will provide either a heat flux for SH ($\dot{Q}_{HP,SH(t)}$ or DHW ($\dot{Q}_{HP,DHW(t)}$ to charge the storage tanks respectively. Depending on the demands of the building $\dot{Q}_{build,SH(t)}$ and $\dot{Q}_{buiild\ ,DHW(t)}$, these heat fluxes will be extracted from the storage tanks, thus the temperature inside the tanks will decay in time due to these demands and heat losses . Once these temperatures reach specified lower limits, the system will determine the best moments to turn ON the HP and charge the tanks to an optimal temperature within specified upper and lower boundaries. These optimal temperatures are determined by the optimization algorithm used here such that the tanks are not overheated unnecessarily, thus the energy costs caused by the HP operation will remain minimized.

Considering this, the following discretized continuous-time equations were obtained:

- Energy balance in the SH tank

$$\frac{dQ_{SH}}{dt} = \dot{Q}_{HP,SH\ (t)} - \dot{Q}_{build,SH\ (t)} - \dot{Q}_{loss,SH\ (t)}$$

$$T_{W,SH\ (t+1)} = T_{W,SH\ (t)} + \frac{\dot{Q}_{HP,SH\ (t)} - \dot{Q}_{build,SH\ (t)} - \dot{Q}_{loss,SH\ (t)}}{\rho_w \cdot Cp_w \cdot V_{w,SH}} * \Delta t \qquad 3\text{-}6$$

- Energy balance in the DHW tank

$$\frac{dQ_{DHW}}{dt} = \dot{Q}_{HP,DHW(t)} - \dot{Q}_{build,DHW\ (t)} - \dot{Q}_{loss,DHW\ (t)}$$

$$T_{W,DHW\ (t+1)} = T_{W,DHW\ (t)} + \frac{\dot{Q}_{HP,dhw\ (t)} - \dot{Q}_{build,dhw\ (t)} - \dot{Q}_{loss,DHW\ (t)}}{\rho_w \cdot Cp_w \cdot V_{w,dhw}} * \Delta t \qquad 3\text{-}7$$

- Energy balance in the household

$$\frac{dQ_{build(t)}}{dt} = \dot{Q}_{build,SH(t)} - \dot{Q}_{loss,build\ (t)}$$

$$T_{room\ (t+1)} = T_{room\ (t)} + \frac{\dot{Q}_{build,SH\ (t)} - \dot{Q}_{loss,build\ (t)}}{C_{m\ ,build} + (V_{air} \cdot Cp_{air} \cdot \rho_{air})} * \Delta t \qquad 3\text{-}8$$

- HP power consumption for SH and DHW

$$P_{HP,SH(t)} = \frac{\dot{Q}_{HP,SH(t)}}{CoP_{SH(t)}} \qquad 3\text{-}9$$

$$P_{HP,DHW(t)} = \frac{\dot{Q}_{HP,DHW(t)}}{CoP_{DHW(t)}} \qquad 3\text{-}10$$

$$P_{HP\ (t)} = P_{HP,SH(t)} + P_{HP,DHW\ (t)} \qquad 3\text{-}11$$

Equation 3-11 does not mean that the HP can operate in SH and DHW modes simultaneously. For the optimization in GAMS, the HP power consumption has been integrated in one single variable to work only with a unique variable.

Thus, if only SH is performed at a specific time, the $P_{HP(t)}$ variable will be equal to $P_{HP,SH(t)}$ and $P_{HP,DHW(t)}$ will be equal to zero. On the other hand, equations 3-6 and 3-7 allow to determine the temperature profile of the water in the SH and DHW tanks, respectively. Through these equations, the change of energy in the storage tanks can be evidenced as a temperature increase is associated with an incoming energy flux, and a decay in the temperature is related to an output heat fluxes due to the demand of the building and thermal losses. Furthermore, equation 3-8 represents the time-dependent temperature of the interior of the building. Through this equation, it can be determined if the building is kept at the desired comfort level at each time during the operation of the system. In addition, equations 3-9 and 3-10 relate the conversion of electricity into heat from the HP during its operation in SH or DHW modes.

In this formulation the time variable *t* is discrete, so the values of the state variables will correspond to its average, while the time step or Δt corresponds to the time resolution of the optimization which is 0.25 *h* (15 minutes). Table 3-2 describes the terms and the parameter values for the optimization problem, and it must be noticed that the volume of the SH and DHW tanks will be changed during a sensitivity analysis in the later sections, for in this table no value is shown. Additionally, the terms for the heat losses of the building and the storage tanks will be developed in the following sections as they depend on the type of materials, their physical properties, and their sizes.

Table 3-2: Terminology of thermal model

Term	Description	Value	Units
Surface Heating (SH) variables			
$\dot{Q}_{HP,SH}$	Heat rate supplied to SH tank from the HP	--------	kW
$\dot{Q}_{build,SH}$	Heat rate demand of household for SH	Demand load profile	kW
$\dot{Q}_{loss,SH}$	Heat rate loss of SH tank	--------	kW
$T_{W,\ SH}$	Water temperature inside SH tank	--------	K
$V_{w,SH}$	Volume of SH tank	--------	m^3
Domestic Hot Water (DHW) variables			
$\dot{Q}_{HP,DHW}$	Heat rate supplied to DHW tank from the HP	--------	kW
$\dot{Q}_{build,DHW}$	Heat rate demand of household for DHW	Demand load profile	kW
$\dot{Q}_{loss,DHW}$	Heat rate loss of DHW tank	--------	kW
$T_{W,\ DHW}$	Water temperature inside DHW tank	--------	K
$V_{w,dhw}$	Volume of SH tank	--------	m^3
Household variables			
T_{room}	Indoor temperature of the building	--------	K
Heat pump variables			
$\dot{Q}_{HP}$	Overall heat rate produced by HP	--------	kW
P_{HP}	Overall HP electric power consumption	--------	kW
$P_{HP,SH}$	HP electric power consumption for SH	--------	kW
$P_{HP,dhw}$	HP electric power consumption for DHW	--------	kW
Parameters			
U_{tank}	Global heat transfer coefficient tanks	$5.98 \cdot 10^{-4}$	kW m^{-2} K^{-1}
U_{build}	Global heat transfer coefficient of building	$6.009 \cdot 10^{-4}$	kW m^{-2} K^{-1}

$A_{tank,\ SH}$	Surface area SH tank	--------	m^2
$A_{tank,\ DHW}$	Surface area of DHW tank	--------	m^2
T_{amb}	Ambient temperature	Weather profile	K
ρ_w	Water's density	993	kg m^{-3}
Cp_w	Water's heat capacity	0.00116	kWh kg^{-1} K^{-1}
$C_{m,\ build}$	Building's thermal capacity	4.755	kWh K^{-1}
V_{air}	Air volume of building	180	m^3
Cp_{air}	Air's heat capacity	0.0002793	kWh kg^{-1} K^{-1}
ρ_{air}	Air's density	1.225	kg m^{-3}
A_{build}	Overall building's area	480	m^2
Δt	Time step optimization	0.25	h
CoP_{SH}	Coefficient of performance of HP for SH	--------	kW_{heat} /kW_{elec}
CoP_{dhw}	Coefficient of performance of HP for DHW	--------	kW_{heat} /kW_{elec}

It must be noted that all the variables will be restricted to upper and lower boundaries by considering technical criteria and recommendations from [33], [28], and[35]. These values are summarized in the following table.

Table 3-3: Boundary values for HP-TES constraints

Parameter	Units	Value
$T_{w,SH\ min}$	˚C	32
$T_{w,SH\ max}$		45
$T_{w,DHW\ min}$		55
$T_{w,DHW\ max}$		65
$T_{room,min}$		17
$T_{room,max}$		20
$P_{HP,max}$	kW	6

3.2.5. Heat storage sizing and distribution heating system

The water storage tanks (WST) are responsible for delivering heat for DHW and SH demands during winter season, while the tank for SH will provide cooling during summer. The sizes of the WST need to be specified, but as DHW and SH demands are dependent on the number of people and their occupancy behavior, it is difficult to predict the exact demand and related it accurately to the size of a thermal storage device. According to [36], heuristic techniques must be applied to calculate their size and validated models are presented to estimate with appropriate accuracy the storage level needed considering the number of household's inhabitants. The following equations have been applied to size the storage tank's volumes for both demands.

$$\boldsymbol{V_{DHW}} = 1.25 \cdot 65 \cdot \left(N_{people}\right)^{0.7} \quad \text{3-12}$$

$$\boldsymbol{V_{SH}} = \frac{\dot{Q}_{PEAK} \cdot 2h}{\rho_w \cdot Cp_w \cdot \Delta T} \quad \text{3-13}$$

where V_{DHW} is the volume of the DHW tank in L, N represents the number of people in the house, and 1.25 represents a safety factor that allows to have sufficient water in the tank. Additionally, V_{SH} is the volume of the SH tank in L, $\dot{Q}_{PEAK}$ represents the yearly SH peak demand of the building (kW), Cp_w corresponds to the water's heat capacity (kWh/kg K), ΔT represent the temperature difference between the upper and lower boundaries values of the SH storage tank, and ρ_w is the water's density (kg/L). Equation 3-12 represents the recommended sizing for storage, and it is intended to supply the maximum heat demand of the year during 2 hours to the building as recommended in [37].

From the heat demand interpolated using equation 3-1 for Delft, the peak heat demand for year 2014 was around 4.6 kW, leading in this way to have a theoretical storage tank size for SH of 793 liters, while for DHW a tank of 215 liters has been determined contemplating there are 4 people living in the house . During the optimization of the HP-TES model this value was considered, and for the PV-BES-EV-HP system this volume was modified multiple times to perform a sensitivity analysis and determine the influence of the storage size on the system's performance. This will be presented in the results section.

SH and DHW storage tanks will present heat losses depending on the site where they are located. It has been considered that both storage tanks will be sited inside the building to reduce the losses as much as possible. To determine the heat loss of each tank, it is necessary to estimate the surface area that is in contact with the surrounding air in the room. Then, the heat losses can be calculated considering the global heat transfer coefficient U_{tank} depending on the material the tank is made of, and the type of insulation. Table 3-4 shows the dimensions of both tanks, and it is important to mention that during the sensitivity analysis the height and radius of the tank will change depending on the considered volume.

Table 3-4: Dimensions of storage tanks

Parameter	Description	Value
$V_{tank,\ SH}$	Volume SH tank	800 L
$V_{tank,\ DHW}$	Volume DHW tank	215 L
$H_{tank,\ SH}$	Height SH tank	2.08 m
$H_{tank,\ DHW}$	Height DHW tank	1.3 m
$R_{tank,SH}$	Radius SH tank	0.35 m
$R_{tank,DHW}$	Radius DHW tank	0.22 m

The following equations have been applied for both tanks:

$$\boldsymbol{V_{tank}} = \pi \cdot R^2 \cdot H \quad \text{3-14}$$

$$\boldsymbol{A_s} = 2\pi R \cdot H + 2\pi R^2 \quad \text{3-15}$$

$$\boldsymbol{\dot{Q}_{loss,SH(t)}} = U_{tank} \cdot A_{s,SH} \cdot \left(T_{w,SH(t)} - T_{room(t)}\right) \quad \text{3-16}$$

$$\boldsymbol{\dot{Q}_{loss,DHW(t)}} = U_{tank} \cdot A_{s,DHW} \cdot \left(T_{w,DHW(t)} - T_{room(t)}\right) \quad \text{3-17}$$

where $A_{s,SH}$ and $A_{s,DHW}$ represent the surface areas of the SH and DHW tanks respectively, $T_{w,SH(t)}$ and $T_{w,DHW(t)}$ are the time-dependent water temperatures in the SH and DHW tanks, and $T_{room(t)}$ is the temperature inside the building.

Additionally, the amount of energy stored in the tanks in kWh during each time step was calculated using equations 3-18 and 3-19, where the temperature of 298.15 K has been chosen as the reference temperature to calculate the thermal difference of the water at each time step

$$\boldsymbol{Q_{stored,SH(t)}} = V_{w,SH} \cdot \rho_{water} \cdot C_{pw,} \cdot \left(T_{w,SH(t)} - 298.15\right) \quad \text{3-18}$$

$$\boldsymbol{Q_{stored,DHW(t)}} = V_{w,DHW} \cdot \rho_{water} \cdot C_{pw,} \cdot \left(T_{w,DHW(t)} - 298.15\right) \quad \text{3-19}$$

Here $Q_{stored,SH}$ and $Q_{stored,DHW}$ represent the amount of heat available in kWh in the SH and DHW tanks respectively at a specific time, and ρ_{water} corresponds to the water's density. Based on the literature review, a floor heating distribution system was selected for SH demand. The minimum temperature at which the distribution system works must be determined to ensure the temperature in the storage tank is high enough to keep the thermal comfort of the building, so the temperature in the tank must be higher or at least equal to a minimum temperature at which the heating system can work. In [28], a model relating the minimum supply temperature of the WST for SH used by

the heating system and the ambient temperature is presented and it has been used here. It is valid for outside ambient temperatures below 15 ˚C.

$$T_{supply,min\ SH} = 273 + a_0 + a_1 \cdot T_{amb\ (t)} + a_2 \cdot T_{amb(t)}^{\ 2} \qquad 3\text{-}20$$

In the equation above, T_{amb} represents the outside ambient temperature in ˚C, 273 represents the conversion factor into Kelvin, and $T_{supply,min\ SH}$ represent the minimum temperature that needs to be supplied from the SH storage tank to the heating system to keep the thermal comfort within the ranges. The coefficients of equation 3-20 are presented in the following table.

Table 3-5: Heating system coefficients

Coefficient	Value	Unit
a_0	32.84	-----
a_1	-0.56	$^{\circ}C^{-1}$
a_2	-0.0051	$^{\circ}C^{-2}$

3.2.6. Building characteristics

Building characteristics such as type of construction materials, level of insulation, and space distribution play an important role in the building's performance to keep the interior thermal comfort within the desirable range. For this research, a typical Dutch house has been chosen based on the studies of [28], [21] and [24], and its main features are presented in tables 3-6 and 3-7. Once the physical dimensions of the building are stated, the global heat transfer coefficient of the entire house must be determined to estimate the heat losses due to the thermal difference among the interior space and the outside environment.

For this research, three types of heat losses have been considered: convection and conduction heat losses through the walls, and heat losses due to natural ventilation . It is important to mention that ventilation losses depend on the specific architecture of the building and the behavior of the inhabitants (i.e opening windows, mechanic ventilation, etc) which are parameters hard to assume. Nevertheless, if appropriate information data about the design of the house and the air changing rate (ACH) is known, this can be added to the model to determine with better accuracy the heat losses due to ventilation. Using information available in [37] and [38] heat losses due to ventilation have been estimated for a typical Dutch terraced house

Table 3-6: Building's physical dimensions

Zone	Material	Length, m	Height, m
Front wall	Brick	10	4
Side wall	Brick	6	8
Roof	Clay	10	5
Windows, door	Glass	-------	------

Table 3-7: Thermal conductivity and convection coefficients

Material	Thickness, m	k, W/m K	h, W/m^2 K
Glass	0.007	0.96	------
Brick	0.15	0.6	------
Insulation	0.02	0.04	------
Clay	0.04	0.7	------
Air interior	-------	------	8
Air outside	-------	------	23

To calculate the global heat transfer coefficient $U_{building}$ equations 3-21 and 3-22 have been used. The global heat transfer coefficient of a material is the sum of the inverse of total thermal resistances for conduction and convection. The thermal resistance for conduction is defined as the ratio of the material's thickness to its thermal conductivity, while the thermal resistance for convection is the inverse of convection's heat transfer coefficient.

$$\boldsymbol{U_{building}} = \frac{1}{R_{building}} = \sum_{i}^{K} \frac{1}{R_{i,conduction}} + \sum_{j}^{F} \frac{1}{R_{j,convection}}, \qquad \left[\frac{W}{m^2\,K}\right] \tag{3-21}$$

$$\boldsymbol{R_{conduction}} = \frac{d_i}{k_i};\ \boldsymbol{R_{convection}} = \frac{1}{h_j} \tag{3-22}$$

where $R_{conduction}$ and $R_{convection}$ are the conductive resistances for conduction and convection expressed in m^2 K/ W , k_i is the thermal conductivity of the material expressed in W/m K, h_i is the convective heat transfer coefficient for the air expressed in W/m^2 K, and d_i corresponds to the thickness of the material expressed in m. Considering the physical dimensions and the type of materials, the total area of the building perpendicular to the heat flow ($A_{building}$) is 312 m^2 , and a global heat transfer coefficient $U_{building}$ of 0.6009 W/m^2 K. In this way, the total heat losses due to convection and conduction in the building's envelope at each time step can be calculated as follows:

$$\dot{\boldsymbol{Q}}_{cond\ (t)} = U_{building} \cdot A_{building} \cdot \left[T_{room(t)} - T_{amb(t)}\right] \tag{3-23}$$

where $Q_{con(t)}$ is the total heat flux loss due to conduction and convection at each time step, Additionally, the thermal capacitance of the building C_m was calculated using the procedures of ISO 13790:2008 [33] having a value of 4.755 kWh for this specific building. On the other hand, heat losses due to natural ventilation have been calculated using equation 3-24 represented by $Q_{vent(t)}$. The air change rate ACH represents the amount of air circulating from outside to the interior of the building to keep an adequate level of fresh air and oxygen, and for this house, it has been calculated as 0.66 h^{-1} based on the study in [38] . Furthermore, the volume-space of the building $V_{building}$ is 480 m^3, assuming there are no divisions or sections for simplicity in the calculations. Therefore, the heat losses due to natural ventilation are:

$$\dot{\boldsymbol{Q}}_{vent\ (t)} = 3.55 \cdot 10^{-4} \cdot V_{building} \cdot ACH \cdot \left[T_{room(t)} - T_{amb(t)}\right] \tag{3-24}$$

The factor 3.55 ·10^{-4} corresponds to the product of the air's density and its heat capacity at an average temperature between the room's temperature $T_{room(t)}$ and the ambient temperature $T_{amb(t)}$, therefore, this factor is expressed in kWh m^{-3} K^{-1}. Finally, the total heat loss of the building is the sum of the convection, conduction, and ventilation heat losses as stated in equation 3-25. This equation has been used in the optimization model's equation 3-8 to determine the room's temperature evolution.

$$\dot{\boldsymbol{Q}}_{loss,build\ (t)} = \dot{Q}_{con\ (t)} + \dot{Q}_{vent\ (t)} \tag{3-25}$$

3.2.7. Optimization HP-TES problem formulation

This section presents the optimal problem formulation for the HP-TES system without considering the PV-BES-EV components. The objective is to determine the optimal power consumption in such a way the consumer's electricity bill be minimized. It is important to mention that the proposed model in this research is a demand-based model, for the heat demand of the building is not reduced nor shifted as the purpose is to follow the demand and let the system find the optimal way to satisfy it. In this way, the optimization problem can be expressed in the following general way:

$$\min_{\boldsymbol{U'(t)}} \sum_{t}^{T} Bill_t\ (x_t, u_t, z_t, d_t) \tag{3-26}$$

$$st.\ \boldsymbol{x_{t+1} = Ax_t + Bu_t + Cz_t}\ , \forall \boldsymbol{t = 1, 2, \ldots . T - 1} \quad \text{3-27}$$

$$\boldsymbol{K_{eq}\, x_t = b_{eq}}\ ;\ \boldsymbol{N_{eq}\, u_t = g_{eq}} \quad \text{3-28}$$

$$\boldsymbol{K_I x_t \leq b_I}\ ;\ \boldsymbol{N_I\, u_t \leq g_I} \quad \text{3-29}$$

$$\boldsymbol{x_t, u_t \geq 0}, \forall \boldsymbol{t = 1, 2, \ldots \ldots T} \quad \text{3-30}$$

$$\boldsymbol{x_1 = x(t_1)} \quad \text{3-31}$$

Equation 3-26 represents the time-varying cost function aimed to be minimized, and it is a function of the state vector *x(t)* that contains all the state variables ($T_{W,DHW(t)}$, $T_{W,SH(t)}$, $T_{room,(t)}$), the steering vector *u(t)* that contains the optimization variables ($P_{HP,SH(t)}$, $P_{HP,DHW(t)}$), *z(t)* is the vector comprehending input data ($\dot{Q}_{build,SH(t)}$, $\dot{Q}_{build,DHW(t)}$, $T_{amb,(t)}$), *d(t)* is the vector of all external signals, in this case the dynamic buying electricity price ($\lambda_{buy(t)}$), and *U'(t)* represents the vector of the decision variables. Based on this general formulation, the HP-TES optimization problem can be stated by using equations 3-6 to 3-11 and add to them boundary, inequality, and equality constraints that will delimit the feasible space where the optimization must occur. Hence, the HP-TES objective function is:

$$\min_{P_{HP\,(t)},\, \lambda_{buy\,(t)}} \sum_{t}^{T} \lambda_{buy(t)} \cdot P_{HP\,(t)} \quad \text{3-32}$$

Furthermore, the state variables are subject to boundary constraints to satisfy the system's requirements according to the following expressions:

$$\boldsymbol{T_{w,SH\,min} \leq T_{w,SH\,(t)} \leq T_{w,SH\,max}}\ , \forall \boldsymbol{t = 1, 2, \ldots . T} \quad \text{3-33}$$

$$\boldsymbol{T_{w,SH\,(t)} \geq T_{supply\,min,SH}}\ , \forall \boldsymbol{t = 1, 2, \ldots . T} \quad \text{3-34}$$

Equation 3-34 allows to ensure that the temperature available in the SH tank must be higher or equal to the required minimum supply temperature of the heating system to keep the thermal comfort of the building.

$$\boldsymbol{T_{w,DHW\,min} \leq T_{w,DHW\,(t)} \leq T_{w,DHW\,max}}\ , \forall \boldsymbol{t = 1, 2, \ldots . T} \quad \text{3-35}$$

$$\boldsymbol{T_{room,min} \leq T_{room\,(t)} \leq T_{room,max}}\ , \forall \boldsymbol{t = 1, 2, \ldots . T} \quad \text{3-36}$$

The decision variables for the heating rate for SH and DHW are not set to any boundary constraints directly, but the power of the heat pump has been limited to a capacity constraint which automatically leads to have optimal values for each heating mode (SH and DHW) . Therefore, the following constraint must be satisfied:

$$\boldsymbol{0 \leq P_{HP\,(t)} \leq P_{HP,max}}\ , \forall \boldsymbol{t = 1, 2, \ldots . T} \quad \text{3-37}$$

As the heat pump can vary its compressor's speed, the heat pump will operate in a partial load mode or in full load mode depending on the necessity of keeping the storage tanks at a certain temperature level. The model will determine when it is more cost effective to completely charge the tanks or to maintain a certain temperature by strictly respecting the constraints of the system.

This formulation of the HP-TES optimization problem was solved in GAMS without the presence of the PV-BES-EV components, and it was observed that the model responded accordingly to the variable electricity price signal $\lambda_{buy(t)}$. The HP operated at times of low prices to charge or maintain the temperature in the storage tanks while minimizing the electricity bill for the consumer. It was evidenced that by using a unique variable to represent the power consumption of the HP ($P_{HP(t)}$), SH and DHW operation modes did not happen at the same time as explained in equation 3-11. This has to do with the fact that if both happen at the same time, either the HP power consumption would be higher than its capacity or the operational costs would increase. Thus, this situation is avoided by the optimization model and it allocates the power consumption for SH and DHW at different times.

Furthermore, the HP's power consumption is influenced by the heat losses of the storage tanks and the tanks size. High heat losses will cause fast temperature decays of the water forcing the HP to operate frequently even when electricity prices become high, and even if the problem exhibits a feasible solution, the results must be analyzed critically considering that the consumer's objective is to minimize as much as possible his electricity costs. Therefore, determining an adequate heat transfer coefficient of the storage tanks, based on the literature review, manufacturer's data, or technical recommendations, is vital to enhance the results of the optimization. On the other hand, sizing of the storage tank plays a vital role in the performance of the system because an oversized tank will lead to unnecessary overheating of the water, thus the power consumption of the heat pump rises, increasing the final energy costs.

3.3. PV-BES-EV-HP model formulation

As explained in section 3-1, this model is result of the integration of the PV-BES-EV model and the formulated HP-TES model above described. Here, the PV production is controlled by a maximum power point tracker (MPPT) that optimizes the amount of energy obtained from the panels such that they operate always at maximum efficiency. Additionally, a multi-port power inverter has been used to connect all the components of the system. Table 3-8 summarizes the parameters of the integrated system. The novelty of the model developed by Vermeer and Ram is the inclusion of the operational degradation of the EV and the BES to account in a more realistic way the operational costs of the EV and BES, and its influence on the cost minimization.

Table 3-8: Integrated system parameters

Symbol	Parameter	Value
$P_{pv\ rated}$	Installed PV capacity power	10 kWp
$P_{EV\ max}$	Maximum EV (dis)charging power	10 kW
$P_{BES\ max}$	Maximum BES (dis)charging power	10 kW
$P_{grid\ max}$	Maximum limit grid	10 kW
$P_{inv\ max}$	Inverter maximum power	10 kW
$E_{EV\ max}$	Maximum EV capacity	80 kWh
$E_{BES\ max}$	Maximum BES capacity	10 kWh
$V_{OC,EV}$	EV voltage	325-430 V
$V_{OC,BES}$	BES voltage	325-430 V

The cost minimization can be achieved by reducing the energy intake from the grid, selling the excess of electricity to the grid, or using as much as possible of the generated PV power. The SGO will provide the electricity price signals for both buying and selling electricity. The model will try to find the optimal points where the operational costs are minimized according to the following objective function:

$$\min_{C_{PV}, C_{EV}, C_{BES}, C_{grid}} C_{total} = \mathbf{min}\left(C_{PV} + C_{BES} + C_{EV} + C_{grid}\right) \qquad 3\text{-}38$$

where C_{PV} corresponds to the installation and investment costs of the PV panels, C_{BES}, and C_{EV}, correspond to the degradation costs of the BES and the EV, respectively due to their operation, and C_{grid} corresponds to the operational

costs of the grid due to the power exchanges of the system with it. In this way, a non-linear programming (NLP) optimization problem was obtained. As mentioned before, GAMS was used to solve the problem by using the CONOPT optimization solver as this is the best algorithm to solve NLP problems according to [39]. In the following sections, a description of the model is presented together with the respective constraints and assumptions considered for the system.

3.3.1. BES degradation costs and capacity lost model

A Nickel-Manganese-Cobalt (NMC) battery has been considered for both the electric vehicle and the stationary battery storage as proposed by [40]. The degradation costs of the stationary battery have been determined by considering a loss of value per kWh (€/kWh) and a loss of capacity during their lifetime operation as proposed in [41]. In the cited study, it is assumed that the first life-value of the battery starts at 100% of its capacity, and the second-life starts at 80% of the initial capacity. During the second-life, the battery's value corresponds to 50% of its initial value. Therefore, the operational costs C_{BES} would be equal to the difference between a new and a degraded battery, and they have been calculated using the following equations:

$$V_{BES}^{2nd} = V_{BES}^{1st} \cdot \frac{E_{BES\,max} - \Delta E_{BES,tot}}{E_{BES\,max}} \quad 3\text{-}39$$

$$C_{BES} = V_{BES}^{1st} \cdot E_{BES\,max} - V_{BES}^{2nd} \cdot \left(E_{BES\,max} - \Delta E_{BES,tot}\right) \quad 3\text{-}40$$

where V_{BES}^{2nd} corresponds to the second-life value of the battery, $\Delta E_{BES,tot}$ represents the degraded capacity of the battery, $E_{BES\,max}$ is the initial capacity, and V_{BES}^{1st} equals to the initial value of the battery. The battery power capacity is limited to 10 kW for both charging and discharging, and a specific distinction between positive and negative battery power has been contemplated. This allows to consider charging, discharging, and converter efficiencies during the operation cycles of the battery. Additionally, a round trip efficiency of 92% has been assumed, meaning the battery has a charging/discharging efficiency of 96%.

According to [42], when the battery's power for charging or discharging is mathematically captured in a unique variable (P_{BES}), simultaneous charging/discharging of the battery is avoided. Besides, the optimization model recognizes that a simultaneous operation is not optimal for cost minimization, and it will intend to find points where charging and discharging occurs separately. Hence, the following equations have been used to model the charging/discharging operation of the battery, and the energy stored by it.

$$P_{BES(t)} = n_{ch} \cdot P_{BES\,(t)}^{pos} - \frac{1}{n_{dis}} P_{BES\,(t)}^{neg} \quad 3\text{-}41$$

$$P_{BES\,(t)}^{pos} \leq P_{BES}^{max} \quad 3\text{-}42$$

$$P_{BES\,(t)}^{neg} \leq P_{BES}^{max} \quad 3\text{-}43$$

$$E_{BES\,(t)} = E_{BES\,(t-1)} + P_{BES\,(t)} \cdot \Delta t, \quad \forall t, t = 2 \ldots\ldots T \quad 3\text{-}44$$

The energy stored by the battery at t=1 and t=t_{final} have been fixed to have a fair comparison in terms of energy/cost. Not fixing the energy at the end of the simulation will lead the system to drain the battery completely as the optimization will try to sell as much as possible of the stored electricity to the grid to produce more revenues and reduce the costs for buying electricity from the grid. Therefore, the capacity of the battery at the end of the simulation horizon must be equal to the capacity at the beginning of the optimization to have a fair comparison of costs.

$$E_{BES\,(t=1)} = E_{BES\,ini} \;\; ; \;\; E_{BES\,(t=t_{final})} = E_{BES\,ini} \quad 3\text{-}45$$

The values of the parameters in equations 3-40 to 3-45 are displayed in table 3-9.

Table 3-9: Parameters Values for BES degradation costs

Parameter	Value	Units
V_{BES}^{1st}	500	€
V_{BES}^{2nd}	250	€
η_{ch}	0.96	-----
η_{disch}	0.96	-----
$E_{BES,ini}$	5	kWh

The state of charge (SOC) of the battery can be calculated as the ratio of the energy stored at time step *t* to the actual limit capacity at the same time step. As the battery degrades with each charging/discharging cycle, part of its capacity will be lost, and this must be considered to determine the actual capacity of the battery to evaluate a more accurate state of charge. At the beginning, the battery's capacity will be equal to its maximum nominal capacity, and as time goes by, the actual capacity will be equal to the starting maximum value minus the capacity lost. This has been modelled through the following equations where the variable $E_{BES,limit}$ represents the actual capacity of the battery at time step t:

$$SoC_{BES\,(t)} = \frac{E_{BES\,(t)}}{E_{BES,limit\,(t)}} \quad 3\text{-}46$$

$$E_{BES,limit\,(t)} = E_{BES\ limit\,(t-1)} - \Delta E_{BES(t)}, \forall t, \qquad t = 2, \dots\dots T \quad 3\text{-}47$$

$$E_{BES\ limit\,(t=1)} = E_{BES,max} \quad 3\text{-}48$$

$$E_{BES\,(t)} \leq E_{BES\ limit(t)} \quad 3\text{-}49$$

The capacity lost $\Delta E_{BES(t)}$ has been calculated using a Li-ion degradation model developed by [43] where the behavior of a single cell has been studied. This model investigates the effects of temperature, current rate, and the ampere-hours processed in the degradation of the cell, however, as the model considers only one cell, the power and voltage of the battery must be scaled down to the voltage and current of one single cell. To do this, [44] proposes a model to establish the relationship between the open circuit voltage (OCV) and the SOC of a battery, and it is shown in equation 3-50. For this research, it has been assumed that the battery is composed of $N_{BES}^{parallel}\ x\ N_{BES}^{series}$ cells to have an OCV of 425 V at full capacity, for in this way both the OCV(t) as a function of the SOC(t) and the current of a single cell can be calculated as:

$$OCV_{BES\,(t)} = N_{BES}^{series} \cdot \left(a_1 \cdot e^{b_1 \cdot SoC(t)} + a_2 \cdot e^{b_2 \cdot SoC(t)} + a_3 \cdot SoC_{(t)}^2\right) \quad 3\text{-}50$$

$$i_{BES}^{cell} = \frac{1000 \cdot P_{BES\,(t)}}{N_{BES}^{parallel} \cdot OCV_{(t)}} \quad 3\text{-}51$$

The value of the parameters in these equations are displayed in table 3-10. Once these variables are estimated, the loss of capacity can be determined using the model of [43] as the percentage of lost capacity respect to the initial battery's capacity. Thus, the capacity's degradation of the battery at any time step, and the total capacity lost has been calculated using the following equations:

$$\Delta E_{BES\,(t)} = \left(c_1 \cdot e^{c_2 \cdot |i_{BES}^{cell}(t)|} \cdot \left|i_{BES\,(t)}^{cell}\right| \Delta t\right) \cdot \frac{E_{BES,max}}{100} \quad 3\text{-}52$$

$$\Delta E_{BES,tot} = \sum_{0}^{T} \Delta E_{BES(t)} \quad 3\text{-}53$$

3.3.2. EV degradation costs and capacity lost model

The degradations costs related to the EV has followed the same reasoning as in the BES section. As for the stationary BES, the EV costs are calculated as the percentage of the degraded capacity due to charging/discharging as showed in equation 3-53 where the 0.2 factor accounts for 20% degradation of the original capacity.

$$C_{EV} = \left(V_{BES}^{1st} - V_{BES}^{2nd}\right) \cdot \frac{\Delta E_{EV,tot}}{0.2\ E_{EV\ max}} \cdot \left(E_{EV\ max} - \Delta E_{EV,tot}\right) \quad 3\text{-}54$$

The degradation of the EV battery has been determined in the same way as for the stationary BES, but it has been assumed that the EV is not available between the times the EV departs from and arrives to the building. To account for this, the binary variable $EV_{av(t)}$ has been introduced having a zero value for the period of the depart and the arrival to the building. During the non-availability of the EV, it is considered the EV is traveling between work and home with an efficiency of 15 kWh/100 Km in a single trip of 30 km. The first-life and second-life parameters for the EV have the same values as the BES in table 3-9.

The power consumed during driving is captured in the variable $P_{drive\,(t)}$ showed in equation 3-55 for all the time the EV is not in the building. Furthermore, it can be established that the EV needs a minimum amount of charge at the departure time to ensure the EV has enough energy when leaving the building. As in the stationary BES, the EV cannot be charged and discharged at the same time, for the same principle of capturing the EV battery's (dis)charging in a unique variable has been applied. All these considerations have been modelled in the following equations:

$$P_{drive(t)} = \frac{15\ kWh}{100\ km} \cdot \frac{d_{round\ trip}}{\Delta t * N_{steps}^{non\ av}} \quad 3\text{-}55$$

$$P_{EV(t)} = EV_{av(t)} \cdot \left(n_{ch} \cdot P_{EV\,(t)}^{pos} - \frac{1}{n_{dis}} P_{EV\,(t)}^{neg}\right) \quad 3\text{-}56$$

$$P_{EV\,(t)}^{pos} \leq P_{EV}^{max} \quad 3\text{-}57$$

$$P_{EV\,(t)}^{neg} \leq P_{EV}^{max} \quad 3\text{-}58$$

$$E_{EV\,(t)} = E_{EV\,(t-1)} + \left[\left(P_{EV\,(t)} - P_{drive(t)}\right) \cdot \Delta t\right], \forall t, t \leq t_{depart}\ \&\ t > t_{arrive} \quad 3\text{-}59$$

$$E_{EV\,(t=1)} = E_{EV,ini} \quad 3\text{-}60$$

$$E_{EV\,(t=t_{depart})} \geq E_{EV,depart} \quad 3\text{-}61$$

The SoC of the EV battery can be determined in the same way as for the stationary BES considering the degradation of its capacity during the charging/discharging cycles. As in the BES, determining the capacity lost is important to establish the actual limit capacity available, and this is represented in the following equations:

$$SoC_{EV\,(t)} = \frac{E_{EV\,(t)}}{E_{EV,limit\,(t)}} \quad 3\text{-}62$$

$$E_{EV,limit\,(t)} = E_{EV,limit\,(t-1)} - \Delta E_{EV(t)}, \forall t, \qquad t = 2, \ldots\ldots T \quad 3\text{-}63$$

$$E_{EV\ limit\,(t=1)} = E_{EV,max} \quad 3\text{-}64$$

$$E_{EV\,(t)} \leq E_{EV\ limit(t)} \quad 3\text{-}65$$

$$OCV_{EV\,(t)} = N_{EV}^{series} \cdot \left(a_1 \cdot e^{b_1 \cdot SoC_{EV}(t)} + a_2 \cdot e^{b_2 \cdot SoC_{EV}(t)} + a_3 \cdot SoC_{EV\,(t)}^2\right) \quad 3\text{-}66$$

$$i_{EV}^{cell} = \frac{1000 \cdot P_{EV\,(t)}}{N_{EV}^{parallel} \cdot OCV_{EV(t)}} \quad 3\text{-}67$$

$$\Delta E_{EV\,(t)} = \left(c_1 \cdot e^{c_2 \cdot |i_{EV}^{cell}(t)|} \cdot \left|i_{EV\,(t)}^{cell}\right| \Delta t\right) \cdot \frac{E_{EV,max}}{100} \quad 3\text{-}68$$

$$\Delta E_{EV,tot} = \sum_{t=1}^{T} \Delta E_{EV(t)} \quad 3\text{-}69$$

The parameters for the BES and EV models to determine the OCV and the capacity lost are summarized in the following table.

Table 3-10: OCV and aging parameters for BES and EV

Parameter	Description	Value
a_1	OCV parameters	3.679
a_2		-0.2528
a_3		0.9836
b_1		-0.1101
b_2		-6.829
c_1	Aging parameters	0.0008
c_2		0.39
$N_{BES}^{parallel}$	Number of cells in parallel in BES	18
N_{BES}^{series}	Number of cells in series in BES	100
$N_{EV}^{parallel}$	Number of cells in parallel in EV	145
N_{EV}^{series}	Number of cells in series in EV	100

3.3.3. PV cost model

As PV is a renewable energy source, normally its operational costs are assumed to be zero, but in this research the model has contemplated the investment and installation costs of the photovoltaic system. According to [45] the LCOE for a rooftop PV system is 0.03 €/kWh in the Netherlands, for the costs for the PV energy are determined by:

$$C_{PV} = \sum_{t=1}^{T} \lambda_{PV} \cdot P_{PV(t)} \cdot \Delta t \quad 3\text{-}70$$

where $P_{PV(t)}$ represents the power production from the panels, λ_{PV} is the LCOE of the panels, and Δt is the step time. There could be moments where the energy production from the PV panel surpasses the energy demand and aggravates the imbalance between the supply and demand. One solution for this problem is the ability of the system to curtail this excess through the house's energy management system (EMS). To account for this, the following equation is used:

$$P_{PV(t)} \leq \eta_{mppt} \cdot P_{PV\,(t)}^{fc} \quad 3\text{-}71$$

3.3.4. Grid and inverter's power balances

For the system represented in Fig. 3-1, two power balances in the multi-port power converter have been developed for simplicity of the modelling. The first one comprehends all the elements connected to the DC side of it (PV, BES, and EV), while the second corresponds to all the elements on the AC side (grid, load, heat pump). Depending on the sign, the variables can represent a power output or input, influencing the direction of the balance. The following equations have been used to calculate these power flows:

$$P_{inv(t)} = P_{PV(t)} - P_{EV\,(t)} - P_{BES(t)} \quad 3\text{-}72$$

$$P_{grid\,(t)} = P_{inv(t)} - P_{load\,(t)} - P_{HP(t)} \quad 3\text{-}73$$

where $P_{inv(t)}$ is the total power balance on the DC side, $P_{EV(t)}$ and $P_{BES(t)}$ represents the power consumption/injection of the EV and BES respectively, $P_{grid(t)}$ corresponds to the power consumption/injection to the grid, $P_{load(t)}$ is the load of the electric appliances of the building, and $P_{HP(t)}$ is the power consumption of the HP for SH or DHW. Equation 3-73 is the one where the HP-TES model developed in section 3.2 and the PV-EV-BES merges to shape the entire optimization problem.

As the system can use or inject energy into the grid, a distinction between the two events have been considered. A positive grid power represents injection of power on the grid at the corresponding selling price $\lambda_{sell(t)}$, while a negative grid power holds for the power intake from the grid at the buying price $\lambda_{buy(t)}$.

The optimization will seek the points where power intake from the grid occurs at low prices, while it will feed back power when the energy price is high. In this way, the power intake, the power injection, and the grid operational costs can be calculated using equations 3-74 and 3-75. Here, the cable's transmission efficiency has been included to account for transmission losses. Besides, to guarantee the grid's stability, the power intake and injection cannot exceed the maximum allowed limit the grid can offer, so capacity constrains have been added.

$$P_{grid(t)} = n_{cable} \cdot P_{grid\,(t)}^{pos} - \frac{1}{n_{cable}} P_{grid\,(t)}^{neg} \quad 3\text{-}74$$

$$C_{grid} = \sum_{t=1}^{T} P_{grid\,(t)}^{neg} \cdot \lambda_{buy(t)} \cdot \Delta t - P_{grid\,(t)}^{pos} \cdot \lambda_{sell(t)} \cdot \Delta t \quad 3\text{-}75$$

$$P_{grid\,(t)}^{neg} \leq P_{grid}^{max} \quad ; \quad P_{grid\,(t)}^{pos} \leq P_{grid}^{max} \tag{3-76}$$

On the other hand, the inverter's efficiency during power conversion is considered. The total power in the inverter DC side can be split in positive ($P_{inv\,(t)}^{pos}$) and negative ($P_{inv\,(t)}^{neg}$) following the same reasoning as before. This is expressed in the following equations:

$$P_{inv(t)} = n_{inv} \cdot P_{inv\,(t)}^{pos} - \frac{1}{n_{inv}} P_{inv\,(t)}^{neg} \tag{3-77}$$

$$P_{inv\,(t)}^{neg} \leq P_{inv}^{max} \quad ; \quad P_{inv\,(t)}^{pos} \leq P_{inv}^{max} \tag{3-78}$$

This concludes the formulation of the optimization problem of the PV-BES-EV-HP system. In this chapter, the model's formulation was explained in detail to show the interaction between the components, and their influence on the power flows of the system. Additionally, the influence of different SH tank sizes on the operational flexibility, and the energy costs of the system was analyzed. Next section will show the results of the optimization of the system.

4. Optimization Results

This chapter presents the results of this thesis. These results were obtained by optimizing the operation of the system during 5 days in winter and summer under a demand response program based on two electricity price signals taken from[46]. The buying and FIT signals slightly differed from each other, being the FIT 10% smaller than the buying price. Additionally, the FIT was halved to ascertain its effect on the behavior and operational costs of the system. The following sections encompass the most relevant findings of the project. Several parameters have been used for the optimization; thus, the following table summarizes their values.

Table 4-1: List of parameters used in the optimization

Parameters HP-TES System			
U_{tank}	Global heat transfer coefficient tanks (SH and DHW)	$5.98 \cdot 10^{-4}$	kW m^{-2} K^{-1}
U_{build}	Global heat transfer coefficient of building	$6.009 \cdot 10^{-4}$	kW m^{-2} K^{-1}
*$V_{W, SH}$	Volume SH tank	*800	L
$V_{W,DHW}$	Volume DHW tank	215	L
T_{amb}	Ambient temperature	Weather profile	K
ρ_w	Water's density	993	kg m^{-3}
Cp_w	Water's heat capacity	0.00116	kWh kg^{-1} K^{-1}
$C_{m, build}$	Building's thermal capacity	4.755	kWh K^{-1}
$V_{building}$	Air volume inside building	480	m^3
Cp_{air}	Air's heat capacity	$2.793 \cdot 10^{-4}$	kWh kg^{-1} K^{-1}
ρ_{air}	Air's density	1.225	kg m^{-3}
A_{build}	Overall building's area	480	m^2
Δt	Time step optimization	0.25	h
f	Factor for natural ventilation	$3.55 \cdot 10^{-4}$	kWh m^{-3} K^{-1}
N	Air change rate	0.66	h^{-1}
a_o	First coeff. COP regression SH	7.8276	-----
a_1	Second coeff. COP regression SH	0.1396	K^{-1}
a_2	Third coeff. COP regression SH	5.5146	K^{-2}
$T_{W,SH\ min}$	Lower temperature boundary for SH	305	K
$T_{W,SH\ max}$	Upper temperature boundary for SH	315	K
$T_{W,DHW\ min}$	Lower temperature boundary for DHW	328	K
$T_{W,DHW,\ max}$	Upper temperature boundary for DHW	338	K
$T_{room\ min}$	Lower temperature boundary for building thermal comfort	290	K
$T_{room\ max}$	Upper temperature boundary for building thermal comfort	293	K
$P_{HP\ max}$	Maximum power capacity of HP	6	kW
Parameters PV-BES-EV System			
a_1	OCV parameters	3.679	--------
a_2	Global heat transfer coefficient of building	-0.2528	--------
a_3	Volume SH tank	0.9836	--------
b_1	Volume DHW tank	-0.1101	--------
b_2	Ambient temperature	-6.829	--------
c_1	Aging parameters	0.0008	--------
c_2	Water's heat capacity	0.39	--------
$N_{BES}^{parallel}$	Number of cells in parallel in BES	18	--------

N_{BES}^{series}	Number of cells in series in BES	100	--------
$N_{EV}^{parallel}$	Number of cells in parallel in EV	145	--------
N_{EV}^{series}	Number of cells in series in EV	100	--------
V_{BES}^{1st}	First-life value BES and EV	500	€
V_{BES}^{2nd}	Second-life value	250	€
η_{ch}	BES/EV charging efficiency	0.96	----
η_{disch}	BES/EV discharging efficiency	0.96	-----
η_{cable}	Cable efficiency	0.99	-------
η_{MPPT}	Maximum Power Point Tracking efficiency	0.98	-------
$\eta_{inverter}$	Inverter's efficiency	0.96	-------
T_{depart}	EV departure time	08:00	h
$P_{pv\ rated}$	Installed PV capacity power	10	kWp
$P_{EV\ max}$	Maximum EV (dis)charging power	10	kW
$P_{BES\ max}$	Maximum BES (dis)charging power	10	kW
$P_{grid\ max}$	Maximum limit grid	10	kW
$P_{inv\ max}$	Inverter maximum power	10	kW
$E_{EV\ max}$	Maximum EV capacity	80	kWh
$E_{BES\ max}$	Maximum BES capacity	10	kWh
$E_{BES,ini}$	Initial BES capacity	5	kWh
$E_{EV,ini}$	Initial EV capacity	35	kWh
$E_{EV,final}$	Final EV capacity	35	kWh
$E_{EV,ini}$	Initial EV capacity	35	kWh
$E_{EV,depart}$	Depart EV charge	50	kWh
$P_{grid\ max}$	Maximum grid power	10	kW
λ_{buy}	Grid energy buying price	------	€
λ_{sell}	Grid energy selling price (FIT)	------	€
λ_{PV}	PV energy price	0.03	€/kWh

Different scenarios have been analyzed during this research. Winter and summer seasons have been considered for the optimization. In this context, winter season is the most relevant to study the behavior of the HP because SH demand is considerably high during this season. On the other hand, summer season is relevant to analyze if the HP can use any excess of PV energy to store it as heat, thus helping in mitigating the effects of variability in the electricity production from renewable sources.

During each season, the influence of the FIT signal on the cost minimization was analyzed, thus it was also determined how renewable energy self-consumption is affected by this signal. Additionally, the influence of the SH tank size in the HP's operation behavior was analyzed only for winter season. The first scenario for winter deals with the cost minimization of the system using the FIT data from [46]. Within this scenario, the SH tank size was varied. As mentioned before, the SH tank was sized using equation 3-13 resulting in a design value of 800 L.

From this value, the size of the SH tank was varied 3 times: 100 L, 400 L and 1000 L, and the volume of the DHW tank has not been changed as it was sized using equation 3-12. The size of this tank was not changed as the aim of this study is to determine the flexibility potential of the HP to schedule a flexible demand, thus SH is the most relevant because DHW cannot be considered a flexible demand as this depends on the behavior of the inhabitants of the house. This is relevant for winter season only because for summer the SH demand is negligible. Therefore, for summer, only the system with an SH tank of 800 L was studied as we must recognize that the same designed tank for winter will be used in summer.

The second scenario deals with the cost minimization of the system using a reduced FIT. This reduced FIT was set to be 50% of the original FIT. Within this scenario, the influence of the SH tank size was not studied, thus only the design value of 800 L was used for winter and summer.

The results of the different scenarios were compared to a based case scenario where the same system was used, however, no cost minimization was performed. In the base case scenario, the FIT was also reduced at 50% of the initial value to have a fair comparison between the different cases. The following tables summarizes the different studied scenarios. Additionally, during this scenario no storage tanks have been used to represent no available flexibility of the HP.

Table 4-2: Studied Scenarios

SCENARIO 1	SCENARIO 2	SCENARIO 3
BASE CASE (NO ENERGY COST MINIMIZATION)	HIGH FIT (ENERGY COST MINIMIZATION)	REDUCED FIT (ENERGY COST MINIMIZATION)

Table 4-3: Influence of SH tank size scenarios

SCENARIO	WINTER	SUMMER
BASE CASE (NO OPTIMIZATION)	NO STORAGE TANK	NO STORAGE TANK
HIGH FIT	100 L	800 L
	400 L	
	800 L	
	1000 L	
REDUCED FIT	800 L	800 L

4.1. Winter season

4.1.1. Heat pump operation behavior

In this section, the results from the HP operation are discussed. The HP power consumption is influenced by the presence of the other devices, the temperature and capacity constraints, the thermal demand of the building, and the buying electricity price signal. Figure 4-1 shows the power profile of the HP for SH during winter for the high FIT case. The top graph displays the HP power consumption versus the buying price, and the power profile versus the temperature of the water in the storage tank in the bottom.

As it can be seen, the HP does not operate at times where electricity prices are the highest, and it shifts its power consumption to the lowest prices to fully charge the SH tank. However, there are times when the HP operates at a minimum power consumption to keep the temperature of the tank close to the low temperature boundary. This has to do with the fact the model determines that during these times it is not necessary nor cost effective to fully charge the tank because the prices are relatively high, but a minimum amount of energy is required to keep the thermal comfort of the building. Since the HP is not connected directly to the building, there is not overheating of the household when the heat pump works. Instead, the HP pre-heats the water in the buffer tank to have enough stored energy to satisfy the demand of the building, offering more flexibility to the system. In this way, the heat demand of the building is not reduced or shifted, but continuously satisfied by the presence of the buffer SH tank.

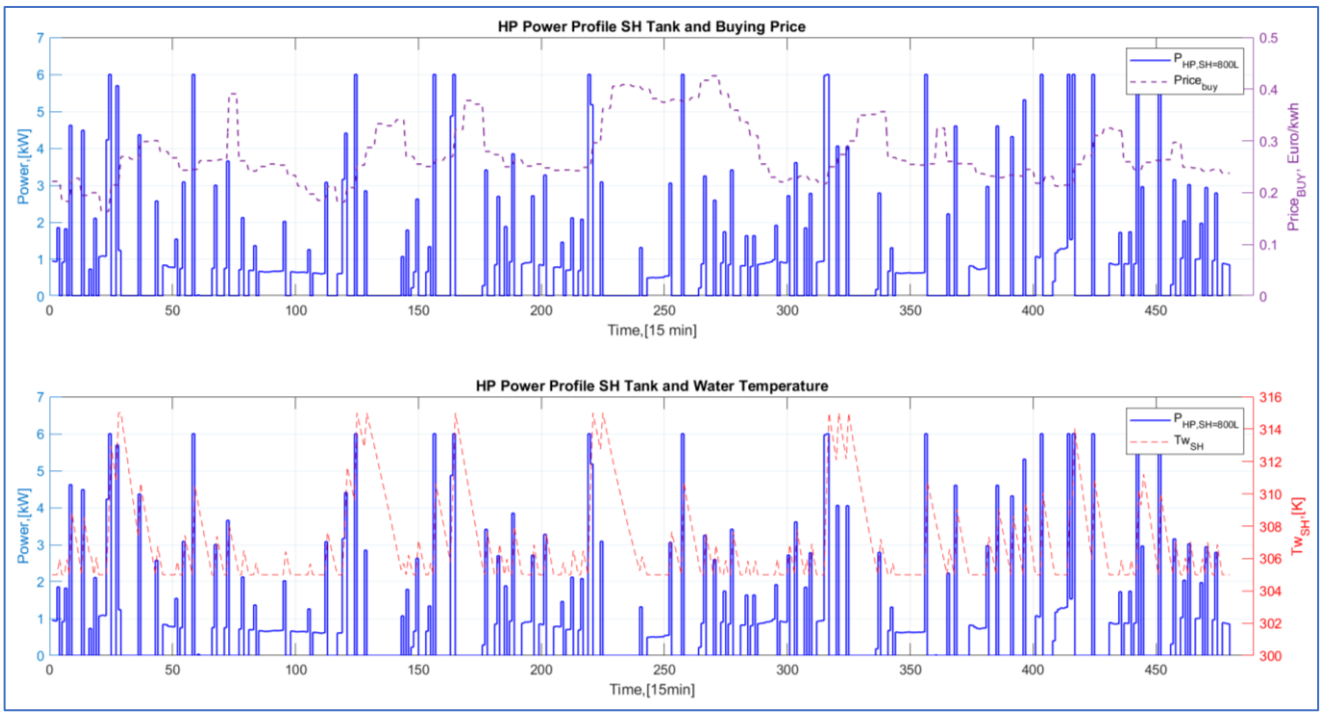

Figure 4-1: Heat pump power profile for SH (High FIT)

On the other hand, when the FIT is halved, there is no significant change in the HP's operation consumption. This can be seen in Figure 4-2 where a comparison of the HP power profile for both cases is displayed. This minimal difference makes sense because in both scenarios the HP tries to minimize its power consumption, but in the reduced FIT, the HP was powered by the BES/EV (see Figure 4-7). Therefore, the FIT itself does not really affect the HP behavior because this device can only withdraw power from the grid.

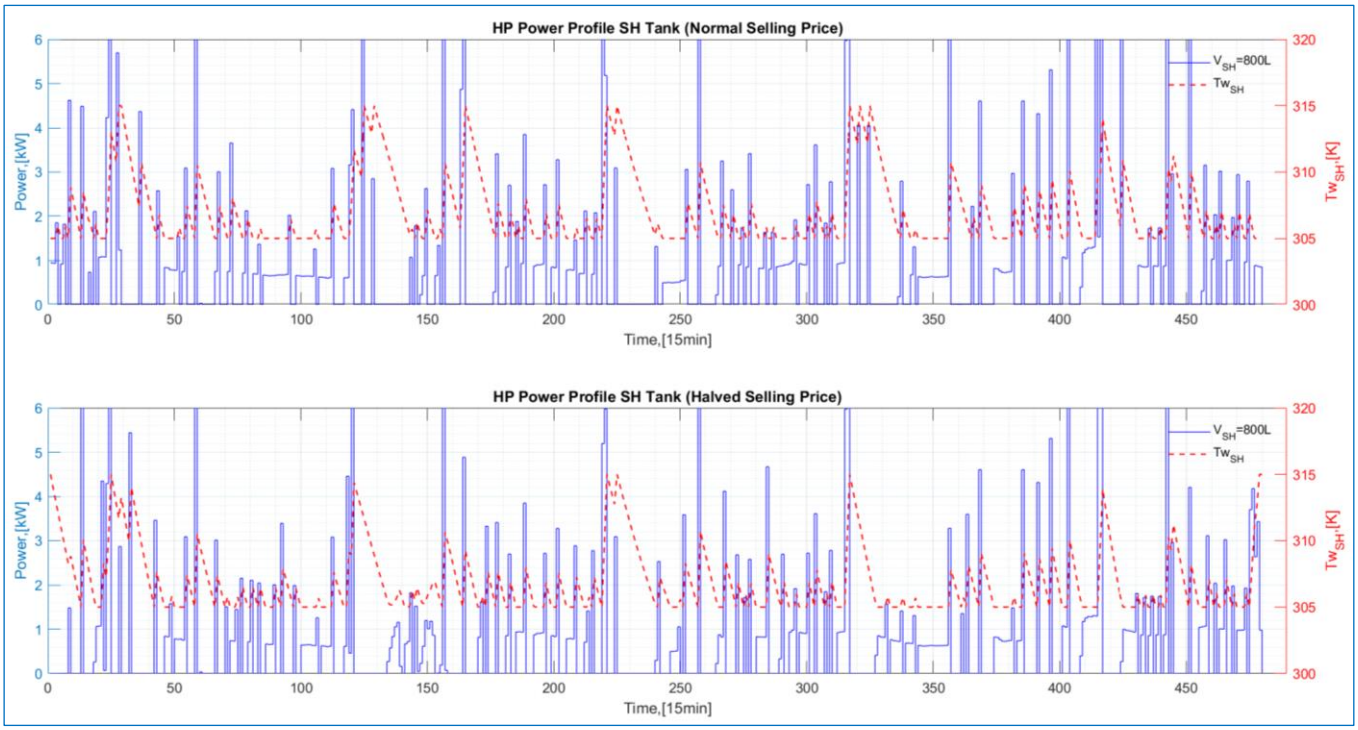

Figure 4-2: HP power profile for SH for normal and halved FIT cases

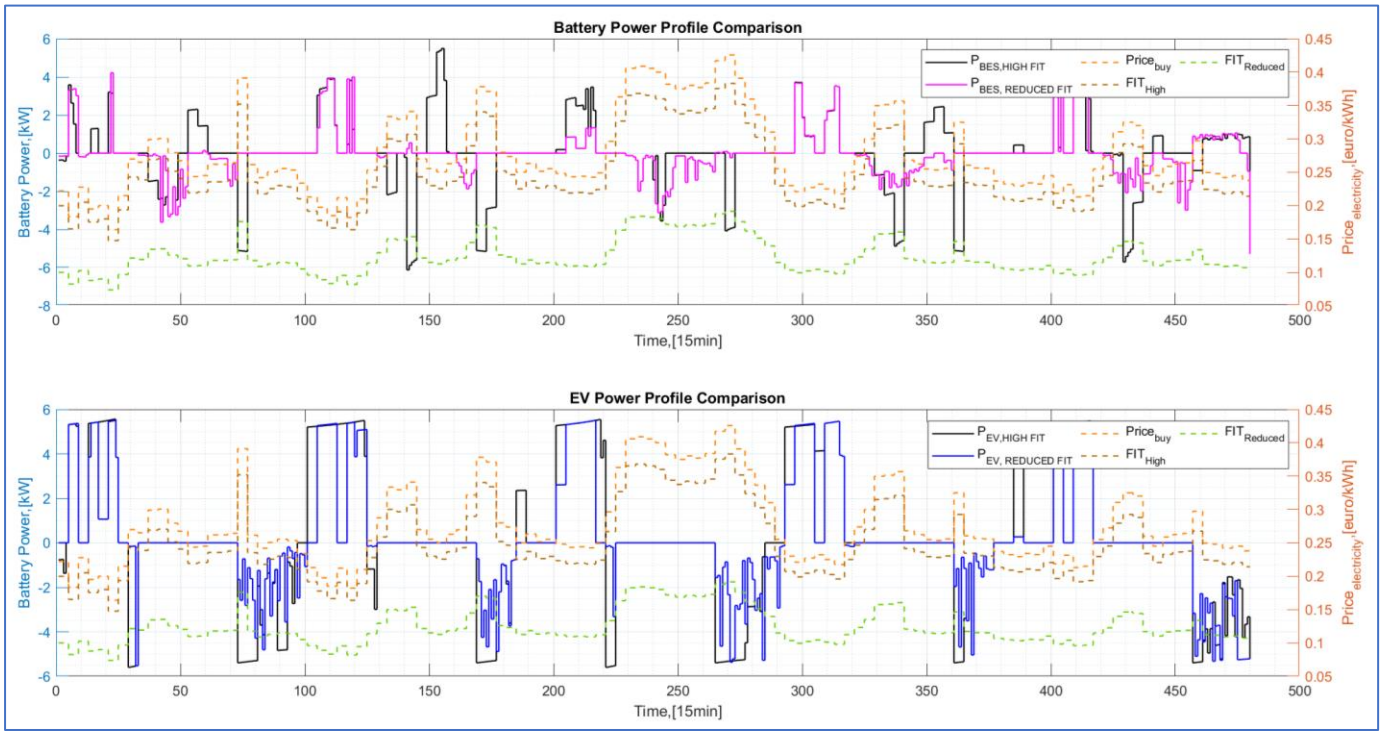

Figure 4-3: BES and EV power profiles for high and reduced FIT cases during winter

Figure 4-3 displays the BES and EV power profiles for the high and reduced FIT cases. In the high FIT scenario, it is evident that the optimized charging strategy is to absorb energy from the grid when the buying prices are low and selling the energy at high prices. Note that the BES and EV during their discharging processes inject most of their energy to grid to get revenues and minimize the costs. When the EV is available at evening, it injects energy to the grid as the selling price is high enough to get more revenues, and it will charge during late night when the buying prices become cheaper.

This has to do with the fact that by having high FIT the minimization strategy is more cost effective when the discharged energy is sold instead of used for self-consumption, thus the system generates revenues and the costs will be minimized. On the other hand, by reducing the FIT to its half, both the BES and EV reduced their depth of discharge and this energy was not injected to the grid but fed into the HP and the load of the electric appliances of the building (see figure 4-7). Also, during charging, the energy consumed by the BES and EV has decreased to minimize the energy costs. This can be evidenced by looking at the width of the positive power profiles, thus a less width profile indicates less energy consumption during those specific times. As result of this, the BES and EV will degrade less than in the high FIT case, thus the degradation costs will be lower in the reduced FIT scenario.

On the HP side for DHW, Figure 4-4 displays the HP power profile for DHW and the water temperature dynamics. DHW will depend on the behavior of the household's inhabitants, so the HP operation is constrained to maintain an adequate temperature level in the DHW tank to satisfy this demand whenever is required. Like the SH case, the HP operates most of the times at the lowest possible prices to minimize the operational costs and keep the constraints satisfied. It can be seen there are sometimes where the HP works at high prices, and this is related to the nature of the DHW demand. Nevertheless, the optimization model makes the HP work in a power level such that the costs at those high prices become reduced by keeping the tank at the low temperature limit.

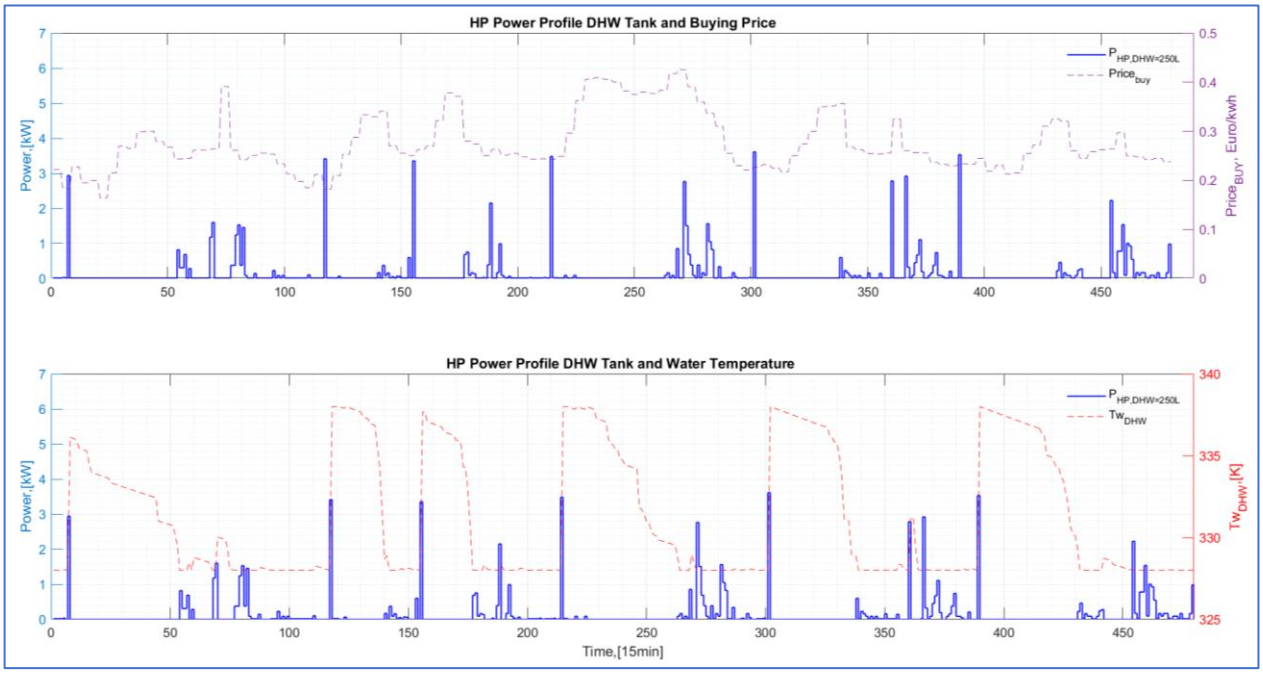

Figure 4-4:Heat pump power profile for domestic hot water (DHW) for 5 days in 15 min resolution

Furthermore, the initial and final temperatures of the storage tanks have been determined by letting the optimization model find the best initial and final points for these variables. From figures 4-1 and 4-3, it is shown that the optimal initial and final temperatures of the storage tanks on each day equal to the lower limits, being 305 K and 328 K for SH and DHW, respectively. This has to do with the fact that at those times, the prices are higher than the next one, therefore, the model decides to make the HP work at a minimum capacity to maintain these temperatures while meeting the building's demands. As explained for the SH, there is no significant difference during the operation of the HP for the high and reduce FIT for DHW either. However, the HP will be fed by the discharge of the BES and EV as showed in figure 4-7.

4.1.2. Building's temperature dynamics, SH and DHW demands

From the energy balance performed in section 3, the temperature of the building can be estimated. Figure 4-3 displays the household's temperature in time, the ambient temperature, and the SH and DHW demands. As expected, when the ambient temperature is low, the SH heat demand increases, and the building is heated up to keep the thermal comfort within the allowed limits.

The demand of the building is of paramount importance because it influences the behavior of the heat pump and its power consumption. High SH demands due to a poor insulation of the building will cause the HP to increase its energy consumption because more heat will be needed to keep an adequate temperature in the storage tank. Therefore, the flexibility potential of the HP will be reduced.

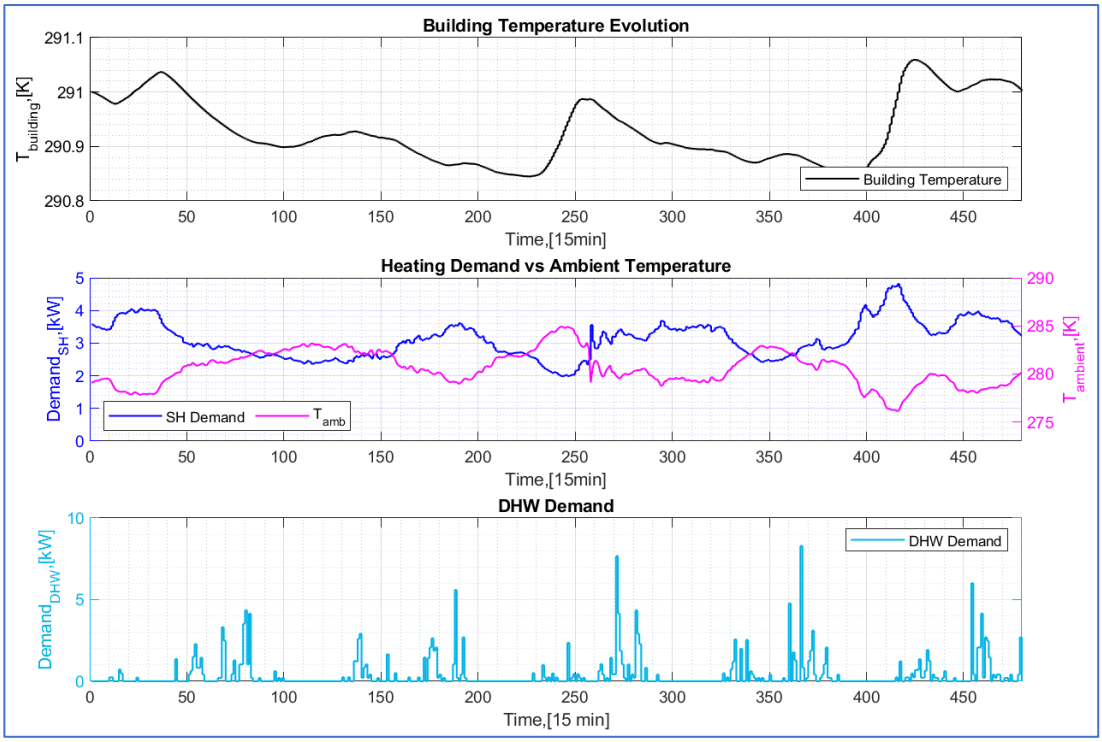

Figure 4-5: Household's temperature, SH and DHW demands

4.1.3. PV-BES-EV-HP system behavior and total grid costs

Figure 4-7 shows the optimized power profiles of the different components of the system for the high FIT case. The simulation was carried out for five days, but for the purpose of appreciation only two days are displayed. The behavior of the system has been split into two parts. The top graph represents the power profiles of the components connected to the DC side of the inverter. The bottom graph corresponds to the AC side of the power converter where the grid, the building's load, and the heat pump are connected. The AC and DC side of the power inverter can be appreciated in the following figure.

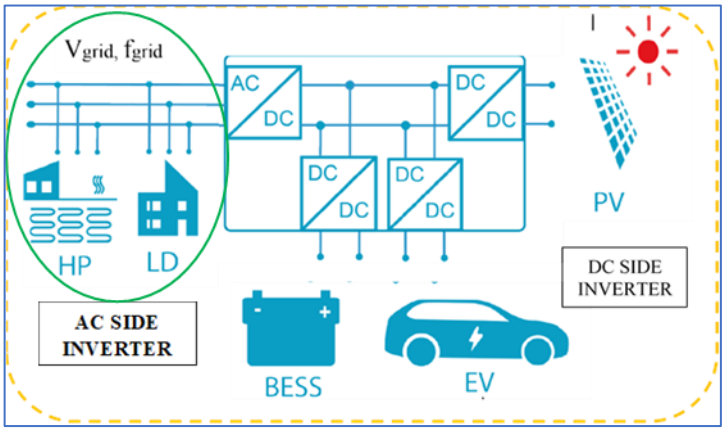

Figure 4-6: AC and DC connections of the different components in the power inverter

Additionally, a sign convention for the direction of the power flows of the components of the system has been used. This is detailed in table 4-4. This sign convention will help to understand better figure 4-7.

Table 4-4: Sign convention for power flows of the all-electric system

Variable	Sign	Convention
P_{grid}	+	Injection of power to the grid
	-	Consumption of power from the grid
P_{BES}	+	Charging/consumption of power
	-	Discharging/injection of power
P_{EV}	+	Charging/consumption of power
	-	Discharging/injection of power
P_{inv}	+	Injection of power
	-	Consumption of power
P_{HP}	+	Consumption of power
P_{Load}	+	Consumption of power

From Figure 4-7, it can be seen there is limited interaction between the BES-EV with the HP and the load of the building (see orange circles). Part of the discharged energy is consumed by the loads, and the excess is sold to the grid. This is result of having high FIT because the minimization strategy is more cost effective when the discharged energy is sold instead of being used for self-consumption of the system. On the PV production side, PV electricity was used mainly to charge the battery at times of not too high prices. Nevertheless, most of the time the system prefers to sell PV energy at the highest FIT to minimize the costs even further (see light blue circle).Therefore, PV self-consumption is not performed. Additionally, the HP operation is influenced by the power consumptions of the BES, EV and the load of the building. Therefore, the HP's power consumption will adapt to not violate the capacity constraint of the grid. For instance, the load of the building between time steps 40-50 is consuming power at high prices, so the optimization determines that either the BES, the EV or the HP will operate with low power consumption to reduce the costs. Consequently, the HP operation is shifted towards the prior or next lower price. Additionally, when the EV is available in the evening, it injects energy to the grid to get more revenues, and it charges during late night when the buying prices become cheaper. This proves that EV when performing V2G can play a vital role in the energy cost minimization and stability of the grid for future energy systems.

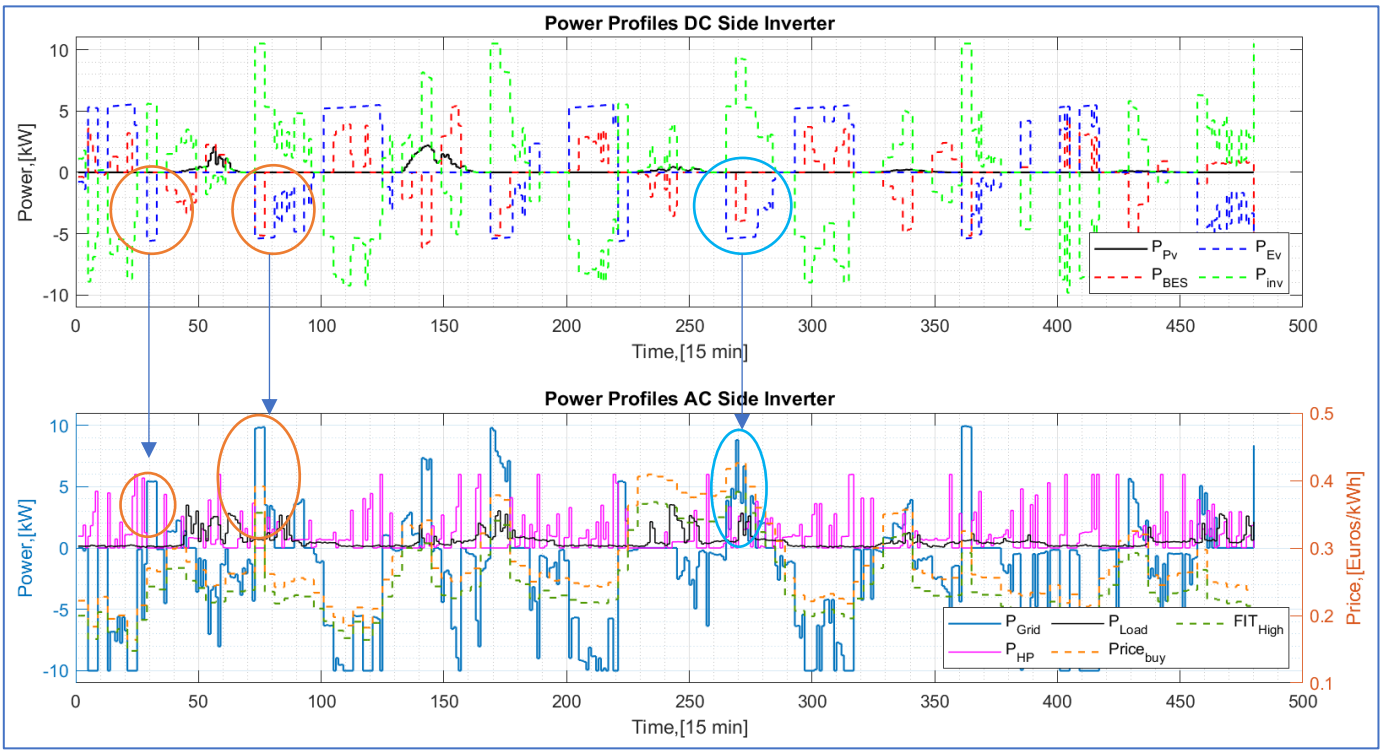

Figure 4-7: System power profiles for high FIT case

On the other hand when the FIT is halved, no selling of energy towards the grid occurs, so the only way for the system to minimize the where operational costs is to enhance self-consumption and reduce the energy intake from the grid. This can be seen in Figure 4-6 where a comparison of the system behavior for the high and halved FIT is displayed .The battery and the EV regulates its energy consumption by decreasing the time needed for charging (see orange circles). Besides, the cycles for charging and discharging are decreased, thus the energy is stored for longer periods. On the other hand, the discharging process is done gradually to feed the load and the HP. Notice how in the high FIT case the BES and EV release all the stored energy to inject it to the grid and generate more revenues, while in the halved price, both discharge gradually while feeding the HP and the load of the building.

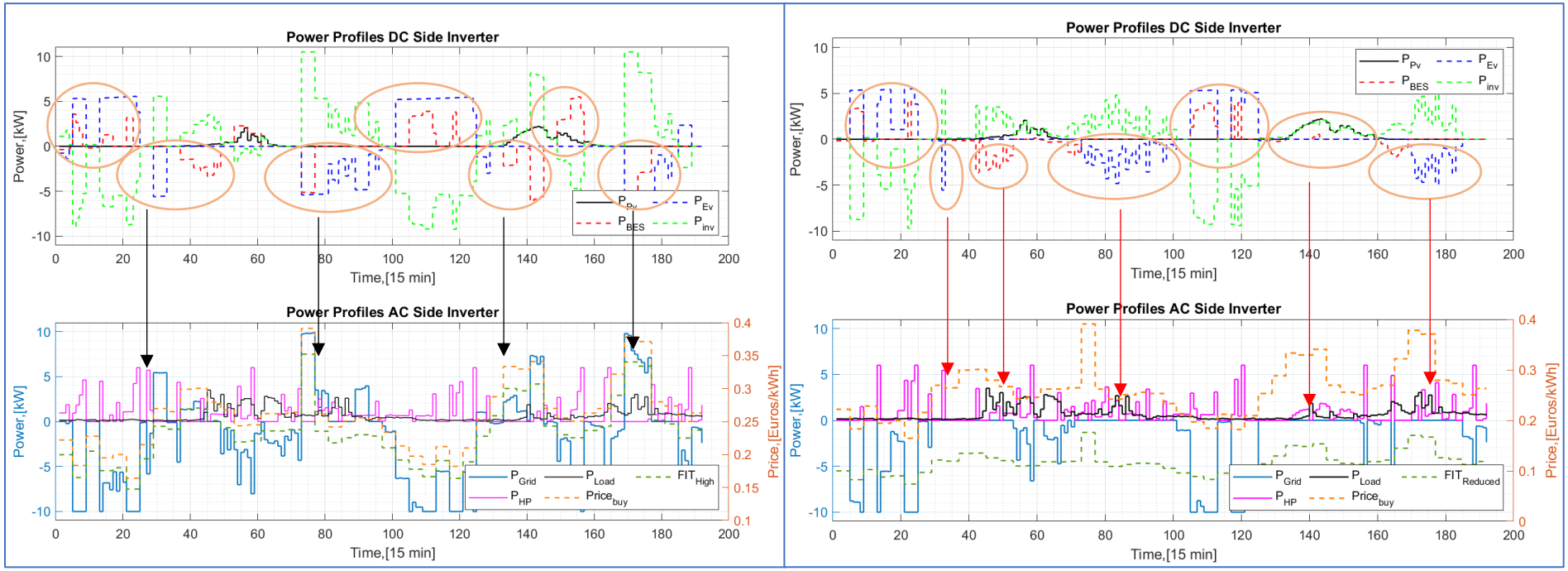

Figure 4-8: System power profiles for high and reduced FIT cases (2 days).

The red arrows indicate the points where self-consumption takes place. In the halved FIT, self-consumption is enhanced to minimize the energy costs because there is no injection of energy towards the grid, thus no revenues are obtained. Consequently, the operational strategy of the system has changed towards reducing the energy intake from the grid by using the BES and EV stored energy. This confirms the hypothesis stated at the beginning of this chapter that decreasing the FIT will enhance self-consumption and reduce the power exchanges with the grid.

It has been analyzed how the cumulative energy of the grid evolves for both cases. Figure 4-9 displays the comparison between the cumulative energy curves of the power intake and power injection for both cases. It is evident that in the reduced FIT no energy is injected to the grid, thus no revenues will be obtained, thus the system reduces its energy intake from the grid to minimize the energy costs as self-consumption has been enhanced. This is of paramount importance for future systems as more renewable energies will be integrated for electricity generation and self-consumption becomes a critical component in the frequency and voltage regulation of the grid. The plateaus formed in the cumulative energy curves give a hint of the flexibility of the system.to reduce the interaction with the grid. In the reduced FIT case, the plateaus in the energy intake curve are wider than in the normal FIT as result of the self-consumption of the system.

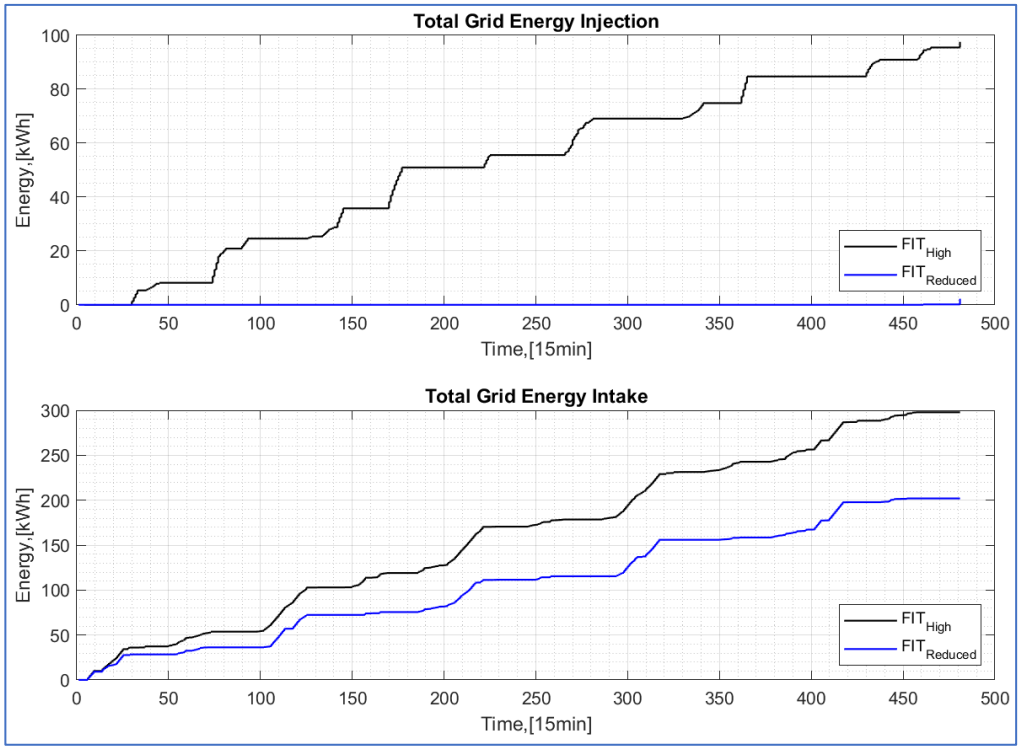

Figure 4-9: Grid cumulative energy curves for normal and reduced FIT cases

The total minimized operational costs have been calculated for the normal and halved FIT cases and compared to a reference case where no optimization was performed. In the non-optimized case, the EV and the BES cannot allocate the injection of energy to the grid as no demand response program is performed. In this way, the BES is charged with the PV production, and it is used to feed the load of the building and the HP in the evening, while the EV is charged upon arrival at 18:00 hours. To represent the HP load, the SH and DHW demands where converted into electricity demands by using an averaged CoP of 3.5 based on the regression model showed in equation 3-9. This intends to simulate the continuous operation of the HP where no operational flexibility is accounted for, so the use of thermal storage components was not included. Additionally, PV costs together with EV and BES degradation costs are also included to determine the total operational energy costs of the system.

Figure 4-10 depicts the behavior of the uncontrolled integrated system for 5 days during winter with an hourly resolution. It is important to notice that under this uncontrolled scheme, the energy consumption takes place at low and high prices. Furthermore, it is clear how the battery charges using the PV energy available, while the excess is fed mainly to the load and the HP. The discharge of the BES in the evening is used by the load and the HP. Besides, the charge and discharge cycles of the battery are considerably lower than in the optimized case. Additionally, the HP power profile is continuous because it is used to directly satisfy the heat demand of the building.

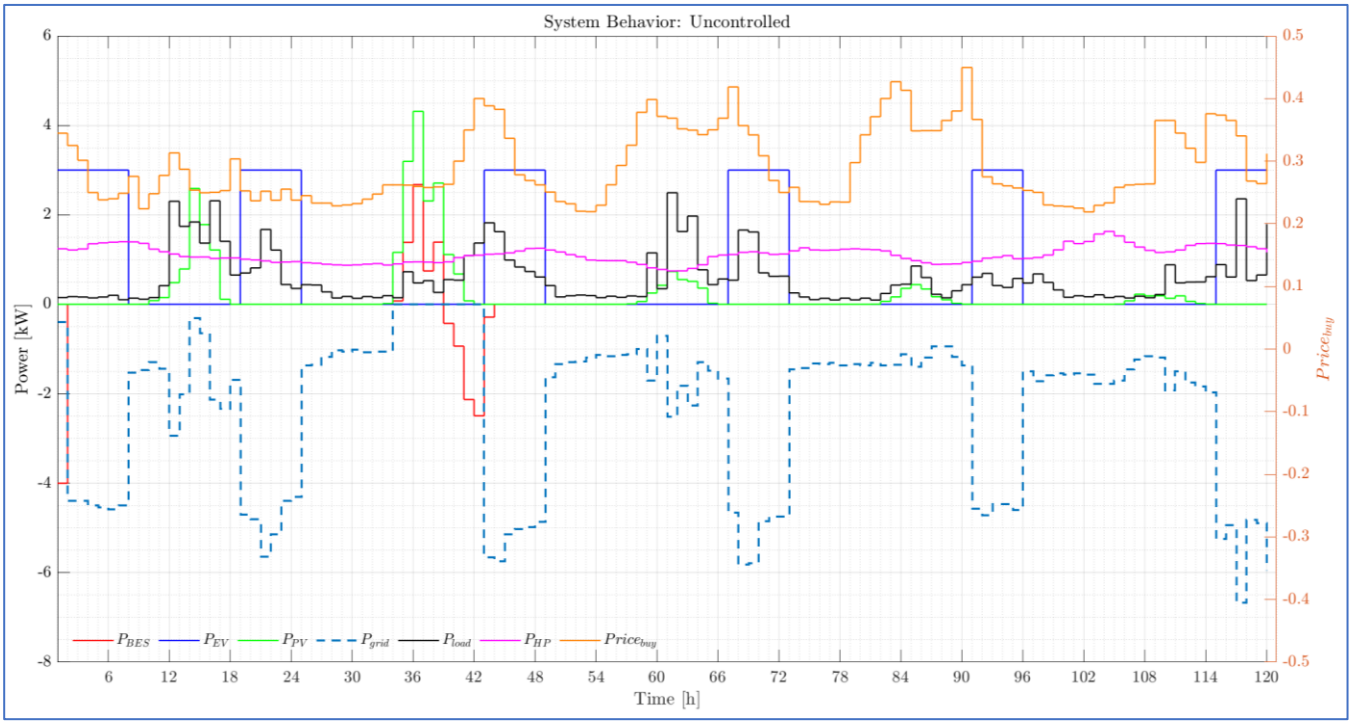

Figure 4-10: System grid operational costs evolution and grid energy intake/injection

Thus, it was calculated that the total minimized energy costs in the high FIT case are 42.92 € per 5 days of operation. This means that during the whole winter season, a total minimized energy cost of 755.40 € will be obtained. On the other hand, the total energy costs of the uncontrolled system are 85.21 € for the 5 days of operation. This means a seasonal cost of approximately 1500 €. In this way, the optimized system generates a net cost reduction of around 50%. Additionally, the degradation costs for the BES and EV are higher in the optimized case than in the non-optimized. This is result of the continuous power exchanges that the EV and BES have with the grid, so more charging/discharging cycles are experienced, thus both degraded further. For the halved FIT case, it was calculated that the total minimized energy costs are 47.26 € per 5 days of operation. This means a seasonal cost of 832 €. Compared to the non-optimized case where the FIT has been also reduced to have a fair comparison, this represents a 45% in costs reduction. Even though the halved FIT case produces 5% less in costs savings, the energy intake from the grid is significantly lower than in the normal FIT. This is result of reducing the interaction with the grid by enhancement of self-consumption. Thus, 28% in the energy consumption from the grid has been reduced. Table 4-5 and 4-6 summarize the results of the comparison between the normal and halved FIT cases with the non-optimized system.

Table 4-5: Optimized (Normal FIT) and Non-Optimized System's TOC Comparison

Non-Optimized											**Δ TOC**
V_{SH} L	**HP kWh**	**Grid Drawn kwh**	**Grid Fed kWh**	**Grid Expenses €**	**Grid Revenues €**	**Grid Cost €**	**PV cost €**	**BES Cost €**	**EV Cost €**	**TOC €**	
----	**118.40**	280.79	0	82.72	0	**82.72**	0.418	1.40	0.67	**85.21**	
Optimized Normal FIT											**- 49.63 %**
V_{SH} L	**HP kWh**	**Grid Drawn kwh**	**Grid Fed kWh**	**Grid Expenses €**	**Grid Revenues €**	**Grid Cost €**	**PV cost €**	**BES Cost €**	**EV Cost €**	**Min. TOC €**	
800	**118.13**	297.84	97.60	68.48	29.90	**38.58**	0.418	1.73	2.19	**42.92**	

*The results correspond to an operation for 5 days.

Table 4-6: Optimized (Reduced FIT) and Non-Optimized System's TOC Comparison Winter

Non-Optimized											Δ TOC
V_{SH} L	HP kWh	Grid Drawn kwh	Grid Fed kWh	Grid Expenses €	Grid Revenues €	Grid Cost €	PV cost €	BES Cost €	EV Cost €	TOC €	
----	**118.40**	280.79	0	82.72	0	**82.72**	0.418	1.40	0.67	**85.21**	
Optimized Reduced FIT											**-44.54 %**
V_{SH} L	HP kWh	Grid Drawn kwh	Grid Fed kWh	Grid Expenses €	Grid Revenues €	Grid Cost €	PV cost €	BES Cost €	EV Cost €	Min. TOC €	
800	**117.65**	201.99	2.23	44.61	0.24	**44.37**	0.418	0.96	1.51	**47.26**	

*The results correspond to an operation for 5 days.

On the other hand, when comparing the high and reduced FIT cases, it can be noticed that the degradation costs for the BES and EV are smaller in the second case. This is result of experiencing less depth discharges and reducing the interactions with the grid, thus less degradation occurs by having a smooth operation of the storage devices.
Additionally, the operational costs of the HP in the normal FIT case and the non-optimized case have been calculated. For the reduced FIT it is not possible to perform this analysis because the HP is fed by the BES and the EV and the grid, so it is not possible to know exactly the individual amount of energy consumed from the grid. Thus, the non-optimized case increases the HP's operational costs because there is no flexibility to shift the power requirement at times of low prices. This can be evidenced by calculating the individual operational cost of the HP in both the uncontrolled and optimized cases as shown in table 4-3. The HP operational costs can be obtained by multiplying the HP's energy consumption with the buying electricity price. For the uncontrolled case, it was calculated that the HP has an operational cost of 36.25 €, while in the optimized case, the HP coupled with a tank of 800 L exhibits an operational cost of 30.14 €. This corresponds to a 17% reduction in the HP's operational costs when flexibility and demand response are integrated.

Table 4-7: HP Operational Costs (OC) Comparison Non-Optimized and Optimized system High FIT

Energy Consumption, kWh		Operational Costs (OC), €		Δ OC
Non-optimized	Optimized	Non-optimized	Optimized	-16.86 %
118.40	118.13	36.25	30.14	

Currently, SH demand is satisfied by local gas boilers, waste heat from power plants, and district heat distribution networks [47]. Therefore, the amount of gas avoided using the heat pump for SH has been calculated. To do this, natural gas from Groningen with a low heating value (LHV_{NG}) of 31.68 MJ/m^3 [48], and a local gas boiler with an 80% of conversion efficiency (η_{boiler}) have been selected as study case. Thus, the amount of gas consumed in normal cubic meters (Nm^3) for SH demand can be calculated as follows:

$$GAS_{consumption} = \frac{\dot{Q}_{building,SH} \cdot 3.6}{\eta_{boiler} \cdot LHV_{NG}} \quad 4\text{-}1$$

As showed in table 4-8, 53.13 m^3 of natural gas can be avoided by using the HP for SH purposes for 5 days of operation. In economic terms, this means a reduction of 6 € in the consumer's heating bill for 5 days. If we consider the entire winter season, this will represent a net saving of 88 €. Additionally, to meet the same amount of energy for SH, the HP consumes 75% less energy that the traditional gas system as result of its high energy conversion efficiency.

Table 4-8: Boiler and HP Energy Consumption and Cost Comparison

Gas Boiler					
SH Demand kWh	**$\eta_{GAS-HEAT}$**	**NG LHV MJ/m³**	**Price* €/kWh**	**Boiler, kWh**	**Gas m³**
374	0.8	31.68	0.077	**467.5**	**53.13**
Heat Pump					
SH Demand kWh	**$\eta_{ELEC-HEAT}$**	**-**	**Price* €/kWh**	**HP_{ELEC} kWh**	**Gas m³**
374	3.5		variable	**118.13**	**0**

In conclusion, the optimized system can produce in average 50% of the energy costs reductions as part of the demand response program. Additionally, with a high FIT, the strategy to minimize the energy costs is to sell energy as much as possible to generate more revenues while consuming power at the lowest possible prices. However, self-consumption is not performed as this is less cost effective. On the other hand, when the FIT was reduced, the system experienced less interaction with the grid. In this context, the energy consumption from the grid decreased in 28% as result of enhancing self-consumption Therefore, it can be inferred that the FIT has a significant impact on the operational strategy of the system to minimize the energy costs.

4.1.4. Influence of SH tank size on HP's behavior

The size of the SH tank was changed to assert its influence on the HP operation. This analysis has been performed only for winter because this is the most relevant case for SH demand. Figures 4-11 and 4-12 display the HP operation and water temperature dynamics for different SH tank's sizes. Although the simulation was carried out for 5 days only the results for two days have been plotted to provide a better visualization of the differences between the cases.

With a small tank, the HP switches ON and OFF several times to meet the SH demand of the building. Here, no peak demands are evidenced, and the HP consumes in average 2 kW. This regular operation results in a flattened power profile, which is preferable from the grid point of view as no submit surges of power will be experienced. According to [49] this type of operation is preferred for cases of centralized electricity production with high storage capacities where a continuous electricity supply to the load must be ensured during times where the renewable resource is not available. On the other hand, when the volume increases, the HP shifts its power demand at times where there is less pressure on the grid. This means that the HP experiences peak demands at times of low energy prices to store enough energy in the tank, thus it will not operate at hours of high demands (high prices). In this way, a high tank produces a load shifting effect. This is a good solution to reduce the curtailment of electricity from renewable energies when the electricity demand is low. Therefore, load shifting potential will allow the integration of renewable sources in the future.

For the DHW tank, the size was remained constant as this is categorized as a non-flexible demand, so it cannot be scheduled as in the case of SH because it depends on the needs of the inhabitants of the house. However, the influence of the size of the SH tank in the operation of the HP for DHW has been included as well as it can be appreciated in Figure 4-13. It is noticed that the SH tank size does not affect considerably the operation of the HP for DHW because as mentioned before this will only depend on the behavior of the inhabitants.

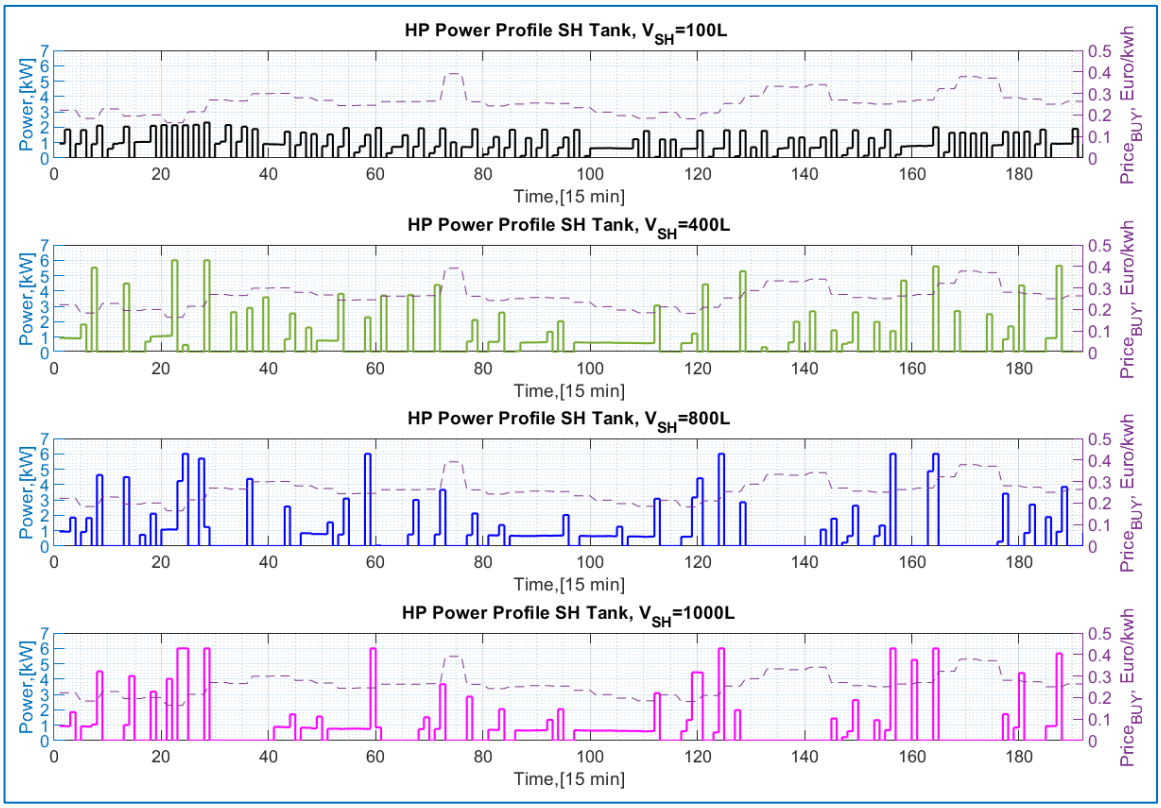

Figure 4-11: Influence of SH tank size on HP operation

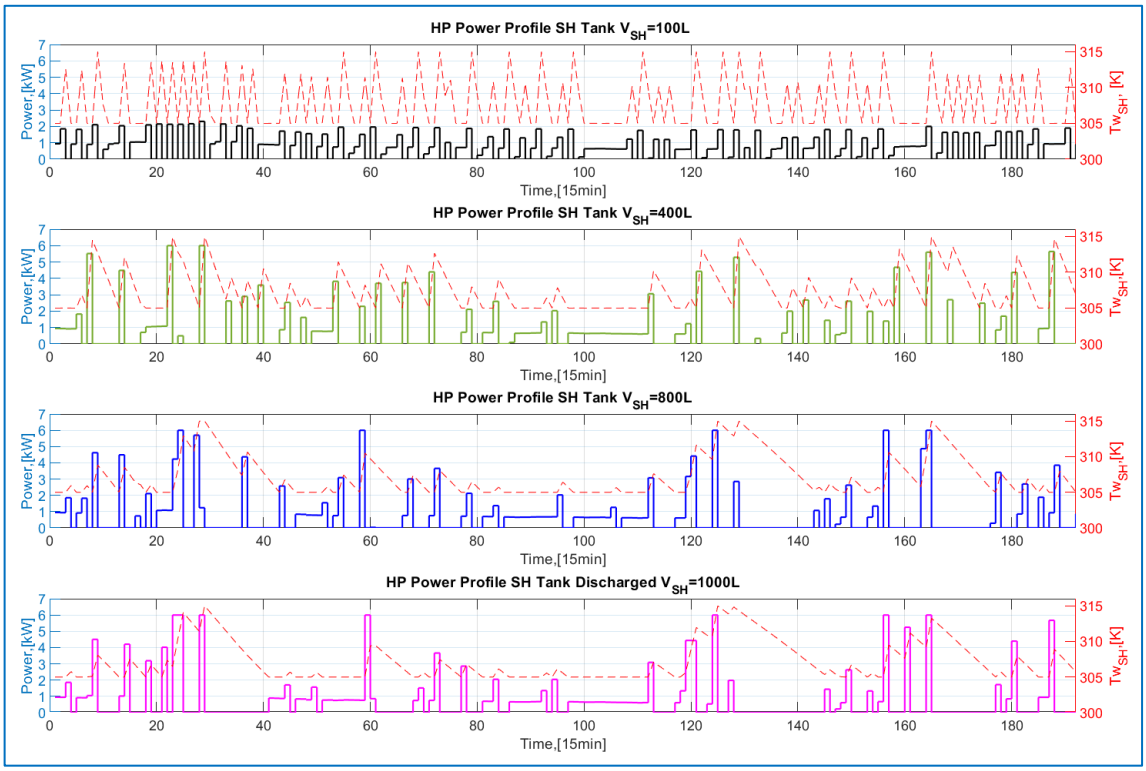

Figure 4-12: Influence of SH tank size on HP operation versus water temperature for SH

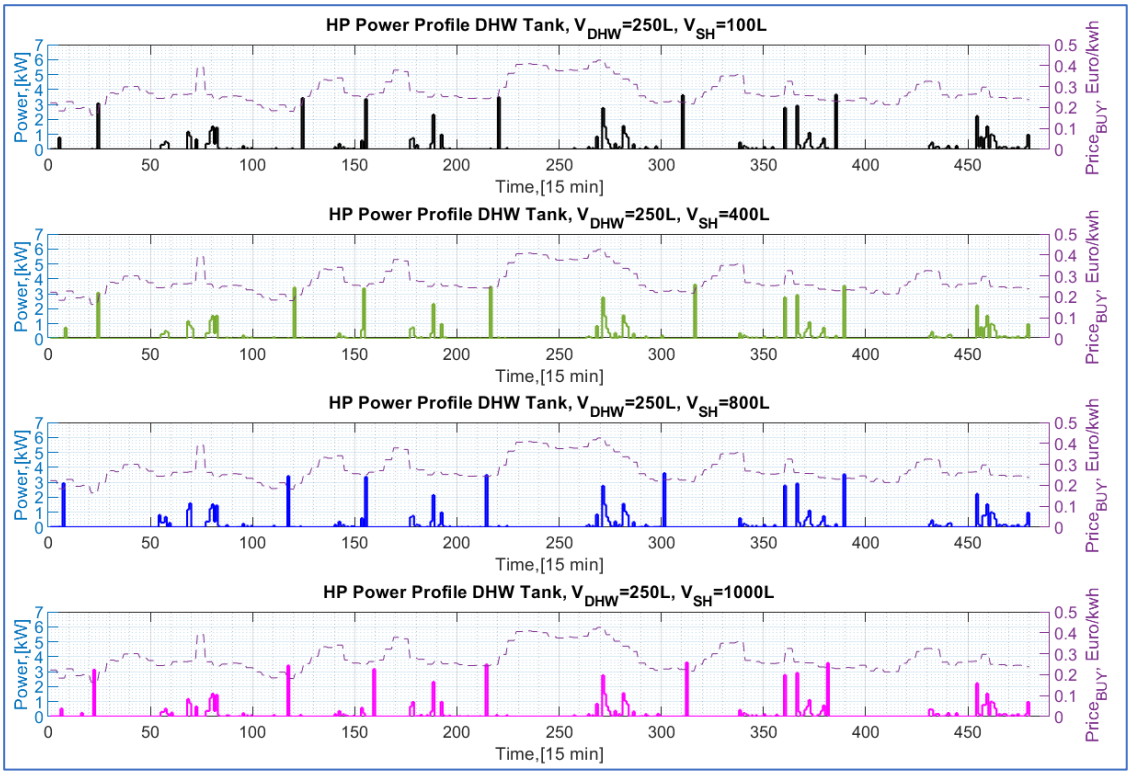

Figure 4-13: HP power profile for DHW for each SH size tank

Concerning the heat losses experienced by the SH tank, it can be seen in Figure 4-14 that when the tank size increases, the heat losses will increase during the entire storage period, thus the HP needs to consume extra power to compensate for these losses.

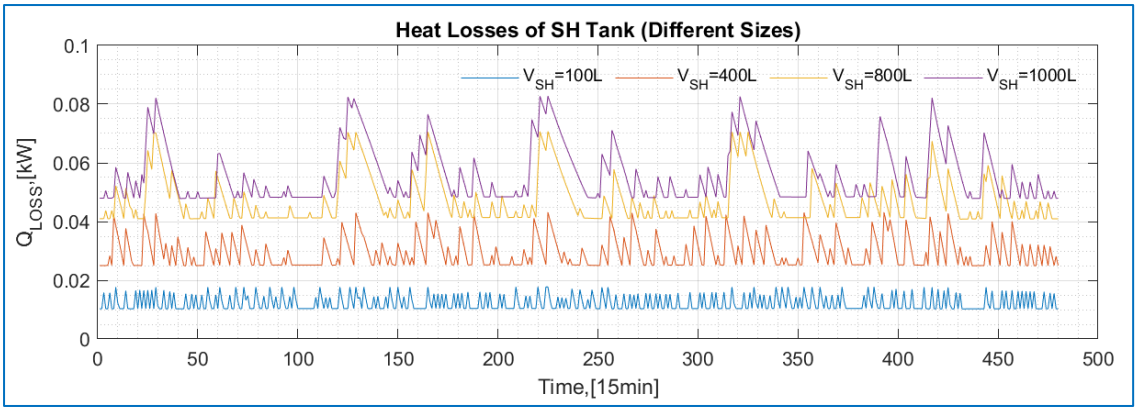

Figure 4-14: Influence of the SH tank size on heat losses

In section 3.2.5, the SH tank was sized to 800 L based on the peak heat demand of the building by equation 3-12. Thus, a fair comparison of the cumulative energy of the HP between the 100 L and the 800 L tanks have been performed to identify the advantages of using a big tank. Figure 4-15 displays the cumulative energy curves for the mentioned sizes. As mentioned before, a higher tank makes the HP consume more power, but more flexibility is obtained. The flexibility can be noticed by the plateaus encircled in orange. They represent the time duration when the HP is not consuming energy from the grid, and the building's SH and DHW demands are met entirely by using the storage tanks. Furthermore, even though the size of the tank is 8 times bigger, the total energy consumption is nearly similar in both cases. Therefore, there is no significant difference between both cases, however, the flexibility potential obtained with the big tank has helped the entire system to reduce the total energy costs. This is showed in

table 4-9 where the energy consumption of the entire system and the minimized costs have been calculated for each tank size.

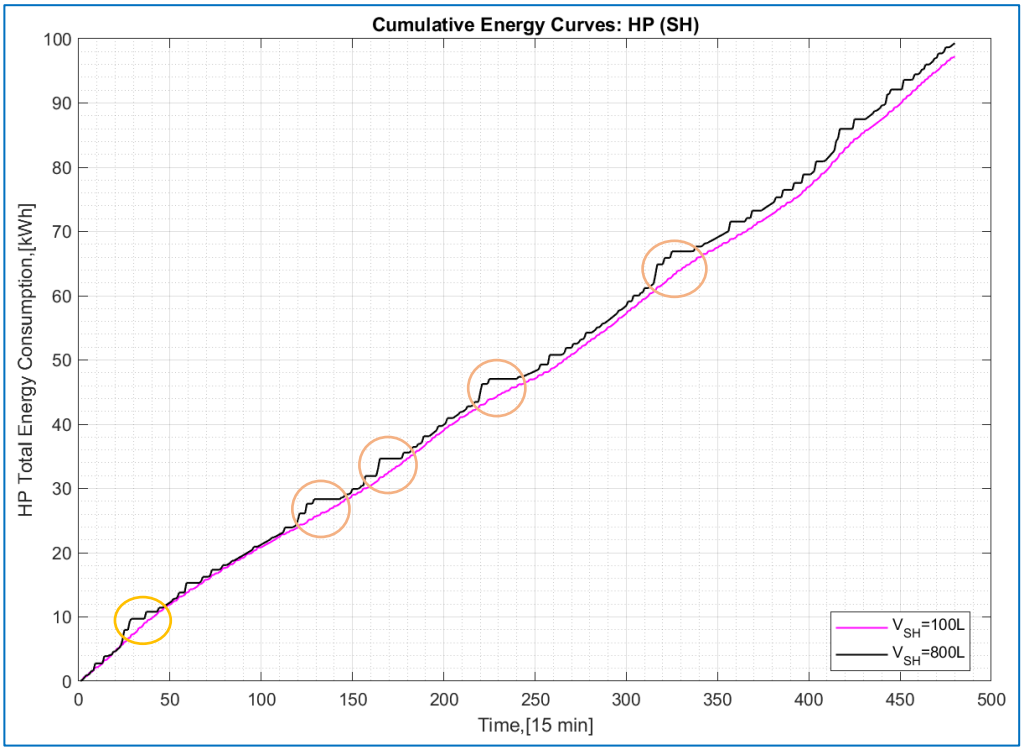

Figure 4-15: Cumulative energy curves for two SH tank sizes

The cost minimization of the system for different SH tank sizes was only performed for the high FIT case because it was demonstrated before that the HP power consumption is not affected by this price signal.

Table 4-9: Influence of Tank's Size on the Minimized TOC (Normal FIT)

V_{SH} L	HP kWh	Grid Drawn kwh	Grid Fed kWh	Grid Expenses €	Grid Revenues €	Grid Cost €	PV cost €	BES Cost €	EV Cost €	Min. Cost €
100	116.09	286.27	88.06	66.10	26.85	39.24	0.418	1.73	2.19	**43.58**
400	116.60	292.89	94.20	67.67	28.77	38.89				**43.23**
800	118.13	297.84	97.60	68.48	29.90	**38.58**				**42.92**
1000	118.83	301.45	100.51	69.37	30.88	38.48				**42.82**

Although with a bigger tank more flexibility is obtained, the reduction in the energy costs is not significative . For instance, a 1000 L tank only generates a reduction of 0.10 € in the total minimized costs when compared to the 800 L case. Thus, using a tank higher than the sized value (800L), obtained in section 3.2.5, will lead to an unnecessary increase in the energy consumption of the system. Considering the minimized energy costs, it is evident that in terms of economics there is not much difference between the costs when using a bigger tank because the HP power consumption remains almost the same. However, the operational strategy of the HP is totally different as demonstrated in Figure 4-11 where with a small tank the HP operates continuously at times of high demands (high buying prices), but with a big tank, the power consumption has been shifted towards times of low demands (low prices). Subsequently, even though the economic benefit is not considerable, the technical benefits are noticeable because the HP can shift its consumption at times of less stress on the grid.

4.2. Summer season

Following the same analysis as in winter, this section will present the results of the optimized system for 5 days of operation. The influence of the FIT on the system's behavior is also studied for this season.

4.2.1. HP operational behavior

Based on the temporal interpolation of the SH using equation 3-1, an average demand of 0.86 kWh per day can be evidenced for the Netherlands. This negligible demand does not motivate a considerable use of the HP as compared to winter. This means that the HP does not require to work at maximum capacity several times, and the model decides that it is better to charge the tank completely once per day at the lowest buying price, happening mostly around 5 and 6 pm. Figure 4-16 displays the operation of the HP for 5 days during summer season.

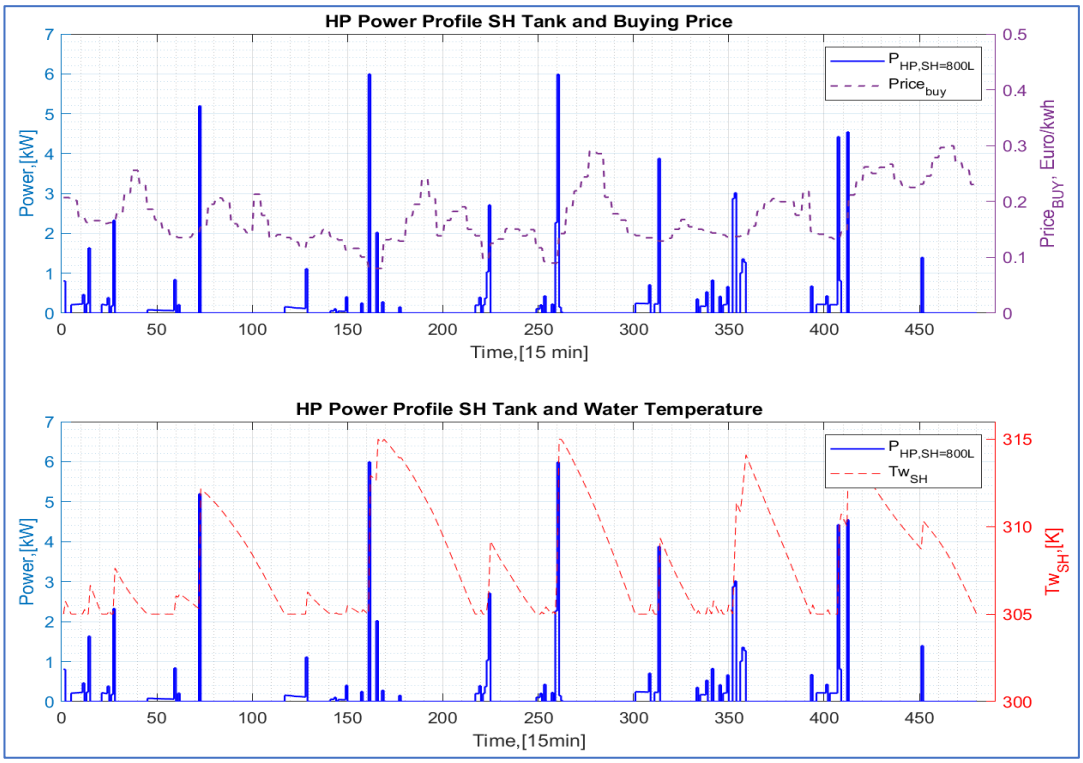

Figure 4-16:HP power profile for SH (High FIT) summer

For the DHW demand, the same data as in winter have been used by assuming the inhabitants do not change their behavior respect to this demand. Therefore, the HP power profile for this demand remains the same, and it is not display in this section.

4.2.2. PV-BES-EV-HP system behavior and total grid costs

Figure 4-17 exhibits the optimized power profiles of the system for the high FIT case. During this season, PV production has a strong participation in the system's operation either for self-consumption or power injection to the grid to increase revenues.

The load and the HP power demands are smaller compared to winter, so it can be expected that the energy costs caused by them will be reduced. As in the winter high FIT case, the operational strategy of the system remains being selling the energy at high prices, and consuming power at low prices. However, the BES, the load, and the HP use part of the PV energy to operate, while in winter this did not happen due to low PV production. At these spots, there is no energy intake from the grid. Nonetheless, a large amount of energy from the PV production, the BES and the

EV are injected to the grid (see black arrows), while self-consumption remains limited even though the system could consume the high PV surplus to reduce the energy consumption from the grid. This means that under a high FIT, self-consumption of renewable energy is not a cost effective strategy for cost minimization.

On the other hand, when the FIT is halved, there is minimum energy sold towards the grid, thus the system has lowered its grid's operational costs by enhancing self-consumption and reducing the energy intake from the grid. In Figure 4-18, a comparison between the power profiles of the system for the high and reduced FIT cases is displayed. It can be noticed that most of the PV is consumed to charge the BES, and if any excess is left, it is injected to the grid. Additionally, the BES and the EV regulates its energy consumption by decreasing the time needed for charging while their depth of discharge has reduced. Besides, their charging/discharging cycles are decreased, since the energy is stored for longer periods, and the discharging process is done gradually to feed the load and the heat pump.

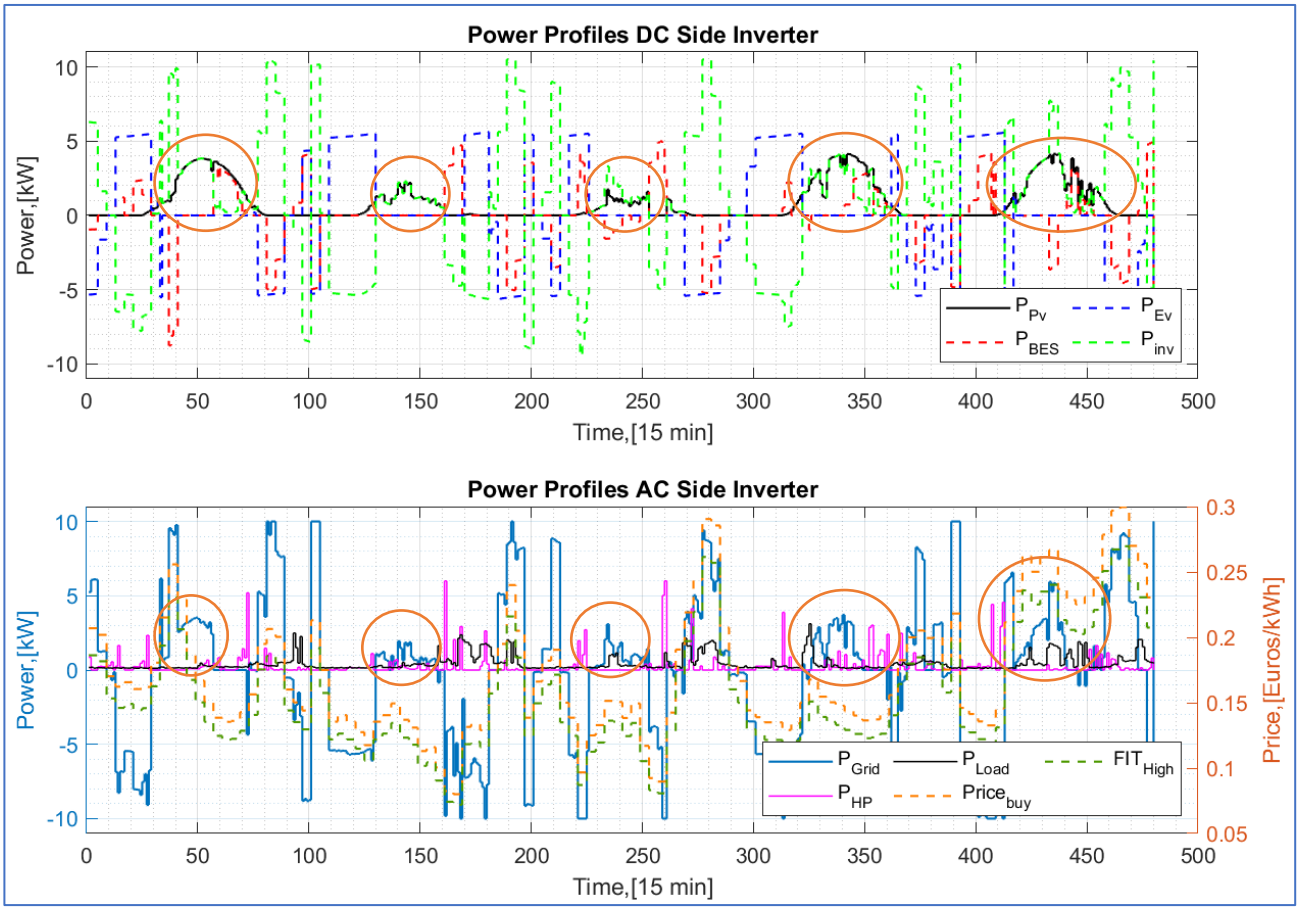

Figure 4-17: System power profiles for high FIT case

In the evening, the BES discharges to meet the demands of the HP and the load, while the EV is barely use for this purpose. Even though the SH demand during summer is almost zero, the coupling of a HP with a thermal system allows to store part of the PV production in the form of heat.

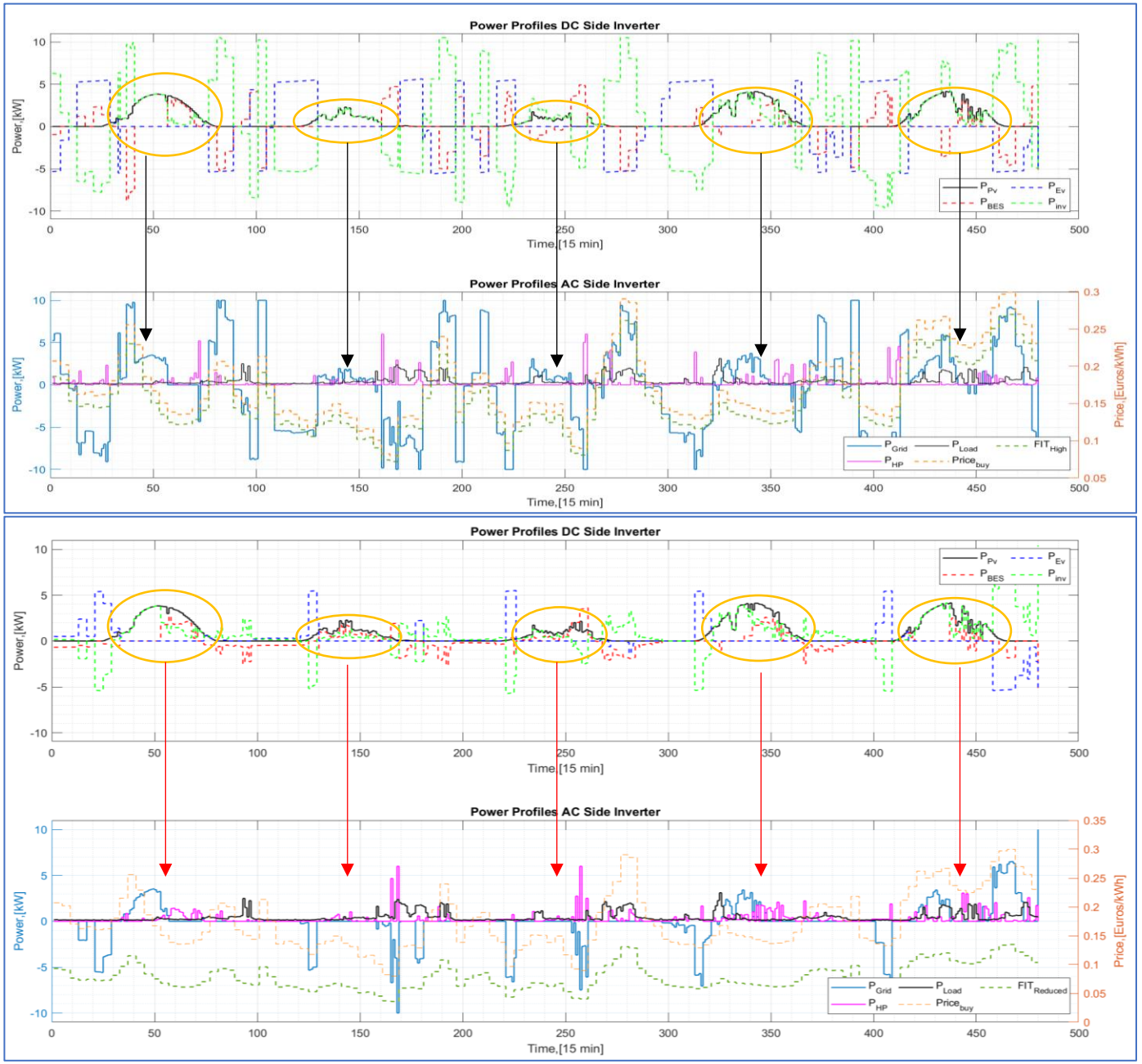

Figure 4-18: System power profiles for high (top) and reduced FIT (bottom)

A comparison between the cumulative energy curves of the power intake and power injection for both cases have been done, and it is showed in Figure 4-19 . Due to enhancement of self-consumption in the halved FIT case, the system has notably reduced the power exchanges with grid. This is of paramount importance for future systems when more renewable energies be integrated for electricity generation. Because self-consumption reduces the demand on the grid, lower amount of energy will circulate through the transmission network decreasing energy losses. Additionally, self-consumption helps to reduce the stress on the grid by decreasing the amount of energy that can be suddenly injected when high FIT may exist. Thus, self-consumption becomes critical to help maintain the voltage and frequency of the grid in cases of high PV and wind electricity production.

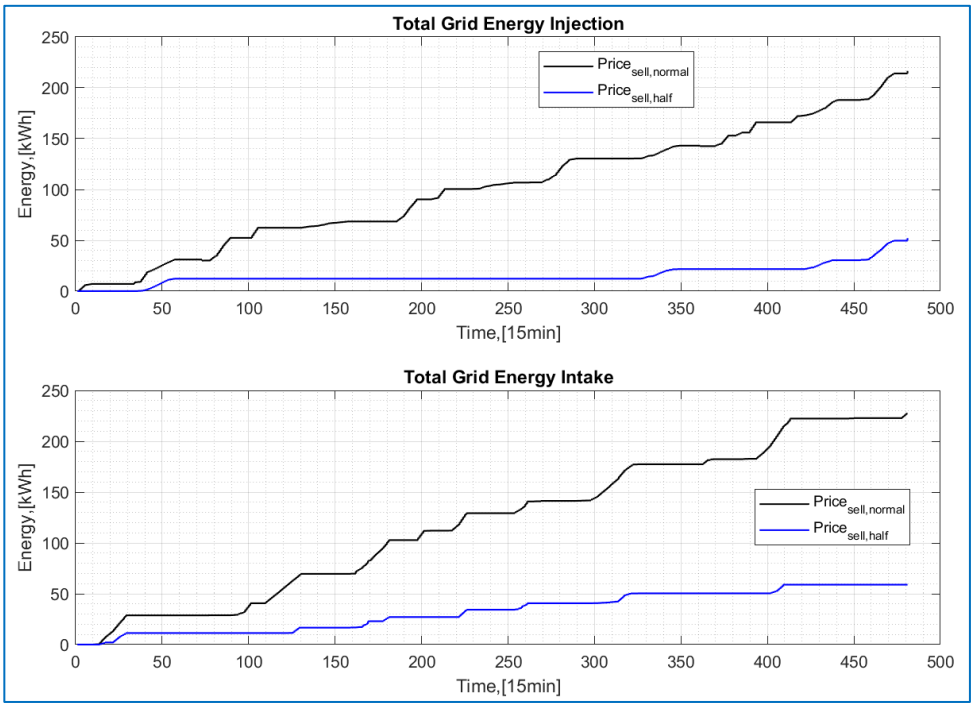

Figure 4-19: Grid cumulative energy curves for high and reduced FIT cases (summer)

The total operational costs of the optimized system for the high and reduced FIT have been calculated and compared to a non-optimized case. In the uncontrolled case depicted in Figure 4-17, the BES charges using the PV energy available, while the excess is partially fed to the load and the HP or injected to the grid. Thus, BES experiences considerable charge and discharge cycles because of high availability of PV energy. On the other hand, the discharge of the BES during the evening is used to feed the electric load of the building and the HP.

In this way, it was calculated that the total minimized energy costs in the high FIT case are -4.88 € for the 5 days of operation. This means that system will generate -87.84 € in revenues for the customer during the whole summer season (90 days) because of the high amounts of energy injected to the grid. On the other hand, the total energy costs of the non-optimized system are 17,47 €. This means a seasonal cost of approximately 314.46 €. Therefore, the optimized system generated a net cost reduction of128% in the high FIT.

For the halved FIT case, it was calculated that the total minimized energy costs are 6.52 € per 5 days of operation. This means a seasonal cost of 117.40 €. Compared to the non-optimized case, this represents a 68% in costs reduction. This is result of reducing the interaction with the grid by enhancement of self-consumption. Thus, both energy consumption and injection have been reduced in 74% and 76%, respectively. Table 4-10 and 4-11 summarize the results of the analysis for the high and reduced FIT cases, respectively.

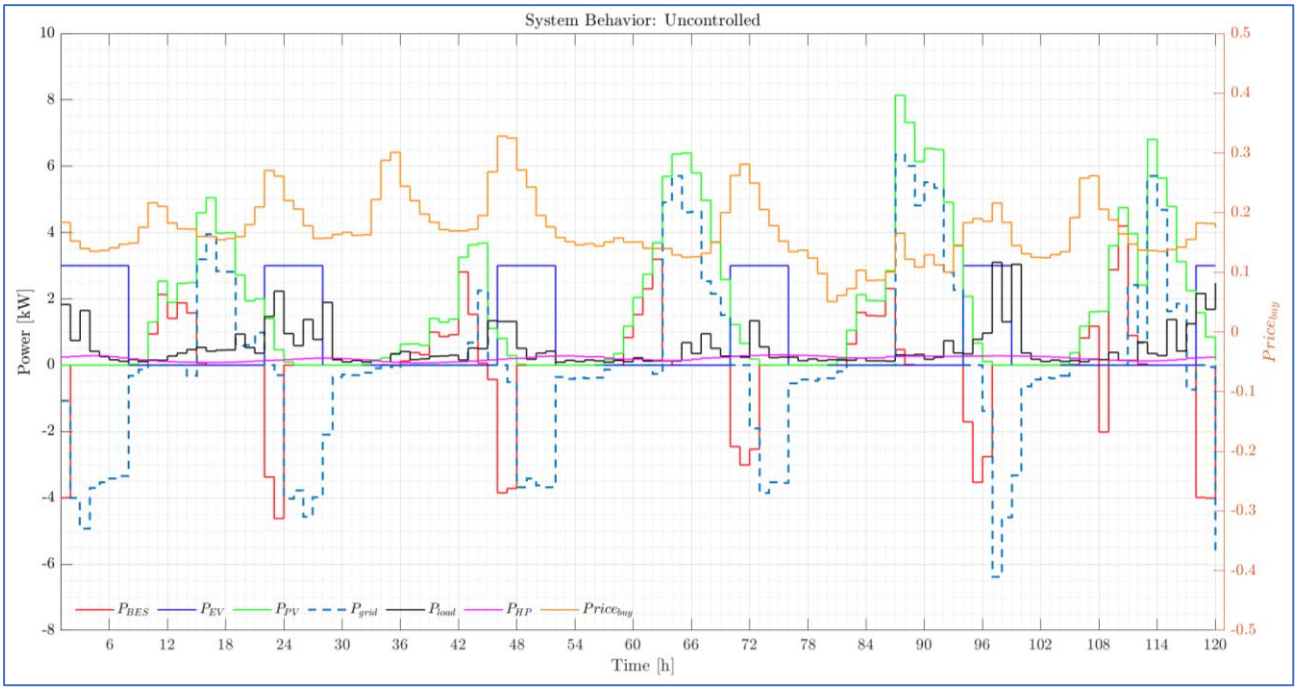

Figure 4-20: Non-optimized system power profile for summer

Table 4-10: Optimized (Normal FIT) and Non-Optimized System's TOC Comparison Summer

Non-Optimized											Δ TOC
V_{SH} L	**HP kWh**	**Grid Drawn kwh**	**Grid Fed kWh**	**Grid Expenses €**	**Grid Revenues €**	**Grid Cost €**	**PV Cost €**	**BES Cost €**	**EV Cost €**	**TOC €**	**-128%**
----	**34.10**	101.67	97.05	18.06	5.83	**12.24**	3.16	1.40	0.67	**17.47**	
Optimized Normal FIT											
V_{SH} L	**HP kWh**	**Grid Drawn kwh**	**Grid Fed kWh**	**Grid Expenses €**	**Grid Revenues €**	**Grid Cost €**	**PV Cost €**	**BES Cost €**	**EV Cost €**	**Min. TOC €**	
800	**33.98**	227.08	216.64	30.69	43.20	**-12.51**	3.16	1.93	2.54	**-4.88**	

Table 4-11: Optimized Reduced FIT) and Non-Optimized System's TOC Comparison Summer

Non-Optimized											Δ TOC
V_{SH} L	**HP kWh**	**Grid Drawn kwh**	**Grid Fed kWh**	**Grid Expenses €**	**Grid Revenues €**	**Grid Cost €**	**PV Cost €**	**BES Cost €**	**EV Cost €**	**TOC €**	**-68 %**
----	**34.10**	101.67	97.05	18.06	2.92	**15.14**	3.16	1.40	0.67	**20.37**	
Optimized Reduced FIT											
V_{SH} L	**HP kWh**	**Grid Drawn kwh**	**Grid Fed kWh**	**Grid Expenses €**	**Grid Revenues €**	**Grid Cost €**	**PV Cost €**	**BES Cost €**	**EV Cost €**	**Min. TOC €**	
800	**33.91**	58.97	52.16	7.23	5.50	**1.73**	3.16	0.96	0.67	**6.52**	

4.3. HP flexibility potential analysis

To determine the flexibility potential of the heat pump during SH operation, it is necessary to establish how much of the SH demand has been satisfied by the storage tank during times of high electricity prices. Due to the flexibility offered by the HP coupled with a storage tank, the HP can be scheduled to operate at low prices to charge the storage tank to have enough energy to cover the SH demand later. This means that the optimization model anticipates to those times where the HP's operation will not be economically feasible for the system, and it forces the HP to operate earlier to minimize the costs while keeping the SH demand met. This results in a load shifting effect where the HP demand has been moved towards times of low energy prices to pre-heat the storage tank. To understand this effect, a load shifting indicator has been calculated according to [49] only for winter where the SH demand is significant. The following equations have been used:

$$LS_{DSM,t} = \frac{P_{HP,t}^{SH} - P_{SH,t}^{Demand}}{P_{SH,t}^{Demand}} \quad 4\text{-}2$$

$$P_{SH,t}^{Demand} = \frac{\dot{Q}_{build,SH,t}}{COP_{SH,t}} \quad 4\text{-}3$$

where $LS_{DSM,t}$ is the load shifting potential of the HP at time step t, $P_{HP,t}^{SH}$ is the power consumption at time step t of the HP for SH when performing a demand response effect, and $P_{SH,t}^{Demand}$ is the power consumption corresponding to the original SH demand converted into electricity power demand. $LS_{DSM,t}$ is positive when the HP increases the power consumption compared to the original demand as it charges the tank to have enough stored energy that can be used later, and it is negative when the HP is turned off and the demand is entirely or partially met by the SH storage tank. If $LS_{DSM,t}$ is equal to -1, the SH demand of the building is entirely satisfied by the energy stored in the storage tank as the power consumption of the HP equals to zero.

The amount of energy that have been shifted can be found by multiplying the values where the LS_{DSM} indicator is negative and the original SH demand. To have a better description of this analysis, Figure 4-21 displays the dynamics of the LS_{DSM} indicator for winter during the five days of operation of the system. Here, the green areas correspond to those times where the SH storage tank covers the SH demand of the building and the HP does not operate because the electricity prices are high, while the blue areas correspond to the times where the electricity prices are low and the HP operates to meet the SH demand of the building and to charge the SH tank. For summer, this analysis was not performed as SH is heavily needed during winter, for it is preferred to study this case. However, if cooling were included during summer, the same analysis could be performed.

In this way, the SH demand has been shifted towards times of low electricity demand by increasing the power consumption of the HP to charge the storage tank, resulting in a demand response effect. Consequently, it was calculated that 56.09 kWh of the SH demand in terms of electricity consumption has been shifted towards low buying price times (low energy demand periods). In other words, 56.09 kWh of electricity has been avoided during times of high buying prices (high energy demand periods), and it has been distributed among times of low demand.

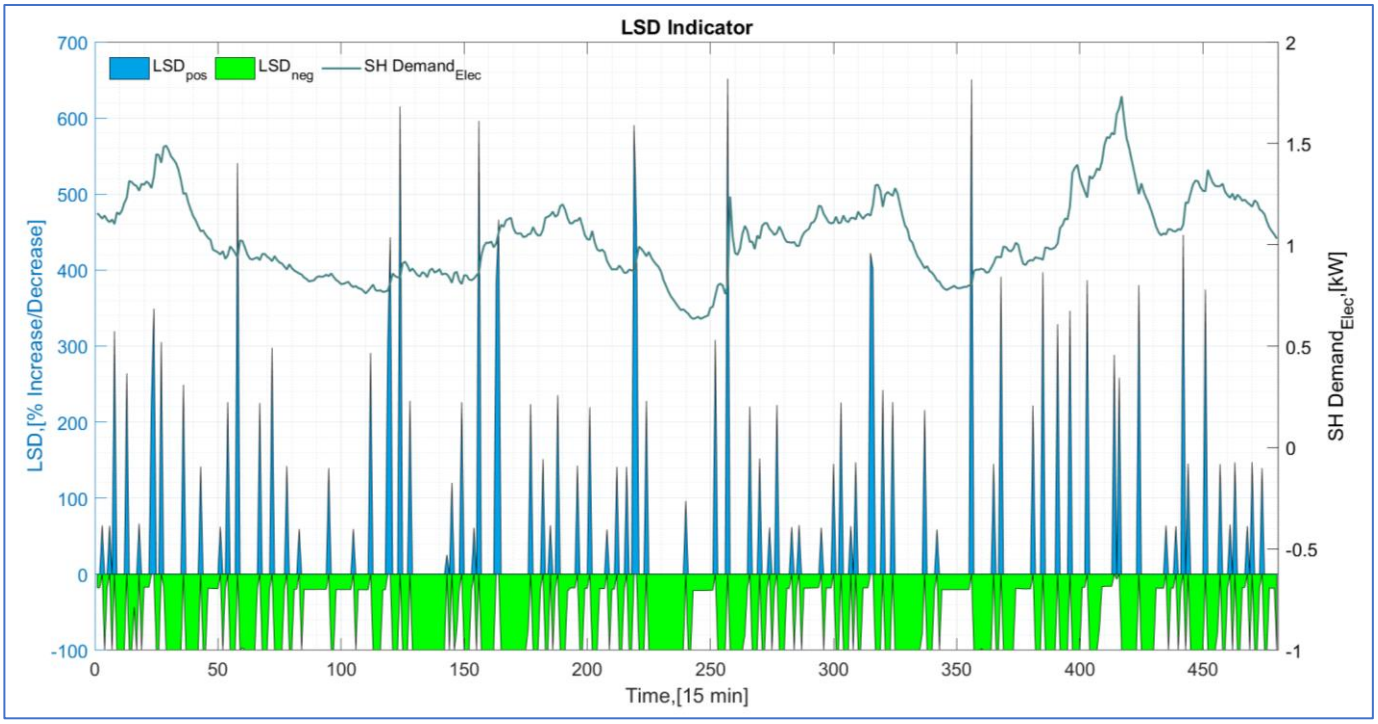

Figure 4-21: Heat pump LS_{DSM} indicator for 5 days of operation in winter

Additionally, the total amount of time that the HP does not operate for SH can be calculated by determining the times where the HP's power consumption during SH mode is equal to zero and $LS_{DSM,t}$ is equal to -1. Based on this, the HP coupled to the 800L SH tank has not operated for 64,5 h during the 5 days of simulation, having in this way an average off-time operation of 12.9 h per day if DHW is not considered. However, DHW needs to be considered in this analysis as this demand cannot be shifted, and as demonstrated in section 4.1.4, DHW demand reduces the operational flexibility of the HP as this demand depends heavily on the behavior of the inhabitants. When DHW is included in this analysis, the HP's off-time operation decreases to 47.25 h per 5 days of operation, representing a decrease in 27% of the off-time operation when only SH demand is included. Therefore, the daily HP's off-time operation including SH and DHW is 9.45 h. These results are valid for the normal and the reduced FIT cases as the HP energy consumption remains the same.

Table 4-12: HP's flexibility potential analysis during winter

SH Demand		**SH + DHW Demand**	
Shifted SH Demand, kWh (electricity)	**HP Off-Time Operation, h/day**	**Shifted SH Demand, kWh (electricity)**	**HP Off-Time Operation, h/day**
56.09	12.9	56.09	9.45

This concludes the results obtained from the analysis of the optimization of this integrated system. In the next two sections the discussion and conclusions from this research are presented together with recommendations for future work.

5. Discussion & Future Work

The developed research intended to determine the flexibility potential of an air source heat pump (ASHP) when integrated into an energy system with PV panels, a battery, and an electric vehicle. Under this scheme, an optimization was performed to schedule the times where each component must operate to meet all the different types of demands while maintaining the total energy costs minimized. In this way, the optimal HP power profile for different cases were obtained and analysed.

The results from the HP's behaviour evidenced how coupling a HP with thermal storage systems can produce a modification of the HP's power profile while providing a demand response effect. Additionally, the results strengthened the role of the thermal inertia of the building as this has a huge impact on the power consumption of the HP. Buildings with low thermal inertia due to its design and configuration will cause a fast decay of the interior's temperature causing the HP to increase its operation hours. This means that the obtained flexibility will also depend on the characteristics of the building. it is established

Looking at HP power profile and the LS_{DSM} indicator results, the HP coupled to the small tank (100 L) worked continuously consuming 2 kW as maximum, resulting in a relatively flattened power profile where no peak demands were observed. Consequently, the HP connected to a small tank for this case did not produce a load shifting response, thus the LS_{DSM} indicator equalled to 0. Nevertheless, an energy conservation effect was generated because there is a reduction of the HP load over all the consumption period to keep SH and DHW demands satisfied when compared to the case with a big tank. Contrarywise, with a big tank (800 L), the HP experienced high-power demands during off-peak hours reaching its maximum capacity of 6 kW, while during peak hours the HP did not operate for about 9.45 h per day. Hence, a load shifting demand response effect was obtained, and the LS_{DSM} indicator reached values bigger than 1 at off-peak hours, while the indicator became equal to -1 at times where the SH and DHW demands were entirely met by the storage tanks.

Thus, the LS_{DSM} indicator provided acknowledgement about the dynamic behaviour of the HP-TES, and its trend suggested the obtained demand response effect, while the time shifting result gave an idea about how long is possible to delay the operation of the flexible device from happening at peak hours. These results can be validated by looking at the findings and conclusions from specialized literature. In [28], [49], [35], and [50], the authors also concluded that small storage systems do not incentive load shifting because the HP works constantly, and that the power consumption of the heat pump remains at low levels. Furthermore, they found that storages with high thermal inertia will delay the energy use for several hours on the range of 4h to 12 h, so more energy autonomy can be provided. However, the energy use of the HP will tend to increase because of the increase of energy losses during the storage period. In this way, the HP results obtained in this research fit consistently with the findings of the cited authors. Unfortunately, these researches did not perform an analysis of the effects of reverse power flows on the grid from the BES or EV as part of their optimization studies.

On the economic side, the results needed to be compared to a reference case in which the system is not subject to a demand response control to strengthen its benefits. Thus, the proposed system demonstrated its feasibility by showing a significant energy cost reduction. In the case with a high FIT, the energy costs were reduced as result of having high power exchanges with the grid, and consequently, large amounts of energy are consumed and injected. In other words, the system showed minimum self-consumption and self-sufficiency as the in-house generated electricity from the PV panels was injected to the grid and not used either to satisfy the building's demand or to charge the BES. These unexpected outcomes motivated to deepen the analysis of the influence of the FIT on the operation of the system. Thereby, it was demonstrated that a low FIT enhanced the self-consumption/self-sufficiency of the system and reduced the energy exchanges with the grid.

Consequently, the FIT is a key variable to be considered when studying these systems as the elements involved will be affected in different ways. Additionally, from the SGO point of view, a low FIT would help to have a better grid stability as it faces fewer power exchanges to satisfy the customer demand, but it would generate less revenues from the energy sold to the customer. For the customer, a low FIT would lead to less revenues as the system will not

inject energy to be sold, so his energy bill reduction will be less attractive to him. Therefore, a proper FIT establishment will be required in the future to ensure high grid stability and an adequate customer's satisfaction.

Additionally, it is important to mention that high PV costs were obtained because of the value of the LCOE of the PV panels used during the simulations for summer. In this case, the cost of producing 1kWh of electricity from PV energy was chosen to be 0.03 €. This led to have considerable PV operational costs that increased the optimized energy cost at the end. However, this LCOE could be assumed to be zero for future works by considering that in the future the penetration of PV systems would be noticeable.

Now that the concept of this future system has been proven to generate considerable energy costs reduction, the research can be extended to a higher level, and further improvements can be made to increase the reliability of the results. Therefore, the following actions are proposed:

- High-level metadata availability for SH and DHW must be enhanced as the ease to access to this information is currently limited. For example, using gas supplier's information and validated in-house gas consumption measurements can help to expand the available data and increase its reliability.
- Include more weather variables for forecasting the SH demand in the temporal interpolation method developed in section 3.3.2. Wind speed and solar irradiation can be added to develop a more concise relationship of the SH demand with weather data. Geographic spatial influence also can be considered to enhance the correlation, as weather variables have their own spatial correlation characteristics [51].
- A more detailed model of the CoP of the heat pump can be used to have a more realistic approach of its performance, as proposed by [31]. In this way, more characteristics of the CoP can be integrated to determine more precisely its electricity consumption and its effects on the demand response potential.
- Replace both storage tanks for a stratified tank to reduce the physical structure of the system such that SH and DHW demands can be met by one single tank. This will lead to have a more sophisticated and accurate heat transfer model which can affect deeply the behaviour of the HP.
- Include investment and installation costs of the HP and the TES and perform an optimization for an entire year such that a more thorough economic analysis can be assessed. Thereby, a levelized cost and return on investment analysis can be performed.
- For summer season, the inclusion of cooling demand and its effects on the HP's flexibility and the system's behaviour can be studied. In this way, storing excess of PV energy as cold during summer could be developed as a new technique to enhance PV self-consumption.
- The proposed integrated system should include more households to have a more thoughtful appreciation of the impacts on the grid when more actors get involved. Therefore, more general conclusions can be drawn to weigh the technical and economic impacts of the introduction of these systems, and to help decision makers to establish policies respect to the development of these projects.

6. Conclusions

This thesis project focused on finding answers to the following research questions regarding the inclusion of heat pumps in an all-electric building under a demand response program. To find answers to these questions, a Non-Linear Programming optimization model was developed and tested in a simulation. The simulations were carried out for winter and summer cases, and they generated remarkable results. Below, a list of these questions and their answers is presented.

- *What is the demand response potential of heat pumps (HP) and thermal storage systems (TES) in all-electric buildings equipped with PV, BES and EV?*

  In Chapter 2, it was described the types of demand respond that can be achieved through the inclusion of flexible devices. During winter, it was found that a heat pump coupled to the 100 L tank resulted in an energy conservation demand response where power peaks were not obtained, however, the heat pump increased its ON/OFF cycles. On the other hand, using an 800 L tank produced a load shifting response where high-power demands of the heat pump were evidenced during low price times, but it provided energy to the house for a longer period before the heat pump needed to switch ON again. When looking at the cumulative energy consumption, there is not a remarkable difference between them as only an increase of 1.72% was evidenced even though the tank was 8 times bigger in the second case. This increase in the energy consumption was result of facing more energy losses when the tank size increased. Additionally, it was found that using a heat pump during winter could lead to a considerable reduction in the gas consumption. This resulted in a cost reduction of 17% in the customer's energy bill by avoiding the consumption of $53m^3$ of gas. Besides, it was demonstrated that a heat pump can satisfy the SH demand of the building by using only 25% of the energy a gas boiler would consume.

  In this way, it was concluded that the demand response potential of the heat pump with an 800 L tank is to shift 56.09 $kWh_{electricity}$ towards times of low energy demands to pre-heat the tank and provide more energy autonomy and flexibility to satisfy the heating demand of the building.

  - *What are the minimized energy costs for this integrated system?*

  The results of the optimization for winter and summer evidenced that high costs reduction could be achieved with the proposed system. It was demonstrated that the FIT signal had a significant influence on the system's cost minimization strategy. A high FIT resulted in a cost minimization through selling high amounts of energy to the grid while with the reduced FIT the minimization was performed by enhancing self-consumption of the PV produced energy and by using the energy stored in the BES/EV.

  During winter, the minimized costs between the high and reduced FIT cases differed approximately by 10%. In average, the optimization resulted in a minimized cost of 8.58 €/day. By assuming that this cost would be the same per each day of the whole season, this would represent a total energy cost of 755 €. When compared to a system where demand response is not performed, the system costs rose to 17.04 €/day, meaning a seasonal energy cost of 1500 €. Therefore, it can be concluded that during winter the proposed system could generate around 50% energy cost reduction when acting under a demand response program.

  For summer, the results in the operational strategy for minimizing the costs remained as in winter. However, the energy savings during the high FIT were almost 2 times higher than in the reduced FIT. In the first case, the system energy costs became negative, generating in average -1 €/day. This means that during the whole season the customer will generate 90 € as revenues. On the other hand, the system caused 3.50 €/day when no demand response was performed, meaning a seasonal cost of 315 €. This represents a 128% in costs reduction due to the type of operational strategy of the system. However, when the FIT was reduced, the costs savings reduced to 68%. The minimized energy costs in this case were 1.30 €/day or 117 € for the entire season.

From the above summary, the research questions and objectives have been accomplished. In addition, some extra conclusions have been established to remark the findings of this study.

- This thesis has offered an option to decouple the transportation and residential sectors from the gas and petrol industries, and to integrate them into one single system which runs entirely on electricity.

- The studied system can generate a considerable reduction in the consumer's energy bill while keeping his energy demand satisfied. Therefore, this can motivate the final users to take part in demand response programs, to rise their willingness to use renewable energies and storage systems in their households, and to become self-sufficient in their energy consumption.

- The developed optimization model can be considered as an intelligent control strategy because it proposes an NLP optimization framework that minimizes the energy costs by scheduling the optimal power consumption as response to the day ahead market price signals. Therefore, this model can control the power demand of the different devices though electricity prices such that the total energy costs can be minimized.

- This system can help to reduce the variability in the electricity production from renewable energies when a low FIT is used because this motivates to self-consume any excess of energy and store it to be used later to keep the demand satisfied.

- The demand response effect obtained by using heat pumps connected to thermal storage system will depend on the size of the storage. A small storage causes an energy conservation response where the power profile of the HP is more stable. This is beneficial in cases of centralized generation as no sudden power surges will occur, ensuring the stability of the grid. For cases of distributed generation or isolated systems from the grid, a load shifting response is more beneficial as the energy consumption can be moved to times of low demands and stored for later use.

- Even though the proposed system can lead to a considerable cost reduction, it is not economically attractive at current electricity prices when compared to the current energy bills. However, in the future, when renewable energies get more involved, this type of systems will become attractive not only in economic terms, but also technical.

- For future systems, renewable energy self-consumption will play a key role in lessening the effects of intermittent electricity production. If the FITs remain sufficiently low, less power exchanges with the grid will be obtained.

7. Bibliography

1. Kreijkes, M., *Looking under the hood of the Dutch Energy System*, T.J.D. Sherwood, Editor. 2017, Clingendael International Energy Program, CIEP: The Hague. p. 1-35.
2. Ministry of Economic Affairs, *Energy Report: Transition to Sustainable Energy*, T. Designers, Editor. 2016, Ministry of Economic Affairs: Netherlands. p. 12.
3. Kern, F. and A. Smith, *Restructuring energy systems for sustainability? Energy transition policy in the Netherlands.* Energy policy, 2008. **36**(11): p. 4093-4103.
4. Centraal Bureau voor de Statistiek. *More wind and solar electricity*. 2018 [cited 2019 2020/03/27]; Available from: https://www.cbs.nl/en-gb/news/2018/09/more-wind-and-solar-electricity.
5. Kosmadakis, G., S. Karellas, and E. Kakaras, *Renewable and conventional electricity generation systems: Technologies and diversity of energy systems*, in *Renewable Energy Governance*. 2013, Springer. p. 9-30.
6. Leavey, S., *Mitigating Power Fluctuations from Renewable Energy Sources*. 2012.
7. Lund, P.D., et al., *Review of energy system flexibility measures to enable high levels of variable renewable electricity.* Renewable and Sustainable Energy Reviews, 2015. **45**: p. 785-807.
8. Eid, C., et al., *Managing electric flexibility from Distributed Energy Resources: A review of incentives for market design.* Renewable and Sustainable Energy Reviews, 2016. **64**: p. 237-247.
9. Ela, E., et al., *Wholesale electricity market design with increasing levels of renewable generation: Incentivizing flexibility in system operations.* The Electricity Journal, 2016. **29**(4): p. 51-60.
10. Eid, C., et al. *Aggregation of demand side flexibility in a smart grid: A review for European market design*. in *2015 12th International Conference on the European Energy Market (EEM)*. 2015. IEEE.
11. Attia, H.A., *Mathematical formulation of the demand side management (DSM) problem and its optimal solution.* 2010.
12. Gellings, C.W. and W.M. Smith, *Integrating demand-side management into utility planning.* Proceedings of the IEEE, 1989. **77**(6): p. 908-918.
13. Hsieh, E. and R. Anderson, *Grid flexibility: The quiet revolution.* The Electricity Journal, 2017. **30**(2): p. 1-8.
14. Fischer, D. and H. Madani, *On heat pumps in smart grids: A review*. Renewable and Sustainable Energy Reviews, 2017. **70**: p. 342-357.
15. Natural Resources Canada's Office of Energy Efficiency, *Heating and Cooling With a Heat Pump*. 2004.
16. Bee, E., et al. *Air-source heat pump and photovoltaic systems for residential heating and cooling: Potential of self-consumption in different European climates*. in *Building Simulation*. 2019. Springer.
17. Rees, S.J., *An introduction to ground-source heat pump technology*, in *Advances in Ground-Source Heat Pump Systems*. 2016, Elsevier. p. 1-25.
18. Wu, R., *Energy efficiency technologies–air source heat pump vs. ground source heat pump.* Journal of sustainable development, 2009. **2**(2): p. 14-23.
19. Patrice Pinel and Markus Brychta, *Checklist for heat pump applications in buildings*, Tim Selke and Marcus Jones, Editors. 2008, Arsenal Research: Vienna, Austria. p. 1-40.
20. Chua, K.J., S.K. Chou, and W. Yang, *Advances in heat pump systems: A review.* Applied energy, 2010. **87**(12): p. 3611-3624.
21. Alvarez Gallardo, M.d.P., *Assessing the Performance of Ground Source Heat Pumps in neighboring medium-size households*, in *Industrial Ecology*. 2013, TU Delft: Delft. p. 1-74.
22. Fischer, D. and K.B. Lindberg. *Potential for balancing wind and solar power using heat pump heating and cooling systems*. in *Solar Integration Workshop*. 2014.

23. Ellerbrok, C., *Potentials of demand side management using heat pumps with building mass as a thermal storage*. Energy Procedia, 2014. **46**(0): p. 214-219.
24. van Etten, M.J., *Simulating the flexibility potential of demand response with heat pumps in the Netherlands*, in *Complex Systems Engineering and Management*. 2017, Delft University of Technology: Delft. p. 1-100.
25. Sichilalu, S., T. Mathaba, and X. Xia, *Optimal control of a wind–PV-hybrid powered heat pump water heater.* Applied energy, 2017. **185**: p. 1173-1184.
26. Steen, D., et al., *Modeling of thermal storage systems in MILP distributed energy resource models.* Applied Energy, 2015. **137**: p. 782-792.
27. Hedegaard, K., et al., *Wind power integration using individual heat pumps–analysis of different heat storage options.* Energy, 2012. **47**(1): p. 284-293.
28. Terlouw, T., et al., *Optimal energy management in all-electric residential energy systems with heat and electricity storage.* Applied Energy, 2019. **254**: p. 113580.
29. Wolf, T., *Model-based Assesment of Heat Pump Flexibility*, in *Teknisk- naturvetenskaplig fakultet*. 2016, Uppsala Universitet: Uppsala. p. 1-76.
30. Hedegaard, K. and O. Balyk, *Energy system investment model incorporating heat pumps with thermal storage in buildings and buffer tanks.* Energy, 2013. **63**: p. 356-365.
31. Saraf, N., *Predictive control for residential capacity controlled heat pumps in a smart grid scenario.* 2015.
32. Edwards, S., I. Beausoleil-Morrison, and A. Laperrière, *Representative hot water draw profiles at high temporal resolution for simulating the performance of solar thermal systems.* Solar Energy, 2015. **111**: p. 43-52.
33. ISO, I.O.f.S., *Energy Performance of Buildings — Calculation of Energy Use for Space Heating and Cooling*. 2008, ISO: Switzerland. p. 162.
34. Mudgal, S., et al., *Energy performance certificates in buildings and their impact on transaction prices and rents in selected EU countries.* European Commission (DG Energy), Paris, 2013.
35. Renaldi, R., A. Kiprakis, and D. Friedrich, *An optimisation framework for thermal energy storage integration in a residential heat pump heating system.* Applied energy, 2017. **186**: p. 520-529.
36. Fischer, D., et al., *Impact of PV and variable prices on optimal system sizing for heat pumps and thermal storage.* Energy and Buildings, 2016. **128**: p. 723-733.
37. Terlouw, T., T. AlSkaif, and W. van Sark. *Optimal Energy Management of All-electric Residential Energy Systems in the Netherlands*. in *2019 IEEE Milan PowerTech*. 2019. IEEE.
38. Nash, S., *Impact of mechanical ventilation systems on the indoor-air quality in highly energy-efficient houses*, in *IVEM, Center for Energy and Environmental Studies*. 2013, University of Groningen: The Netherlands.
39. Corp., G.D. *GAMS*. [cited 2020 19-08-2020]; Available from: https://www.gams.com/products/gams/gams-language/.
40. Laslau, C., L. Xie, and C. Robinson, *The Next-Generation Battery Roadmap: Quantifying How Solid-State.* Lithium-Sulfur, and Other Batteries Will Emerge after, 2020.
41. Kelly, K., et al., *Battery Ownership Model-Medium Duty HEV Battery Leasing & Standardization.* 2015, National Renewable Energy Lab.(NREL), Golden, CO (United States).
42. Garifi, K., et al., *Control of Energy Storage in Home Energy Management Systems: Non-Simultaneous Charging and Discharging Guarantees.* arXiv preprint arXiv:1805.00100, 2018.
43. Wang, J., et al., *Degradation of lithium ion batteries employing graphite negatives and nickel–cobalt–manganese oxide+ spinel manganese oxide positives: Part 1, aging mechanisms and life estimation.* Journal of Power Sources, 2014. **269**: p. 937-948.
44. Baccouche, I., et al., *Improved OCV model of a Li-ion NMC battery for online SOC estimation using the extended Kalman filter.* Energies, 2017. **10**(6): p. 764.

45. Mouli, G.R.C., et al. *Economic and CO2 emission benefits of a solar powered electric vehicle charging station for workplaces in the Netherlands*. in *2016 IEEE Transportation Electrification Conference and Expo (ITEC)*. 2016. IEEE.
46. Epexspot. *Market Data*. 2020 [cited 2020 07/04]; Available from: https://www.epexspot.com/en/market-data.
47. Niessink, R. and H. Rösler, *Developments of Heat Distribution Networks in the Netherlands*. 2015.
48. Rabou, L.P., et al., *Micro gas turbine operation with biomass producer gas and mixtures of biomass producer gas and natural gas.* Energy & fuels, 2008. **22**(3): p. 1944-1948.
49. Arteconi, A. and F. Polonara, *Assessing the demand side management potential and the energy flexibility of heat pumps in buildings.* Energies, 2018. **11**(7): p. 1846.
50. Sánchez, C., et al., *Optimised Heat Pump Management for Increasing Photovoltaic Penetration into the Electricity Grid.* Energies, 2019. **12**(8): p. 1571.
51. Boissonnade, A.C., L.J. Heitkemper, and D. Whitehead, *Weather data: cleaning and enhancement.*

8. Appendices

8.1. Appendix A: Percentile Analysis SH Data Temporal Interpolation

The percentile analysis for the temporal interpolation of the SH demand data is presented. This analysis was performed in MATLAB using the built-in function *prctile* and the curving fitting tool. Figure 8.1-1 represents the temporal interpolation regression for the SH demand data without a percentile analysis. Here the fitting correlation showed an $R^2 = 0.4798$, thus it was rejected.

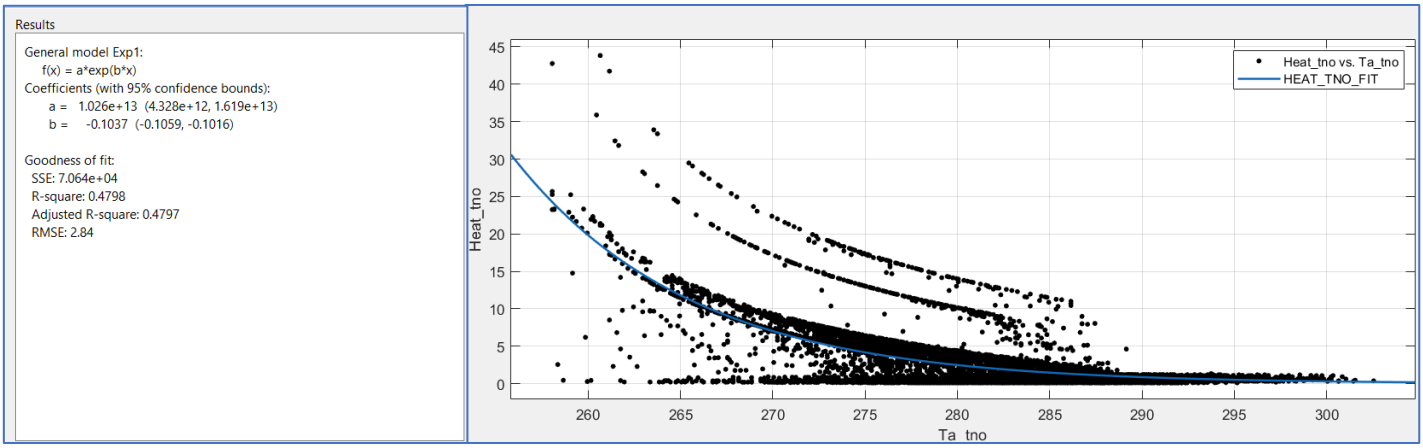

Figure 8.1-1: SH demand data distribution (no percentile)

Figures 8.1-2, and 8.1-3 display the temporal interpolation analysis for percentiles 90, and 25, respectively.

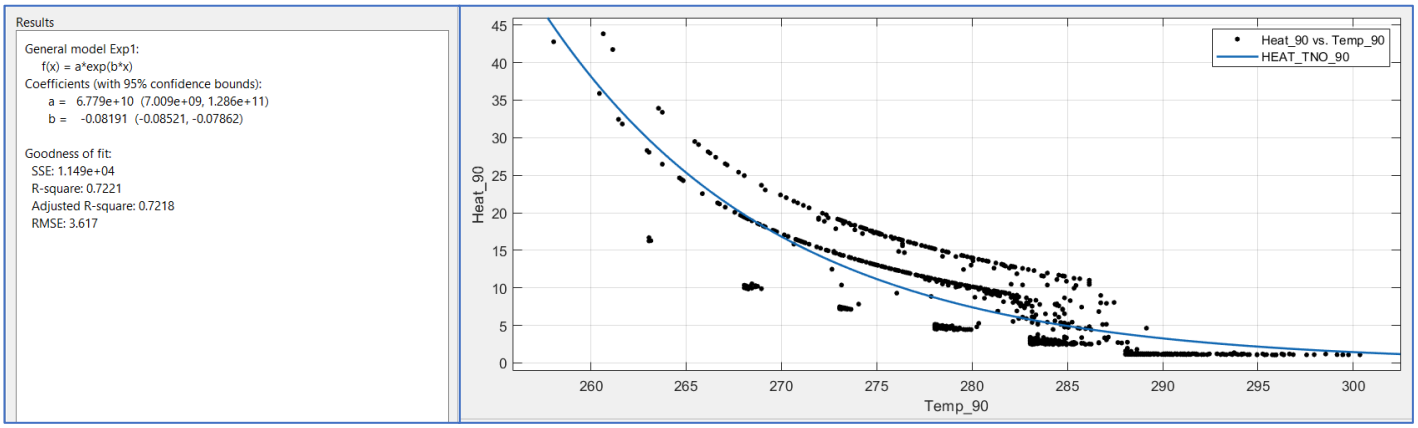

Figure 8.1-2: SH demand data distribution for Percentile 90 (P90)

In, Figure 8.1-1, it is seen that the SH demand data is strongly grouped within values between 0 and 15 kWh, however, the percentile 90 has included values higher than 15 kWh. Although in this percentile an $R^2 = 0.7221$ is obtained, the fitted values correspond to the most scattered ones, thus the least probable to occur. Therefore, this fitting correlation cannot be used to perform the temporal interpolation because it will overestimate the SH demand, having less reliable results.

In the percentile 25 (P25), it is clear how a considerable percentage of the data are used to perform the fitting correlation. In this percentile, values with high occurrence frequencies have been integrated, and those ones which deviate from this tendency are eliminated by the tool. Therefore, it was decided that this correlation can be used to perform the temporal interpolation described in section 3-1.

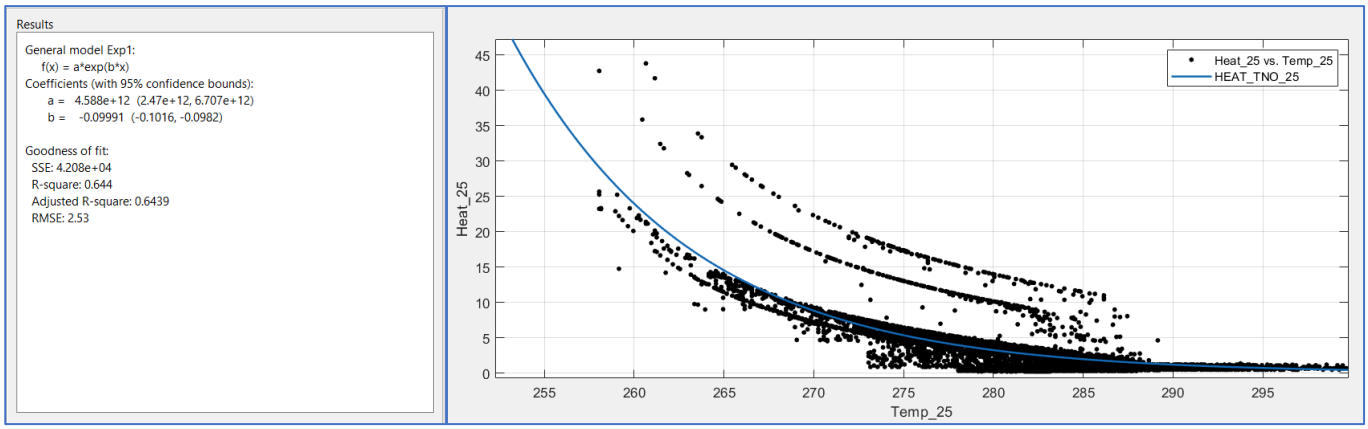

Figure 8.1-3: SH demand data distribution for percentile 25 (P25)

8.2. Appendix B: BES and EV Power Profiles for Winter

Figure 8.2-1 displays the power and energy profiles for the BES during winter for high FIT case. It is seen that the BES consumes power during the lowest buying electricity prices, and it sells its energy at times of high FIT prices. This is result of the operational strategy of the PV-BES-EV-HP system to minimize its total energy costs under the demand response program. Figure 8.2-2 displays the power and energy profiles of the EV where the same behaviour as the BES is evidenced.

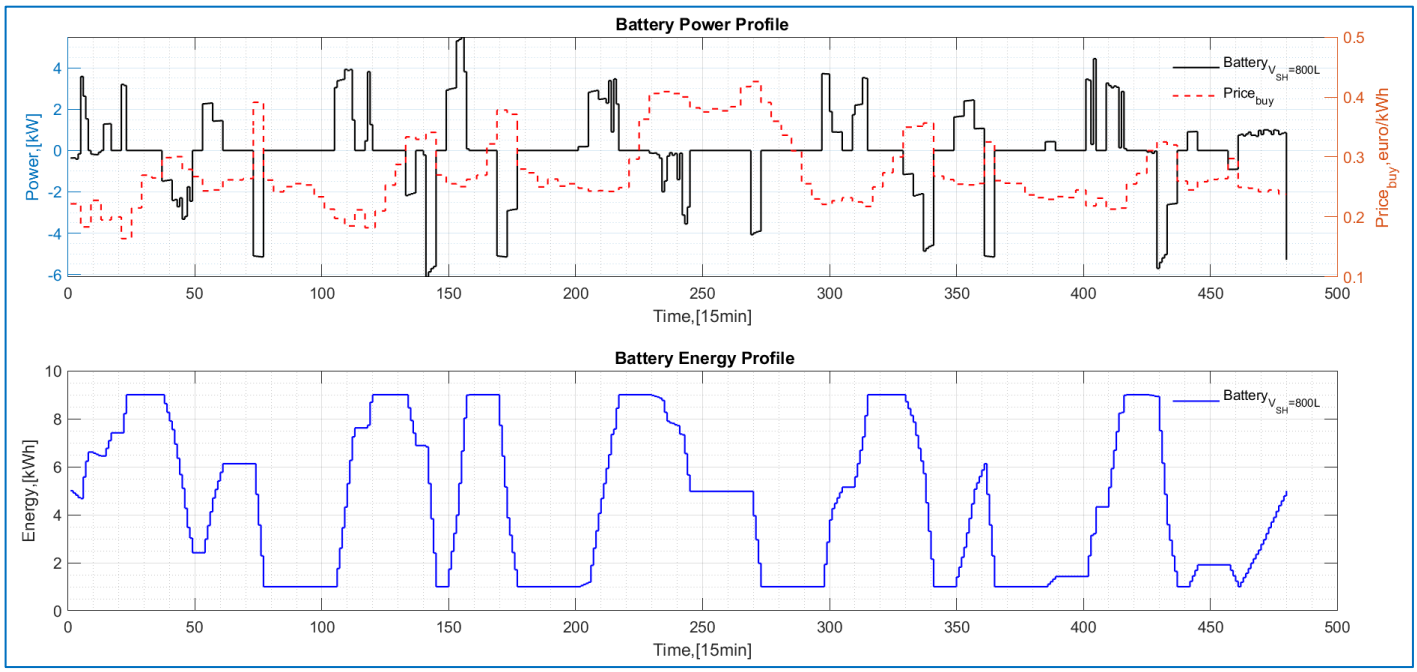

Figure 8.2-1: BES optimized power and energy profiles (Winter-High FIT)

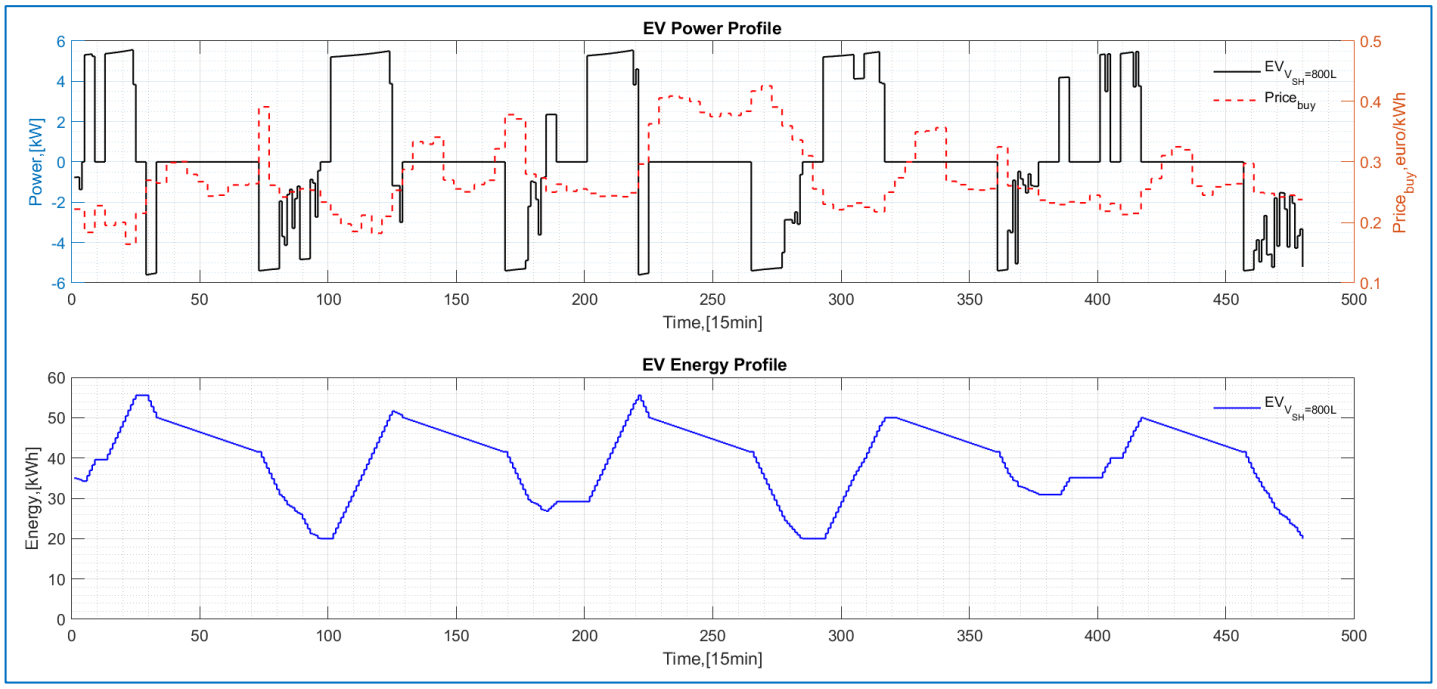

Figure 8.2-2: EV optimized power and energy profiles (Winter-High FIT)

8.3. Appendix C: Grid Operational Costs

Figure 8.3-1 shows the grid's cumulative energy curves for consumption and injection due to power exchanges of the optimized system during winter . In the bottom graph, the grid costs evolution for the high FIT case is plotted. The grid costs have been calculated by multiplying the energy consumption or injection with the respective buying or selling electricity price at each time step of the optimization.

$$E_{intake(t+1)} = E_{intake(t)} + P^{Neg}_{Grid(t)} \cdot \Delta t \quad 8.3\text{-}1$$

$$E_{injection(t+1)} = E_{injection(t)} + P^{Pos}_{Grid(t)} \cdot \Delta t \quad 8.3\text{-}2$$

$$Cost_{Grid\ intake(t+1)} = Cost_{Grid\ intake(t)} + P^{Neg}_{Grid(t)} \cdot \Delta t \cdot \lambda_{buy(t)} \quad 8.3\text{-}3$$

$$Cost_{Grid\ injection(t+1)} = Cost_{Grid\ injection(t)} + P^{Pos}_{Grid(t)} \cdot \Delta t \cdot \lambda_{sell(t)} \quad 8.3\text{-}4$$

$$Total\ Cost_{Grid\ (t+1)} = Cost_{Grid\ intake(t+1)} - Cost_{Grid\ injection(t+1)} \quad 8.3\text{-}5$$

Where $E_{intake(t)}$ is the energy consumption from the grid, $E_{injection\ (t)}$ is the energy injected to the grid, $Cost_{Grid\ (t+1)}$ is the cumulative cost for the energy consumed or injected to the grid, and Total $Cost_{Grid(t+1)}$ is the total cumulative grid cost.

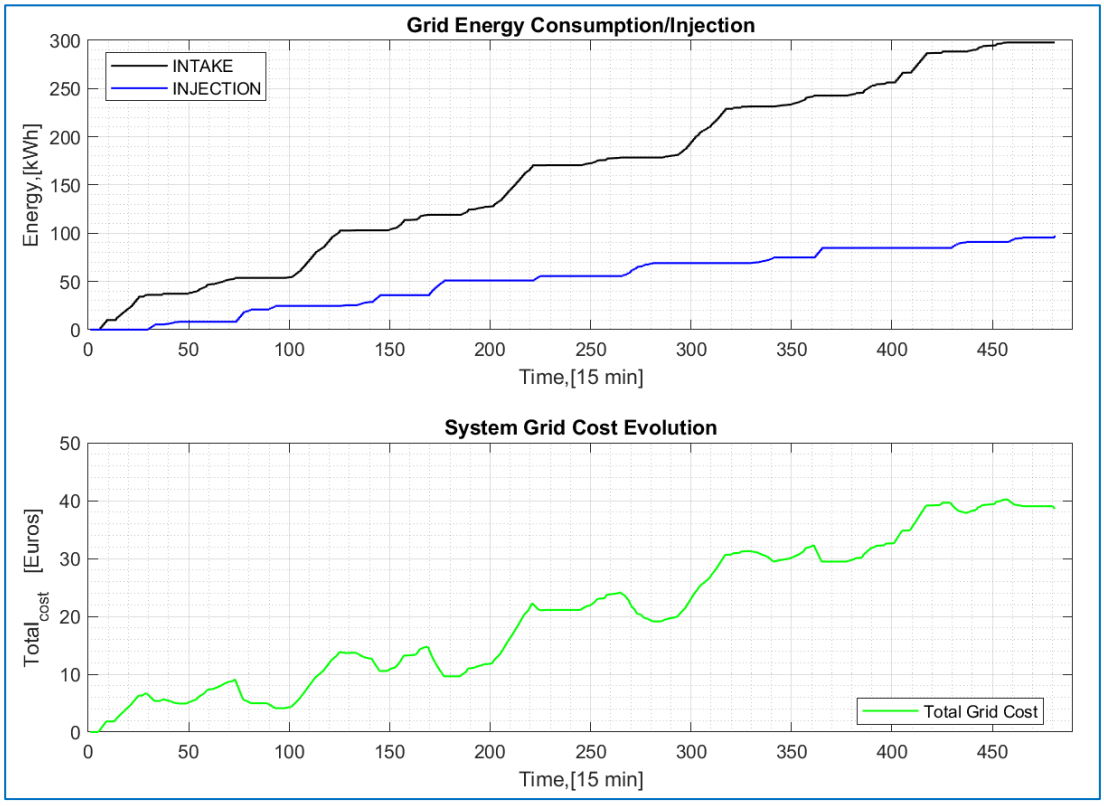

Figure 8.3-1: System grid's operational costs and cumulative energy curves (Winter High FIT)

The same analysis was performed to calculate the total grid costs for the reduced FIT case in winter, and for summer.

8.4. Appendix D: Building's Temperature Summer

Figure 8.4-1 displays the temperature of the building, the SH and DHW demands for summer. In this case, the temperature of the building will increase because the outside air is warmer than the interior of the building, thus the household experiences heat gains due to convection, conduction, and natural ventilation. The SH demand is remarkably low compared to winter. However, this demand was calculated using equation 3-1 to have a fair comparison between both winter and summer seasons

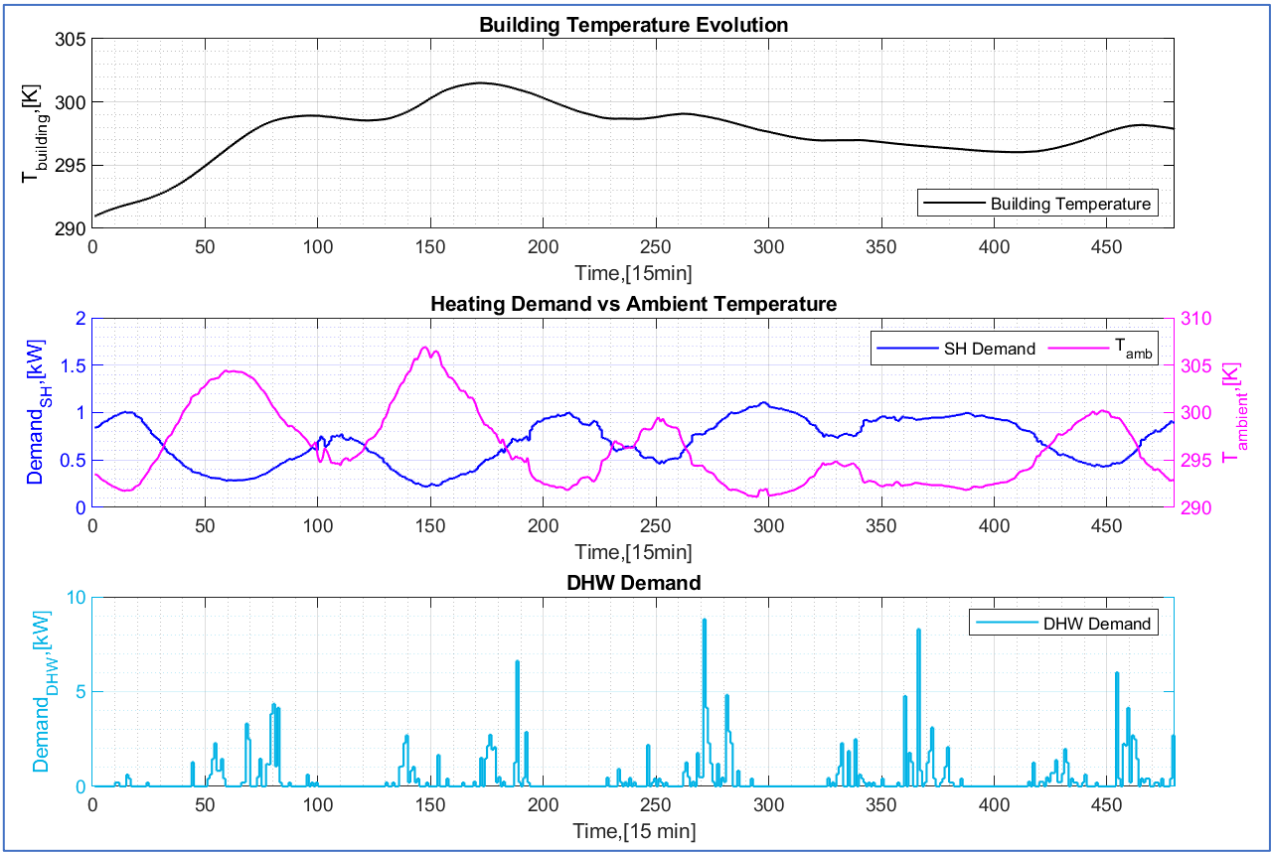

Figure 8.4-1: Building's temperature, SH and DHW demands for summer (five days)

8.5. Appendix E: ASHP Technical Data

Figure 8.5-1 displays the technical data of the air source heat pump (ASHP) used in this research project. These data were used to determine the COP correlation described in section 3.2.4. The data were provided by Mr. Maurice Rebel, Senior Account Manager from LG Electronics in the Netherlands.

THERMA V Monobloc Type Product Data

6. Performance Data

6.2 Heating Oparation

■ **Maximum Heating Capacity (Include defrost effect)**

◆ **ZHBW056A0 [HM051M U43]**

Outdoor Temperature [°C DB]	Water flow rate 15.81 LPM								Water flow rate 9.9 LPM				Water flow rate 7.9 LPM			
	LWT 30 °C		LWT 35 °C		LWT 40 °C		LWT 45 °C		LWT 50 °C		LWT 55 °C		LWT 60 °C		LWT 65 °C	
	TC	COP	TC	COP	TC	COP	TC	COP	TC	COP	TC	COP	TC	COP	TC	COP
-25	3.79	1.88	3.67	1.75	3.54	1.63	3.42	1.50	-	-	-	-	-	-	-	-
-20	4.22	2.51	4.09	2.01	3.96	1.86	3.83	1.72	3.70	1.57	-	-	-	-	-	-
-15	4.66	2.42	4.52	2.27	4.38	2.10	4.25	1.93	4.11	1.77	3.97	1.60	-	-	-	-
-7	5.50	3.18	5.50	2.99	5.50	2.79	5.50	2.60	5.50	2.41	5.50	2.21	5.50	2.02	-	-
-4	5.50	3.36	5.50	3.14	5.50	2.93	5.50	2.71	5.50	2.49	5.50	2.28	5.50	2.06	5.50	1.91
-2	5.50	3.51	5.50	3.25	5.50	3.04	5.50	2.83	5.50	2.63	5.50	2.42	5.50	2.21	5.50	2.01
2	5.50	3.52	5.50	3.45	5.50	3.25	5.50	3.04	5.50	2.83	5.50	2.63	5.50	2.42	5.50	2.21
7	5.50	4.84	5.50	4.50	5.50	4.16	5.50	3.82	5.50	3.49	5.50	2.70	5.50	2.59	5.50	2.47
10	5.50	5.14	5.50	4.78	5.50	4.42	5.50	4.06	5.50	3.70	5.50	3.35	5.50	2.99	5.50	2.63
15	5.50	6.12	5.50	5.66	5.50	5.20	5.50	4.73	5.50	4.27	5.50	3.81	5.50	3.35	5.50	2.88
18	5.50	6.45	5.50	5.96	5.50	5.48	5.50	4.99	5.50	4.50	5.50	4.01	5.50	3.53	5.50	3.04
20	5.50	6.67	5.50	6.17	5.50	5.66	5.50	5.16	5.50	4.65	5.50	4.15	5.50	3.65	5.50	3.14
35	5.50	8.31	5.50	7.68	5.50	7.05	5.50	6.43	5.50	5.80	5.50	5.17	5.50	4.54	5.50	3.91

◆ **ZHBW076A0 [HM071M U43]**

Outdoor Temperature [°C DB]	Water flow rate 20.12 LPM								Water flow rate 12.6 LPM				Water flow rate 10.0 LPM			
	LWT 30 °C		LWT 35 °C		LWT 40 °C		LWT 45 °C		LWT 50 °C		LWT 55 °C		LWT 60 °C		LWT 65 °C	
	TC	COP	TC	COP	TC	COP	TC	COP	TC	COP	TC	COP	TC	COP	TC	COP
-25	4.82	1.99	4.67	1.73	4.51	1.48	4.36	1.22	-	-	-	-	-	-	-	-
-20	5.38	2.47	5.21	1.98	5.05	1.77	4.88	1.56	4.72	1.35	-	-	-	-	-	-
-15	5.93	2.38	5.76	2.22	5.58	2.06	5.41	1.90	5.23	1.74	5.06	1.58	-	-	-	-
-7	7.00	3.15	7.00	2.96	7.00	2.77	7.00	2.58	7.00	2.38	7.00	2.19	7.00	2.00	-	-
-4	7.00	3.33	7.00	3.11	7.00	2.90	7.00	2.68	7.00	2.47	7.00	2.25	7.00	2.04	7.00	1.89
-2	7.00	3.51	7.00	3.21	7.00	3.01	7.00	2.81	7.00	2.60	7.00	2.40	7.00	2.19	7.00	1.99
2	7.00	3.52	7.00	3.42	7.00	3.21	7.00	3.01	7.00	2.81	7.00	2.60	7.00	2.40	7.00	2.19
7	7.00	4.69	7.00	4.50	7.00	4.16	7.00	3.82	7.00	3.47	7.00	2.68	7.00	2.57	7.00	2.45
10	7.00	5.14	7.00	4.78	7.00	4.42	7.00	4.05	7.00	3.69	7.00	3.33	7.00	2.96	7.00	2.60
15	7.00	6.02	7.00	5.57	7.00	5.12	7.00	4.67	7.00	4.21	7.00	3.76	7.00	3.31	7.00	2.86
18	7.00	6.34	7.00	5.87	7.00	5.39	7.00	4.92	7.00	4.44	7.00	3.96	7.00	3.49	7.00	3.01
20	7.00	6.56	7.00	6.07	7.00	5.57	7.00	5.08	7.00	4.59	7.00	4.10	7.00	3.60	7.00	3.11
35	7.00	8.17	7.00	7.56	7.00	6.95	7.00	6.33	7.00	5.72	7.00	5.10	7.00	4.49	7.00	3.88

Figure 8.5-1: ASHP Therma V Monobloc Type technical data LG Electronics